

Ultrafiltration and Nanofiltration Multilayer Membranes Based on Cellulose

Dissertation by

Sara Livazovic

In Partial Fulfillment of the Requirements

For the Degree of Doctor of Philosophy

King Abdullah University of Science and Technology, Thuwal,

Kingdom of Saudi Arabia

June 2016

EXAMINATION COMMITTEE APPROVALS FORM

The dissertation of Sara Livazovic is approved by the examination committee.

Committee Chairperson: Prof. Dr. Suzana P. Nunes

Committee Co-Chair: Prof. Dr. Suzana P. Nunes

Committee Members: Prof. Dr. Klaus-Viktor Peinemann, Prof. Dr. Peiyong Hong, Prof. Dr. Sacide Alsoy Altkinkaya

COPYRIGHT PAGE

© June 2016

Sara Livazovic

All Rights Reserved

ABSTRACT

Ultrafiltration and Nanofiltration Multilayer Membranes Based on Cellulose

Sara Livazovic

Membrane processes are considered energy-efficient for water desalination and treatment. However most membranes are based on polymers prepared from fossil petrochemical sources. The development of multilayer membranes for nanofiltration and ultrafiltration, with thin selective layers of naturally available cellulose, has been hampered by the availability of non-aggressive solvents. We propose the manufacture of cellulose membranes based on two approaches: (i) silylation, coating from solutions in tetrahydrofuran, followed by solvent evaporation and cellulose regeneration by acid treatment; (ii) casting from solution in 1-ethyl-3-methylimidazolium acetate ([C2mim]OAc), an ionic liquid, followed by phase inversion in water.

In the search for less harsh, greener membrane manufacture, the combination of cellulose and ionic liquid is of high interest. Due to the abundance of OH groups and hydrophilicity, cellulose-based membranes have high permeability and low fouling tendency. Membrane fouling is one of the biggest challenges in membrane industry and technology. Accumulation and deposition of foulants onto the surface reduce membrane efficiency and requires harsh chemical cleaning, therefore increasing the cost of maintenance and replacement. In this work the resistance of cellulose

membranes towards model organic foulants such as Suwanee River Humic Acid (SRHA) and crude oil have been investigated.

Cellulose membrane was tested in this work for oil-water (o/w) separation and exhibited practically 100 % oil rejection with good flux recovery ratio and membrane resistivity. The influence of anionic, cationic and ionic surfactant as well as pH and crude oil concentration on oil separation was investigated, giving a valuable insight in experimental and operational planning.

ACKNOWLEDGMENTS

I would like to thank my supervisor Prof. Dr. Suzana P. Nunes for taking me as her PhD student and going on this journey together with me. Thank you for your time and patience, scientific and life related discussions. Especially thank you for coming to my wedding. I thank my committee members, Prof. Dr. Klaus-Viktor Peinemann, Prof. Dr. Peiyong Hong and Prof. Dr. Sacide Alsoy Altinkaya for agreeing to be part of my committee and for their valuable comments. I am thankful for working with WDRC members, for their help, support and encouragement, especially Dr. Faisal Wali, Dr. Zhenyu Li, Dr. Rodrigo Valladares for and Nigel Metge their help in the beginning of my PhD. I am most thankful for learning from staff from Analytical and Imaging and Characterization Core Lab how to operate different equipment.

To my amazing NPM members, I was so lucky and blessed to be in a group with all of you, you are all very kind, smart and helpful and each one of you contributed to my growth as a scientist and as a person. Very, very big thank you goes to my family, my mother for her love and support, my father and grandparents as well as my friends. I am grateful to Craig Kershaw from Human Resources for his help and understanding regarding my mothers' stay at Kaust.

I couldn't do this without my husband Samir who threatened he will kill anyone that makes me sad. Your unconditional support and calmness get me through it all.

I am most grateful to God for my health, my family and friends and for all the blessings he bestowed upon me and guided me through difficult times.

TABLE OF CONTENTS

EXAMINATION COMMITTEE APPROVALS FORM.....	2
COPYRIGHT PAGE.....	3
ABSTRACT.....	4
ACKNOWLEDGMENTS.....	6
TABLE OF CONTENTS.....	7
LIST OF ABBREVIATIONS.....	9
LIST OF SYMBOLS.....	11
LIST OF FIGURES.....	12
LIST OF SCHEMES.....	15
LIST OF TABLES.....	16
1. Motivation.....	17
1.1. Objective.....	20
2. Introduction.....	21
2.1 Currently Available Membranes for Ultra- and Nanofiltration: Advantages and Drawbacks.....	22
2.1.1. Inorganic Ultrafiltration Membranes.....	24
2.1.2. Inorganic Nanofiltration Membranes.....	26
2.1.3. Organic Ultrafiltration Membranes.....	28
2.1.4. Organic Nanofiltration Membranes.....	30
2.1.5. Block Copolymer Membranes.....	31
2.2. Fouling.....	31
2.3. Oil-Water Separation.....	37
2.3.1 Relevance and Different Available Processes.....	38
2.4 Cellulose.....	41
2.4.1 Short History of Cellulose.....	42
2.4.2. Cellulose Structure and Analysis.....	44
2.4.3 Methods of Cellulose Solubilization and Processing.....	46
2.4.3.1 Cellulose Xanthogenate.....	47
2.4.3.2 Cuprammonium Process.....	48
2.4.3.3 Cyclic Amine Oxides.....	48
2.4.3.4 N-methylmorpholine-N-oxide.....	49
2.4.3.5 Cellulose in Ionic Liquids.....	49
2.4.4. Cellulose Nanomaterials and Applications.....	52
2.4.5 Cellulose Membranes.....	54
3. Methodology.....	57
3.1 Materials.....	57
3.1.1. Cellulose Modification by Silanization and Regeneration.....	57
3.1.2. Cellulose Membranes from Solutions in Ionic liquid.....	58
3.1.3. Fouling Evaluation of Cellulose Membranes.....	59
3.1.4. Oil-Water separation by Cellulose Membrane.....	59

3.2. Membrane Preparation.....	60
3.2.1. Cellulose Modification by Silanization and Regeneration	60
3.2.1.1. Preparation of Trimethylsilyl Cellulose	60
3.2.1.2. Preparation of Regenerated Silyl Cellulose.....	61
3.2.2. Cellulose Membranes from Solutions in Ionic Liquid	62
3.2.2.1. Preparation of multilayer membranes with polyamide selective layer	63
3.2.3. Fouling Evaluation of Cellulose Membranes	63
3.2.4. Oil-Water Separation by Cellulose Membrane	63
3.3. Experimental Methods of Characterization	64
3.3.1. Chemical Characterization.....	64
3.3.2. Morphological Characterization.....	64
3.3.3. Surface Characterization	66
3.3.4. Permeance Measurement.....	67
3.3.5. Rejection Measurement and Permeate Characterization.....	69
3.3.6. Fouling Characterization.....	71
3.3.6.1. Extent of Fouling (Humic acid, BSA and γ -globulin)	71
3.3.7. Oil-Water Separation	72
3.3.7.1. Extent of Fouling in Experiments with Oil in Water Emulsion and Real Produced Water	72
3.3.7.1.1. Turbidity.....	74
3.3.7.1.2. Oil in Water Analysis.....	74
4. Results and Discussion.....	75
4.1. Cellulose Modification by Silanization/Regeneration	75
4.2. Cellulose Membranes from Solutions in Ionic Liquid	89
4.2.1. Stability of Cellulose/Ionic Liquid Membranes in Organic Solvents.....	94
4.3. Fouling Evaluation of Cellulose Membranes	95
4.3.1. Fouling Evaluation with Bovine Serum Albumin, Gamma Globulin and Humic Acid.....	97
4.4. Oil-Water Separation by Cellulose Membranes	103
5. Conclusion.....	125
5.1. Summary of Research Conclusions	125
5.1.1. Cellulose Membrane Prepared via Silanization and Regeneration	125
5.1.2. Cellulose Membrane Prepared with Ionic Liquid	125
5.1.3. Low Fouling Tendency of Cellulose/Ionic Liquid Membranes Towards Humic and Non-Humic Foulants	126
5.1.4. Complete Removal of Crude Oil with Cellulose/Ionic Liquid Membranes	126
5.2. Recommendations for Future Research.....	127
5.2.1. Scale-up Potential, Environmental Impact and Recovery of Ionic Liquid	127
5.2.2. Cellulose Membranes in Biomedical Application	131
REFERENCES.....	133
APPENDICES.....	145
LIST OF PUBLICATIONS AND CONFERENCES.....	147

LIST OF ABBREVIATIONS

[C2mim]OAc	1-ethyl-3-methyl imidazolium acetate
AFM	Atomic Force Microscopy
AGU	Anhydroglucose units
Al ₂ O ₃	Aluminum (III) oxide
ALD	Atomic layer deposition
ATRP	Atom transfer radical polymerization
ATR-FTIR	Attenuated total reflectance mode
BSA	Bovine serum albumin
CA	Cellulose-acetate
CAB	Cellulose acetate butyrate
CAP	Cellulose acetate propionate
CeO ₂	Cerium (IV) oxide
COD	Chemical oxygen demand
CTAB	Hexadecyltrimethylammonium bromide
DMAc	N,N-dimethylacetamide
DMF	N,N-dimethylformamide
DR	Flux decay ratio
<i>E. coli</i>	Escherichia coli
FESEM	Field emission scanning electron microscopes
FO	Forward osmosis
FRR	Flux recovery ratio
FTIR	Fourier Transform Infrared Spectroscopy
GO	Graphene oxide
GPC	Gel-permeation chromatography
HEMA	2-hydroxyethyl-methacrylate
IP	Interfacial polymerization
L2MM	Hydrophilic polyurethane additive
LiCl	Lithium chloride
LMH	Lm ⁻² h ⁻¹
LMH/bar	Lm ⁻² h ⁻¹ bar ⁻¹
MB/D	Million barrels per day
MF	Microfiltration
MWCO	Molecular weight cut-off
NF	Nanofiltration
NIPS	Non-solvent induced phase separation
NMMO	N-methylmorpholine-N-oxide
NMP	1-methyl-2-pyrrolidone
NOM	Natural organic matter

NPs	Nanoparticles
NTU	Nephelometric Turbidity Unit
O/W	Oil in water
OSPAR	Convention for Protection of the Marine Environment of the North-East Atlantic
PAN	Polyacrylonitrile
PBI	Poly[2,2'-(m-phenylene)-5,5'-dibenzimidazole]
PEG	Polyethylene glycol
PEGDE	Poly(ethylene glycol) diglycidyl ether
PES	Polyethersulfone
PET	Polyethylene terephthalate
PI	Polyimide
PPM	Parts per million
PPM	Polypropylene
PRO	Pressure retarded osmosis
PSU	Polysulfone
PTFE	Polytetrafluoroethylene
PVA	Poly vinyl alcohol
PVDF	Polyvinylidene fluoride
RO	Reverse osmosis
SDBS	Sodium dodecylbenzylsulfonate
SiC	Silicon carbide
SiO ₂	Silicon dioxide
SRHA	Suwanee River Humic Acid
SS	Suspended solids
TEM	Transmission Electron Microscopy
TiO	Titanium (II) oxide
TiO ₂	Titanium (IV) oxide
TIPS	Thermally induced phase separation
TMP	Trans-membrane pressure
Tween 80	Polysorbate® 80
UF	Ultrafiltration
USEPA	United States Environmental Protection Agency
UV-VIS	Ultraviolet-visible spectroscopy
WHO	World Health Organization
ZnO	Zirconium (II) oxide
ZrO ₂	Zirconium (IV) oxide
γ - globulin	Gamma globulin

LIST OF SYMBOLS

A	Membrane area (m^2)
K_c	Coefficient for cake filtration
K_b	Coefficient for complete blocking
K_i	Coefficient for intermediate blocking
K_s	Coefficient for standard blocking
V	Cumulative permeate volume (L)
t	Filtration time (s)
DR	Flux decay ratio (%)
FRR	Flux recovery ratio (%)
J_0	Initial permeate flux ($\text{Lm}^{-2}\text{h}^{-1}\text{bar}^{-1}$)
J_p	Produced water permeance ($\text{Lm}^{-2}\text{h}^{-1}\text{bar}^{-1}$)
J_{wi}	Pure water permeance ($\text{Lm}^{-2}\text{h}^{-1}\text{bar}^{-1}$)
J_{wc}	Recovered water permeance ($\text{Lm}^{-2}\text{h}^{-1}\text{bar}^{-1}$)
R	Rejection (%)
C_f	Solute concentration in the feed (mg/L)
C_p	Solute concentration in the permeate (mg/L)

LIST OF FIGURES

Figure 1. Fouling mechanisms	34
Figure 2. Cellulose structure with reducing and non-reducing end along with repeating anhydroglucose unit (adapted from reference ¹⁰³)	44
Figure 3. Inter and intra-molecular hydrogen bonds formed in cellulose (adapted from reference ¹⁰³)	45
Figure 4. Classification of cellulose solvents suitable as medium for chemical functionalization reactions (adapted from reference ¹¹¹)	47
Figure 5. Flat sheet membrane machine at KAUST	62
Figure 6. Cross-flow set-up	68
Figure 7. Dead-end set-up	69
Figure 8. Cross-flow experiment. Legend: (1) Feed tank; (2) Thermostatic bath (if needed); (3) Gear pump; (4) Membrane module; (5) Pressure gauge; (6) Valve; (7) Retentate return; (8) Permeate collection with electronic balance and (9) Computer for data collection.	73
Figure 9. FTIR spectra of non-modified microcrystalline cellulose (black), TMS-cellulose (blue) and regenerated cellulose (red); inset: expanded spectra at low wavelength range.	77
Figure 10. NMR ¹ H spectrum of trimethylsilyl cellulose (silylated cellulose).	78
Figure 11. Surface FESEM image and X-ray diffractograms of (a) dry polyacrylonitrile porous membrane coated with 1 wt% silylated cellulose in THF, followed by regeneration with acid treatment; X-Ray diffractograms of (b) unmodified cellulose and (c) regenerated cellulose.	80
Figure 12. PEG rejections of cellulose membranes prepared by coating with different concentrations of silylated cellulose on PAN porous supports, followed by regeneration with acid solutions: (a) cellulose coating and (b) cellulose coating with polyamide layer.	82
Figure 13. Surface (FESEM image) of a dry (a) PAN porous membranes and (b, c) the same membrane coated with polyamide by interfacial polymerization: (b) dry and (c) cryo images of wet membranes.	83
Figure 14. Surface (FESEM image) of (a) PVDF porous membranes and (b, c) the same membrane coated with polyamide by interfacial polymerization: (b) dry and (c) cryo images of wet polyamide/PVDF membrane.	84
Figure 15. FESEM images of membranes prepared by interfacial polymerization on asymmetric porous polyacrylonitrile supports coated with 1 wt% regenerated cellulose: (a) cross section and (b, c, d) surface images of (a, b) dry and (c, d) cryo wet membranes.	86
Figure 16. Thin polyamide layer formed by interfacial polymerization on supports of different porosities: (a) PAN, (b) PVDF and (c) cellulose coating on porous PAN. Membrane soaked in diamine aqueous solution (yellow) in contact to trimesoyl chloride organic solution (green). Right: Probable water permeation path. (Adapted from reference ¹⁵⁸)	87
Figure 17. Cross section (FESEM) images of membranes prepared from (a) 2, (b) 5 and (c) 10 wt % cellulose solutions in [C2mim]OAc by casting on polysulfone asymmetric porous supports and immersion in water.	91

Figure 18. X-Ray diffractogram of cellulose after dissolution in [C2mim]OAc and immersion in water; inset: AFM and FESEM images of coating surfaces prepared with 5 wt % cellulose/[C2mim]OAc solution.	92
Figure 19. PEG rejections of cellulose membranes prepared from solution in [C2mim]OAc coated on PSU and PEI porous supports or directly on polyester nonwoven.	94
Figure 20. A) BSA solution permeance (1 gL ⁻¹) for membranes prepared from 2 %, 5 %, 10 % and 14 % cellulose/ionic liquid solutions. B) Flux recovery and BSA permeance for 2 wt % and control PSU membrane.	98
Figure 21. Humic acid structure (adapted from ¹⁷²)	99
Figure 22. Pure water permeance and water permeance in the presence of humic acid for membranes prepared from 2, 5 and 10 wt. % cellulose solutions.	100
Figure 23. Water permeance in the presence of humic acids for commercial PVDF and PSU membranes as well as PSU membranes prepared in our lab (control).	101
Figure 24. Pure water permeance and water permeance with humic acid for a membrane prepared from a 1 wt % cellulose solution	102
Figure 25. Oil-water filtration experiment	106
Figure 26. Three surfactants used in the experiment: (a) sodium dodecylbenzenesulfonyl (SDBS); (b) hexadecyltrimethylammonium bromide (CTAB) and (c) Polysorbate 80 (Tween 80) ¹⁷⁵	107
Figure 27. (a) Zeta potential of a membrane prepared from 2 wt % cellulose solution, measured with water at different pH values and (b) Zeta potential of surfactant-oil droplets in water for an emulsion containing 200 ppm crude oil and 20 ppm SDBS, CTAB and Tween.	110
Figure 28. Zeta potential	110
Figure 29. CTAB-oil droplet at low pH	112
Figure 30. SDBS-oil droplet at high pH	113
Figure 31. Flux recovery ratio for filtration of emulsions with SDBS, CTAB and Tween through 5 wt % cellulose membrane.	114
Figure 32. Emulsion permeance through 5 wt % cellulose membranes containing SDBS, CTAB and Tween and 200, 500 and 1000 ppm of crude oil at pH 8.	115
Figure 33. Emulsion permeance through 5 wt % cellulose membrane, containing SDBS, CTAB and Tween and 200, 500 and 1000 ppm of crude oil at pH 4 and pH 11.	116
Figure 34. Pure water permeance, emulsion permeance and recovered water permeance for PSU and membranes prepared from 2 wt %, 5 wt % solutions with 200 ppm crude oil and 20 ppm SDBS at pH 8. Inset: rinsed membranes after filtration.	119
Figure 35. TEM images of membrane cross sections after filtration of oil-water emulsions containing 200 ppm of crude oil and SDBS at pH 8. A 2 wt % cellulose membrane is shown on the left side and polysulfone is shown on the right.	120
Figure 36. Feed (a), retentate (b) and permeate (c) for emulsions with 200 ppm, 500 ppm and 1000 ppm oil with SDBS at pH 8 filtered through 2 wt % cellulose membranes.	121
Figure 37. Real produced water permeance with time using membranes prepared from 2, 5 and 10 wt % cellulose solutions in ionic liquid.	123

Figure 38. Real produced water permeance with time for unmodified PSU membrane.....	124
Figure 39. Recovery of ionic liquid by (a) membrane process and (b) distillation process.....	128

LIST OF SCHEMES

Scheme 1. Schematic representation of cellulose and 1-ethyl-3-methylimidazolium acetate [C2mim]OAc covalent binding.....	123
Scheme 2. Silylation and regeneration of cellulose.....	74

LIST OF TABLES

Table 1. Contact angle of investigated membranes.....	79
Table 2. Cellulose diffractogram and polymorphs.....	81
Table 3. Performance of membranes prepared from silylated cellulose/THF solution on PAN porous support, followed by regeneration in acid.	82
Table 4. Water permeance of membranes constituted by layers of interfacial polymerized polyamide on regenerated cellulose and on PAN porous support.	88
Table 5. Water permeance and solute rejection for multilayer membranes prepared from Cellulose/[C2mim]OAc.....	93
Table 6. Pure water permeance and rejection for BSA and gamma globulin for 2 %, 5 %, 10 % and 14 % cellulose/ionic liquid membranes	98
Table 7. Droplet size and zeta potential of 200 ppm oil in water emulsion with SDBS at pH 4, 8 and 11.	108
Table 8. Droplet size and zeta potential of 200 ppm oil in water emulsion with CTAB at pH 4, 8 and 11.	108
Table 9. Droplet size and zeta potential of 200 ppm oil in water emulsion with Tween 80 at pH 4, 8 and 11.	108
Table 10. Feed, retentate and permeate concentrations for emulsions with 200, 500 and 1000 ppm oil with SDBS at pH 8 for 2 wt % cellulose membrane.....	122

1. Motivation

Since the 1960s with the introduction of Loeb-Sourirajan asymmetric cellulose-acetate (CA) membranes, membrane research and application had an exceptional growth. Reverse osmosis (RO) dominates as water desalination technology, providing clean drinking water for vast population living in places, where freshwater is scarce. In addition, nanofiltration (NF) and ultrafiltration (UF) membranes, capable of removing suspended solids, bacteria and viruses along with nanofiltration resistance towards divalent salts are used as RO pretreatment. Membranes have been implemented in dairy, beverage, and textile industry along with pharmaceutical and oil industry.

For the last 50 years, scientists are trying to obtain a perfect membrane with properties close to 100 % rejection, no flux decline, no fouling, indefinite operability and reduced cost. The success in one characteristic means however collateral damage in another. RO membranes are capable of rejection of more than 99 % of monovalent salts, maintaining high flux, but with high pressure requiring a lot of energy. NF and MF membranes have higher fluxes and don't require high pressures but they cannot provide drinking water quality.

In order to achieve higher fluxes and improve selectivity, membrane surface should be tailored in a way that fits our desired characteristic. Hydrophilic membranes promote water transport, as well as decreased foulant attachment. Hydrophobic

membranes, preferably used for gas separation are also used for solvent filtration and membrane distillation.

The hydrophilicity/hydrophobicity of the solute to be rejected will affect the decision on the type of the membrane needed.

Cellulose membrane prepared with ionic liquid combines the most abundant natural material, dissolved in one of the least toxic solvents. The membranes are smooth, hydrophilic and dense, plentiful of OH groups on the surface contributing to hydrophilicity as well as negativity. This type of surface allows fast water transport i.e. the water permeability yet rejecting the foulants.

Due to vast amount of hydrogen bonds cellulose is insoluble in water and majority of organic solvents, leaving only a handful of solvents capable of disrupting the hydrogen bonds. These solvents are predominantly toxic and include several additional steps in synthesis to get to the final cellulose.

Imidazolium based ionic liquid with acetate anion is listed as the least toxic among other ionic liquids. It dissolves cellulose in one-step process and yields a membrane via phase inversion. The membrane exhibited high permeance and good resistivity towards the foulants, showing steady flux during long-term experiment with humics and 100 % oil in water separation.

Conditions under which separation takes place influence the efficiency of rejection. Feed water characteristics, membrane surface and operational conditions impact the rejection trend. Foulant-foulant and membrane-foulant interactions as well as their charge interplay shape the ability of membrane to reject or adsorb a certain

foulant. During seawater or brackish water filtration together with humics there are other organics such as biopolymers and proteins and inorganic substances e.g. monovalent and divalent salts that improve or deteriorate rejection.

In the oil and gas industry process, water is injected into the oil well in order to increase the pressure and stimulate oil production. This is referred as water flooding. The water that comes out of the well is called produced water and it is initially seawater or brackish water with high salinity. Besides high salt concentration produced water also contains different hydrocarbons and heavy metals picked up on the way out of the well. The composition of crude oil and the well and therefore produced water depends on the age of crude oil, well location and soil composition. Different separation methods are used with different efficiency. Even after partial oil removal, additional separation steps can be required, depending on the target application.

In many applications, not only in the petrochemical industry, oil-in-water emulsions have an important role. They are commonly stabilized by the addition of surfactants, which reduce interfacial tension between the oil and water.

Various salts and additives found in the produced water affect the removal efficiency of the membrane. The pH of the solution controls the charge of the ions and solutes in the solution and on the membrane surface. Protonation and deprotonation might occur both between foulant-foulant and membrane-foulant interfaces.

Improved oil separation with relatively steady permeability using membrane technology increase the water quality and the amount of water that can be reused for agricultural and livestock purposes, as well as for further treatment. Complete oil removal with only salt can be treated with RO membrane and achieve even drinking water quality.

Understanding the role of surfactants, salt and pH on membrane selectivity can shape future experiment and help improve the separation.

1.1. Objective

The overall objective of this work was to prepare membranes from pristine cellulose using reduced number of steps and more environmentally friendly solvents and/or proposing new methods for cellulose thin coatings. The membranes should be resistant to fouling with reasonable permeability and efficient selectivity.

2. Introduction

Water scarcity and access to clean water are major problems worldwide, directly affecting around 1.2 billion people, one-fifth of the world's population.¹ While seawater desalination has been an indispensable strategy in the Middle East as a source of drinking water, water treatment is essential everywhere in the world to assure sustainable life quality with high environmental standards. This includes treating municipal and agriculture wastes and recycling industrial effluents. Increasing need for safe drinking water, purification of effluents with small pollutant molecules and recovery of valuable products has placed membrane separation processes such as nanofiltration (NF) among the fastest growing technologies. The global membrane-based technology market for the treatment of industrial water and wastewater has been estimated to reach \$5.5 billion in 2015, driven by different applications and motivations in different continents.² With economic growth, many countries are facing an enormous challenge of water pollution. For example, 55% of the groundwater in China has been reported to have poor water quality, while 78% of urban rivers are polluted to an extent that they might not serve as drinking water source anymore.^{3,4} In European countries, which have been intensively fighting to reach high level of water quality, wastewater treatment has satisfactorily reduced the content of regular pollutants, but there is an increasing concern with emerging new pollutants such as endocrine disrupters. Besides environmental aspects, water reuse might become mandatory to bring

water autonomy to desert areas in the Middle East far from the coast and therefore with restrict access to seawater. Water availability has also been a question of security and a reason for potential conflict in many countries. Membrane technology is recognized as energy efficient, easy to scale-up and environmentally friendly, with large perspective of expanding its application with the growing need of implementing more sustainable industrial processes. Membranes have been optimized with selectivity/permeation characteristics useful for quite diverse separation tasks. However the membrane manufacture itself could be much more sustainable and greener than it is now.^{5, 6}

2.1 Currently Available Membranes for Ultra- and Nanofiltration: Advantages and Drawbacks

For more sustainable membrane manufacture two aspects have to be taken into consideration: (i) the membrane material and (ii) the manufacture process. Most membrane materials are produced from petrochemical sources. The most applied membrane manufacture process involves non-solvent induced phase separation (NIPS), solution casting followed by immersion in water. Large amount of solvents like N,N-dimethylformamide (DMF), N,N-dimethylacetamide (DMAc) or 1-methyl-2-pyrrolidone (NMP) are frequently used for phase inversion. Furthermore membranes are frequently prepared as multilayers, with the asymmetric porous support being only the substrate, which is coated by additional solutions, constituted also by solvents, which are environmentally harmful. There is an

increasing discussion on the possibility of banning their application in large scale and the need for finding alternatives at least for part of the manufacture processes.

The need for the highest possible rejection and least permeability decline is higher than ever. Increase in human population and need for industry has made a huge impact on the amount of drinking water available for all the people. Desalination and wastewater treatment by membrane technology is capable of removing more than 99 % of total suspended and dissolved solids including everything from big macromolecules to smallest ions of salt, providing fresh and clean water for millions of people. Increased amount of places coping with water scarcity increased the need for faster and more efficient water treatment. Membranes need to deliver desalted and disinfected water fast in larger amounts. When designing a membrane two main characteristics need to be satisfied, high permeability and high solute rejection. Besides that, membranes should have mechanical, chemical and thermal stability as well as antifouling property and endurance.

To achieve this several factors should be taken into consideration; membrane material and process, method of operation and operational cost, module of operation and possibility of scaling-up, overall cost of maintenance, operations, cleaning and replacement.

Membrane material and fabrication are the main point of interest since the performance of the membrane solely depends on membrane physical and chemical properties, surface characteristics and pores size.

Nanofiltration and ultrafiltration membranes have pore sizes between 0.001 μm – 0.01 μm and 0.01 μm – 0.1 μm , respectively. UF membranes are often used in food and beverage industry, wastewater treatment and removal of proteins, viruses and bacteria while NF is most often used for water softening since they are capable of removing divalent salts. Both NF and UF are used in a desalination plant as a pretreatment and increasing the lifespan of RO membranes by rejecting bigger ions, molecules and macromolecules hence allowing only monovalent salts to pass.

2.1.1. Inorganic Ultrafiltration Membranes

Inorganic material has promising chemical and thermal stability but membranes are quite fragile and challenging to manage, overall cost is too high and scaling-up is restricted at this point. Nevertheless, inorganic material such as Al_2O_3 , TiO_2 , ZrO_2 , ZnO , and SiO_2 nanocrystals, composites $\text{TiO}_2\text{-SiO}_2$, $\text{TiO}_2\text{-ZrO}_2$, and $\text{Al}_2\text{O}_3\text{-SiC}$, nanocomposites (Ag-TiO_2 , Zn-CeO_2 , and zeolites) as well as ceramics (TiO_2 and TiO_2 -composites) have been extensively studied.

The most exploited material in ceramic membrane application is photocatalytic TiO_2 where charge separation is induced by light i.e. photons. Most favorable application of TiO_2 is disinfection, specifically *E. coli*⁷⁻⁹ and removal of organic pollutants mainly dyes and humics.¹⁰⁻¹⁴ Efficiency of TiO_2 membrane is evaluated by degradation rate of the pollutants and membrane permeability.

Katsaros et al. (2012)¹⁵ reported $20 \text{ Lm}^{-2}\text{h}^{-1}\text{bar}^{-1}$ and successful decomposition of azo-dye via TiO_2 photocatalysis. Liu and Sun et al. (2012)⁹ investigated bacteria inactivation and dye degradation via Ag/TiO_2 nanofiber UF membrane and reported 99.9 % and 80.0 %, respectively, with $5\text{-}20 \text{ Lm}^{-2}\text{h}^{-1}$ at 1-4 bar. Zhang and Sun et al. (2009)⁸ used multifunctional TiO_2 nanowire UF membrane for water treatment where they reported membrane exhibits both anti-fouling and anti-bacterial behavior with reported permeability of $12.2 \text{ Lm}^{-2}\text{h}^{-1}\text{bar}^{-1}$. Zhang and Sun et al. (2008)¹⁰ grafted multifunctional TiO_2 nanotube into MF membrane via liquid-phase deposition, yielding a UF membrane with photodegradation of humic acid via photocatalytic activity with reported permeability of $15\text{-}33 \text{ Lm}^{-2}\text{h}^{-1}$ at 0.5-2 bar.

Besides most commonly used material TiO_2 , Al_2O_3 and SiC are gaining more interest. Boffa et al. (2014)¹⁶ prepared a nearly defect free SiC UF membrane on SiC support via extensive organic synthesis for UF applications. The reported permeability was $0.05\text{-}0.06 \text{ Lm}^{-2}\text{h}^{-1}\text{bar}^{-1}$ and polyethylene glycol (PEG) (100 kDa) retention 93 %. The same group prepared $\text{Al}_2\text{O}_3/\text{SiC}$ UF membrane, where commercially available SiC tubes were used as carrier for Al_2O_3 UF membrane. The membrane showed high permeability ranging from 10 to 3000 $\text{Lm}^{-2}\text{h}^{-1}$ at 10 bars and PEG (8 and 35 kDa) retention of approximately 75 %.

Incorporation of nanoparticles into inorganic material for water treatment and remediation is an attractive technique due to the known antimicrobial activity. Some nanoparticles, such as silver and copper can promote disinfection (waterborne pathogens). Others have degradation capability via photocatalysis.¹⁷⁻²⁶

Matsuyama et al. (2014)²⁷ prepared a stacked UF membrane comprised of silver nanoparticle layers using layer-by-layer deposition with molecular weight cut-off (MWCO) of 500 kDa (dextran).

2.1.2. Inorganic Nanofiltration Membranes

Graphene based materials incorporated in membranes for water treatment and purification are a blistering topic in the membrane technology for water treatment applications mainly due to the high permeability. Out of the graphene based material family, graphene oxide (GO) is the most used one, most likely because of availability and relatively low cost. Desirable characteristics of graphene and graphene based materials are hydrophilicity, which enhances the water transport desired for nanofiltration membranes with good selectivity, mechanical stability which gives them robustness and tunable nanopores for implementation in different applications. Mi and Hu (2013)²⁸ were one of the first to report a 4-10 times higher permeability ($80\text{-}276 \text{ Lm}^{-2}\text{h}^{-1}$ at 10 bars) than conventional NF membranes, using cross-linked GO membrane prepared via layer-by-layer process. Xu et al. (2013)²⁹ prepared inorganic NF membranes using ultrathin sheets of chemically converted graphene for water purification. Membranes showed high retention for organic dyes (99 %) and intermediate retention of ion salts (20-60 %) whilst having high pure water permeance ($21.8 \text{ Lm}^{-2}\text{h}^{-1}\text{bar}^{-1}$). Graphene-oxide membranes are being investigated by different groups, targeting desalination with the expectation of exceptional high water permeance.³⁰⁻³²

Together with graphene, carbon-nanotubes became interesting material in the field of membrane technology due to their mechanical strength, relatively low cost and potential antimicrobial property quite desirable in water purification field.³³⁻³⁶ But the main reason to explore carbon nanotubes for membranes is the advantage of lack of friction for water transport, which could lead to extremely high fluxes. Yoon et al. (2014)³⁴ prepared vertically aligned carbon-nanotubes exhibiting three times higher water permeance compared to conventional membranes with 2 log less bacterial adhesion.

Although quite attractive, the preparation of inorganic membranes requires very complex and extensive methods such as water-assisted thermal chemical vapor deposition method³⁴, hydroiodic acid vapor and water-assisted delamination³⁰, drop casting, spraying or spin coating, Langmuir-Blodgett method and vacuum filtration³⁷ for carbon based membranes, electrostatic interaction of polyelectrolyte-stabilized nanoparticles (NPs) with layer-by-layer deposition for inorganic nanoparticles²⁷, grafting and liquid-phase deposition¹⁰, alkaline hydrothermal synthesis, followed by a filtration and hot-press process⁸, polyol synthesis⁹ for TiO₂ incorporation and pyrolysis of allylhydrido polycarbosilane in the presence of submicron α -SiC particles for SiC-SiC deposition. These techniques require harsh chemicals and even with some low cost material, there is still great limitation of scale-up processes.

2.1.3. Organic Ultrafiltration Membranes

Although inorganic membranes are receiving more and more attention in recent years, polymeric membranes are irreplaceable at this moment when it comes to large industrial applications and water treatment. Different polymers and methods of preparation can tune the pore size, structure and properties. Techniques such as grafting and cross-linking provide control characteristics and desired properties. Most commonly used polymers for organic membrane fabrication are polysulfone (PSU)³⁸, polyethersulfone (PES)³⁹, polyvinylidene fluoride (PVDF)^{40, 41}, polyacrylonitrile (PAN)^{42, 43}, polytetrafluoroethylene (PTFE), polyimide (PI), polypropylene (PP), poly vinyl alcohol (PVA) and cellulose acetate and cellulose nitrates.⁴⁴⁻⁴⁶

Polysulfone and polyethersulfone are most common polymers in membrane fabrication. Different approaches have been used to improve even more the performance of polysulfone-based membranes. Some examples are mentioned here. Polysulfone blended with poly[2,2'-(m-phenylene)-5,5'-dibenzimidazole] (PBI) showed increased permeability ($355 \text{ Lm}^{-2} \text{ h}^{-1}$) and higher BSA rejection (69 %), when compared to pristine polysulfone ($228 \text{ Lm}^{-2} \text{ h}^{-1}$ and 36 %), respectively.⁴⁷ Xie et al. (2015) functionalized polysulfone with triazole ring via click chemistry to improve anti-fouling property of UF membrane.⁴⁸

Other additives such as poly (ethylene glycol methyl ether) are used for enhancing the hydrophilicity of polysulfone membranes.⁴⁹ Derlon et al. (2014)⁵⁰ studied gravity-driven UF membranes that require very low pressure. They stated that

presence of thin and young biofilm on the membrane surface improved the quality of permeate although further filtration will cause accumulation of organic matter triggering permeate deterioration.

For enhancement of polyethersulfone hydrophilicity various additives (hydrophilic, amphiphilic and inorganic), surface functionalization (carboxyl, sulfonated and PEG functional groups), surface grafting techniques, coating methods, chemical treatments and polymer blends were investigated for membrane functionalization in order to increase the permeability.³⁹

Blend of polyimide and microporous polyethersulfone submitted to atomic layer deposition (ALD) was investigated for the purpose of enhancing the selectivity by tuning the surface morphology. Rejection increased with increasing number of ALD cycles.⁵¹

Cellulose-acetate nanofibers prepared via freeze-extraction with permeance of $3540 \text{ L m}^{-2} \text{ h}^{-1} \text{ bar}^{-1}$ showed ferritin rejection of 90.7 %.⁴⁶ Hollow fiber membranes prepared from cellulose acetate derivatives cellulose acetate butyrate (CAB) and cellulose acetate propionate (CAP) via thermally induced phase separation (TIPS) method showed good anti-fouling property towards BSA and humic acid.⁴⁵

Hydrophilic polyurethane additive, known as L2MM, was added to PVDF membrane during phase inversion process. Two types of additives, L2MM(PEG-600) and L2MM(PEG-200) were used and the reported permeance was six times higher than that of pristine PVDF membranes.⁵² Another type of additive, nano-chitin whisker

was added as the reinforcement tool via non-solvent induced phase separation process to the PVDF membrane in order to impart fouling.⁵³

By grafting 2-hydroxyethyl-methacrylate (HEMA) on the top of polyethylene terephthalate (PET) membrane, a pH-responsive membrane was obtained via atom transfer radical polymerization (ATRP). The results showed that the grafted membranes reveal pH-response permeation towards environmental solutions.⁵⁴

2.1.4. Organic Nanofiltration Membranes

For improved removal of cadmium (98 %), polysulfone membrane was modified by addition of amphiphilic IGEPAL in a PSU/IGEPAL/NMP system via immersion precipitation process. IGEPAL CA-630 is a nonionic, non-denaturing detergent. Its official IUPAC name is octylphenoxy polyethoxy ethanol and it is a registered trademark of Rhodia. Reported permeability reached maximum $70 \text{ Lm}^{-2}\text{h}^{-1}$ at 10 bars.³⁸

To improve fouling resistance on RO and NF membranes, poly(ethylene glycol) diglycidyl ether (PEGDE) was grafted to surface of commercial RO (XLE) and NF (NF90). Modified membranes exhibited better resistance to fouling when compared to pristine, non-grafted membranes, although further addition of poly(ethylene glycol) diglycidyl ether (PEGDE) didn't continue to improve the membrane performance.⁵⁵

2.1.5. Block Copolymer Membranes

Block copolymer membranes have high porosity together with narrow tunable pore-size distribution, with high permeability and tailored selectivity. Self-assembly of copolymers lead cylindrical pore morphology with governable surface characteristics and chemistry.⁵⁶⁻⁵⁸

Future trends in membrane technology have to focus on developing new membrane material and solvents that have desired surface properties for longer durability and fouling resistance. Fabrication and membrane processing should include less operational steps with decreased usage of harsh chemicals.

One of the main motivations of this work is to substitute at least part of the solvents used in the multilayer membrane manufacture by greener alternatives. We propose the production of membranes based on natural cellulosic materials, in which ionic liquid is employed for coatings. One-step cellulose dissolution in ionic liquid is a fast process capable of replacing extensive cellulose dissolutions processes. The natural abundance of cellulose is attractive. The large amount of OH groups contributes to hydrophilicity, which provides high permeability and good fouling resistance.

2.2. Fouling

Membrane efficiency is mainly measured in terms of water permeance and solute selectivity. The lower the pressure the less energy does the process require. All types of membranes will eventually lose its initial permeance and filtration rate will

decrease with time. To maintain steady permeance, trans-membrane pressure has to increase.

Flux reduction with time by accumulation of solutes, particles and colloids near the membrane surface, which may lead to adsorption or deposition, is known as fouling. If the system operates under constant trans-membrane pressure, the permeance will decline with time, whilst operating under constant permeance the trans-membrane pressure will increase to maintain the same conditions. One of the biggest nemeses of the membranes overall is fouling.⁵⁹

Fouling decreases the membrane productivity, due to the accumulation of particles of different origin on the membrane. Less productivity means permeate with poor quality, more energy consumption and overall increase of plant operation cost. Membranes have to be replaced more often or backwash has to be implemented more frequently. In general, fouling causes severe financial and industrial losses so it is necessary to reduce it. Fouling can be caused by organic (rigid and flexible biopolymers, fulvic and humic compounds) and inorganic scaling (silica, minerals etc.) compounds.⁶⁰

Organic compounds responsible for organic fouling are referred to as natural organic matter (NOM) and they are classified as humic and non-humic substances and can be found in surface water and ground water as well as soil (humics). Humics are high molecular weight substances that can be of aquatic or terrestrial origin. Concentration of humics in the Red Sea water is 0.389 mgL^{-1} and 0.671 mgL^{-1} in the Arabian Sea water, representing 51.2 % and 39.4 % of total dissolved organic

carbon. For comparison, biopolymers represent 11.7 % and 12.6 % of total dissolved organic carbon in the Red Sea water and Arabian Sea water, respectively.⁶¹

Aquatic humics have lower molecular weight than the accompanying terrestrial ones, they are more difficult to remove and present dominant foulant. Presence of divalent salt cations such as Ca^{2+} and Mg^{2+} increase fouling rate due to the bridge formed between the cation-humic-membrane surfaces.

Non-humic NOM foulants are proteins, polysaccharides, sugars and polyoxyaromatics.

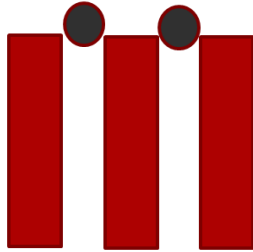
In order to find the appropriate solution for the fouling problem, the understanding of the foulant-foulant as well as foulant-surface interactions has to take place.

Fouling can be classified as reversible and irreversible, backwashable and non-backwashable. Reversible fouling is due to the complete pore blockage, partial pore blockage and cake filtration whilst irreversible fouling is due to the internal pore blockage and adsorption of foulants onto the membrane surface.⁶² Non-backwashable fouling cannot be removed with hydraulic backwash but it can be removed by chemical cleaning. On the other hand, irreversible fouling cannot be completely removed with chemical cleaning or any other method (backwash, flushing, wiping) and membrane will not recover its original permeance.⁵⁹

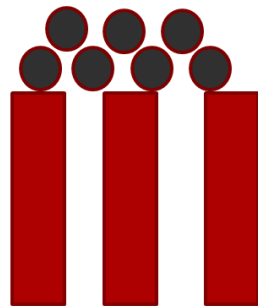
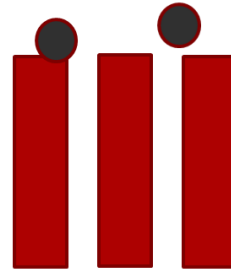
Several factors cause fouling; the composition of feed (type of foulant used, pH, ionic strength, and concentration), hydrodynamic conditions (permeance, cross-flow speed etc.) and membrane properties such as roughness, charge, functional groups

and hydrophilicity.⁶⁰ Fouling takes place either due to the cake formation and/or pore blockage (Figure 1).

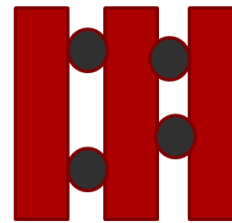
a) Complete blockage



b) Partial blockage



c) Cake filtration



d) Internal blockage

Figure 1. Fouling mechanisms

To quantify the extent of fouling, flux recovery ratio, and total flux loss were calculated based on following equations;

Flux recovery ratio;

$$FRR = \left(\frac{J_{wc}}{J_{wi}} \right) \times 100 \% \quad (1)$$

Flux decay ratio;

$$DR = \frac{(J_{wi} - J_p)}{J_{wi}} \times 100 \% \quad (2)$$

where J_{wi} is the initial pure water permeance, J_p is permeance measured with a solution, which might include potential foulants, and J_{wc} is the pure water permeance after rinsing the membranes and measuring J_p , respectively.

Reversible fouling is not a threat as big as irreversible fouling, because the foulants can be mechanically removed by hydraulic backwash. Irreversible fouling cannot be mechanically or chemically removed, the membrane needs to be either replaced or operate under diminished efficiency.

As mentioned before, several factors affect the rate of fouling. Foulant-foulant and membrane-foulant electrostatic and hydrophobic interactions are the main reason for adsorption or lack of it. Further understanding of both behaviors could give a valuable insight prior to usage of membrane for under fouling conditions.

Besides fouling, concentration polarization causes decrease in permeance. Concentration polarization represents the occurrence of higher concentration of solutes near the liquid-membranes interface causing higher osmotic pressure and

decreased permeance. Concentration polarization can be removed with backwash. Fouling presents deposition of foulants onto the membrane surface. In case of adsorption and internal pore blockage, irreversible fouling takes place and foulants cannot be removed neither by backwash or chemical cleaning. Concentration polarization can promote fouling by increasing foulant concentration during longer period of time.⁶⁰

If a foulant cake layer is formed on the surface, it becomes more hydrophobic and therefore, oil droplets can penetrate, decreasing the rejection in oil-water separations.⁶³

Pressure can cause an increase in cake layer formation, which results in oil droplets not being able to penetrate through the thick layer, therefore increasing the rejection. If the feed contains suspended and colloidal particles of different sizes, a secondary layer might form, reducing the flux and increasing the rejection.

For understanding the mechanism of fouling the influence of pH is of a great meaning to elucidate charge related characteristics. Over wide range of pH, membrane functional group tend to protonate and deprotonate which will result in different membrane charge and surface zeta potential. Solute rejection and water permeance will depend on the membrane-solute charge and zeta potential either by causing electrostatic repulsion or attraction. Besides membrane functional groups, varying pH will also cause changes within the solute ions in the solution as well.⁶⁴⁻⁶⁶

The laws and regulations regarding the oil and gas effluent quality are becoming stricter therefore increasing the need for membranes with desirable separation

without severe permeance loss, as well as with high stability and durability. In Australia, permitted oil and gas limit for offshore effluent is 30 ppm daily or 50 ppm instantaneous.⁶⁷ In China the maximum monthly average limit of oil and gas effluent is 10 ppm while chemical oxygen demand (COD) limit is 100 ppm.⁶⁸ According to the Convention for Protection of the Marine Environment of the North-East Atlantic (OSPAR), annual average limit of the amount of dispersed oil in produced water allows discharges in the sea up to 40 ppm.⁶⁹ According to United States Environmental Protection Agency (USEPA), the maximum limit for oil and gas effluent is 42 ppm (daily average), while the monthly average limit is 29 ppm⁷⁰ Based on World Health Organization (WHO), regarding the turbidity of the effluent, ideal turbidity when measured in Nephelometric Turbidity Unit (NTU) should be below 1 NTU or on average cases below 5 NTU.⁷¹ According to European Standards, total hydrocarbons in the oil and gas effluent should be lower than 10 ppm while oil concentration should be less than 5 ppm.⁷²

2.3. Oil-Water Separation

Oily wastewater is one of the biggest by-products of food industry, chemical and petrochemical industry and, in largest percentage, petroleum refineries. According to the International Energy Agency⁷³, for every barrel of crude oil produced, seven to ten barrels of water need to be treated. 97 million barrels per day were produced worldwide in late 2015, reaching 35 billion barrels per year globally. Predictions for 2016 as a whole, non-OPEC output is expected to decline by 0.6 million barrels per

day (mb/d), to 57.1 million barrels per day (mb/d), therefore there is an extreme need for produced water management and more efficient separation.

Oil in the water can be classified as floated or dispersed oil, where the oil droplets size is higher than 10 μm and they can be removed mechanically. Other cases might have oil droplets with size less than 10 μm . They are then classified as emulsified oil creating oil in water (O/W) emulsion.

2.3.1 Relevance and Different Available Processes

Emulsified oil is difficult to remove due to its small size by using common techniques such as physical treatment, chemical treatment and biological treatment.^{74,75} Gravity separation, flocculation, coagulation and air flotation are not effective in removing micron and submicron sized oil droplets in the emulsion.⁷⁶⁻⁷⁹

The EARTH Canada Corporation developed a technology called TORR™ that stands for Total Oil Remediation and Recovery. They use a multi-stage adsorption and separation system that has an adsorbent media, the polyurethane based Reusable Petroleum Adsorbent (RPA®), an oleophilic, hydrophobic, nontoxic, coalescing agent capable of removing and recovering oil droplets. The drawback of adsorption systems is cost and the need for frequent regeneration of materials and waste generation.⁸⁰

Hydrocyclone were first used to de-sand and de-oil wastewater. The hydrocyclone pretreated the raw produced water removing solids and oil content by 73% and

54%, respectively. Cyclones combine centrifugal forces and gas flotation to separate water, oil and gas.^{81, 82}

Membranes have become a powerful technology in oil in water separation due to the tailored pore sizes, applicable for wide range of oil droplets sizes ranging from 0.1-10 μm .⁸³ Hydrophobic membranes, including polysulfone, polyethersulfone, polyacrylonitrile can separate oil droplets from water, but with severe fouling.^{84, 85} Modification of surface making them more hydrophilic has become a trend with methods such as surface graft polymerization⁸⁶⁻⁸⁸, surface coating^{89, 90} and surface segregation.⁹¹⁻⁹⁴ These techniques have been performed on hydrophobic and hydrophilic membranes, as well as ceramic. However, they require additional steps which increasing cost and preparation time.

UF membranes are one of the most effective systems for oily wastewater treatment due to its low cost, small space requirements and no need for additives. Lia et al. (2006)⁹⁵ studied a tubular UF model equipped with polyvinylidene fluoride membranes modified by inorganic nano-sized aluminum particles to treat oilfield-produced water. Bilstad and Espedal et al. (1996)⁹⁶ compared MF and UF membranes in pilot trial to treat the North Sea oilfield-produced water. Results showed that UF, but not MF, could meet effluent standards for total hydrocarbons and dissolved constituents. By UF membrane treatment with molecular weight cut-off (MWCO) between 100,000 and 200,000 Da, the total hydrocarbon concentration could be reduced from 50 mg/L to 2 mg/L (96% removal). Benzene, toluene, and

xylene (BTX) were reduced by 54%, and some heavy metals like Cu, and Zn were removed to the extent of 95%.

Lee et al. (2005)⁹⁷ tested a hydrophilic UF membrane of 0.01- μm pore size, in crossflow mode, to treat oilfield-produced water. Oil and gas concentration after UF could be reduced to less than 2 mg/L. The preferred feed-water specifications for ideal performance of UF for oil and solids removal was less than 50 and 15 ppm, respectively.

Jiang et al. (2009)⁸³ stated that oil/water separation improved with cellulose grafted polyacrylonitrile membranes. They showed that the membranes could reject 100 % of high-speed vacuum pump oil using ultraviolet-visible spectroscopy (UV-VIS).

Li et al. (2006)⁹⁸ prepared hollow fiber membranes from cellulose/monohydrate N-methylmorpholine-N-oxide (NMMO \cdot H₂O)/polyethylene glycol (PEG 400) through the immersion precipitation technique. The membranes showed good antifouling properties but the permeability was relatively low, 7.67 L/(m² h) under an operation pressure of 0.1 MPa.

Ceramic membranes are interesting topic in membrane technology field and recently have more attention in the produced water industry.⁹⁹ Due to their inorganic composition they possess competitive mechanical and chemical stability, can withstand higher temperatures, high oil concentration and harsh cleaning agents.¹⁰⁰ Although they tolerate high temperatures, the expansion may cause problems with sealing between membrane and the housing.¹⁰¹ They are brittle, which makes it difficult to handle, they are quite expensive compared to polymeric

membranes and are challenging to scale up given the cost and currently available ratio of membrane area and permeability.

Chen et al. (1991)¹⁰² tested performance of ceramic crossflow MFs to separate oil, grease, and suspended solids from produced water. Permeate quality for dispersed oil and gas was 5 mg/L and for suspended solids was less than 1mg/L.

Tao and Ma et al. (2015)⁷⁴ investigated reversible and irreversible fouling on ceramic membranes. They stated that specification and type of the crude oil affect the droplet size and zeta potential which later affects the separation efficiency in the ceramic membrane test.

2.4 Cellulose

For the manufacture of multilayer membranes, by dip coating, a solvent is needed, which dissolves the coating polymer without damaging the substrate. The coating layer is usually responsible for the selectivity and the porous substrate, which is frequently made of polysulfone, poly(vinylidene fluoride) or polyacrylonitrile, improves the mechanical stability without compromising flux. Multilayer membranes have been successfully applied for gas separation, pervaporation, nanofiltration and reverse osmosis. However the application of cellulose coating for multilayer membranes has been hindered by the lack of solvent for cellulose, which would not damage the morphology of the porous polymeric support. Cellulose¹⁰³ is one of the most abundant natural materials and has been used as starting material

for membrane manufacture for long time. However cellulose can be hardly dissolved in common solvents due to strong hydrogen bonds and crystallinity. Chemically modified cellulose in the form of cellulose acetate has been successfully used in large scale for instance as reverse osmosis hollow fibers for seawater desalination or more recently as commercialized flat-sheet membrane for forward osmosis. However the use of cellulose itself has been restricted by the availability of industrial process for dissolution, which is currently done in aggressive medium, by chemical modification and regeneration.

2.4.1 Short History of Cellulose

Cellulose presents one of the most abundant, renewable polymer resources available today worldwide. It has been assessed that by photosynthesis, 10^{11} - 10^{12} tons are synthesized annually in the form of seed hairs of the cotton plant, although mostly cellulose is combined with lignin and hemicelluloses in the cell wall of woody plants.¹⁰⁴ Cellulose has been used for many centuries as a construction material, mainly in the form of intact wood and textile fibers such as cotton or rayon, or in the form of paper and board. Cellulose is an adaptable starting material for chemical conversions, for example in production of artificial threads and films as well as a variety of various derivatives used in several areas of both industry and everyday life.¹⁰⁵

Cellulose occupies a unique place in the annals of polymers. As early as 1838, Payen recognized cellulose as a ultimate substance and created the name cellulose.¹⁰⁶

Cellulose as a precursor for chemical modifications has been used even before its polymeric nature was recognized and well understood. Milestones on this pathway were the discovery of cellulose nitrate by Schönbein in 1846, the preparation of Schweizer's reagent, i.e., a cuprammonium hydroxide solution representing the first cellulose solvent¹⁰⁷ in 1857, and the synthesis of an organo-soluble cellulose acetate by Schützenberger in 1865.¹⁰⁸

The origin of cellulose chemistry as a branch of polymer research can be traced back to the fundamental experiments of H. Staudinger in the 1920s and 1930s on the acetylation and deacetylation of cellulose; these experiments resulted in the concept of polymer-analogous reactions.¹⁰⁹ According to this concept, functional groups of macromolecules; in the case of cellulose predominantly hydroxyl groups; can undergo the same kind of reactions as the corresponding low-molecular compounds. Further, it was observed that the supramolecular structure of the polymer may play an important role in determining the rate and final degree of conversion, as well as the distribution of the functional groups, which has been well recognized for cellulose. The scale of cellulose structure is ranging from few nanometers to several microns with tensile strength as high as Kevlar.¹¹⁰

Today, the evolution of analytical and synthetical instrumentation has paved the way for exploration of cellulose nanomaterials. Novel forms of cellulose materials are called cellulose whiskers, cellulose nanocrystals, microfibrilated cellulose, cellulose nanofibrils and nanofibers, cellulose crystallites and bacterial cellulose.

2.4.2. Cellulose Structure and Analysis

Cellulose is an abundant polymer consisting of the β -(1-4) glucose linkage with repeating D-glucopyranose units (anhydroglucose units (AGU)).¹⁰³ Besides the AGU units, the molecular structure of cellulose consists of non-reducing end group and reducing end group shown in Figure 2.

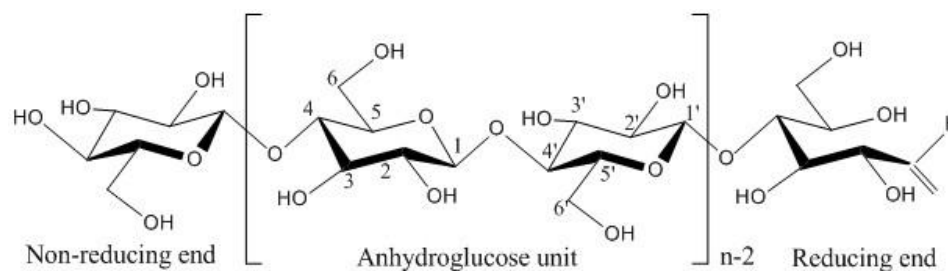


Figure 2. Cellulose structure with reducing and non-reducing end along with repeating anhydroglucose unit (adapted from reference¹⁰³)

The molecular structure of cellulose usually adopts the lowest free energy conformation, which results in cellulose's free hydroxyl groups, positioned on C-2, C-3 and C-6 atoms, in the equatorial plane, while the hydrogen atoms are positioned in the axial plane.¹⁰⁴ Hydrogen bond in the cellulose structure is the main reason of cellulose insolubility in water and most of the common solvents. Hydroxyl groups can also be further reacted, allowing easy grafting and growing of polymeric

segments from the surface, which could further decrease fouling or introduce specific groups to tailor selectivity.

Throughout the history of cellulose discovery and various modifications as well as implementations of the cellulose in different facets of industry, several efforts have been dedicated to enhance its solubility. But the main challenge, which has hindered the use of cellulose as coating for composite membranes, or for the preparation of membranes by phase inversion, remained its insolubility in most organic solvents.

Inter and intra-molecular hydrogen bonds of cellulose are the main of reason for cellulose insolubility. The hydrogen bonds are not easily broken, without compromising the supramolecular structure. The type of inter and intra-molecular hydrogen bonds formed in the cellulose are presented in Figure 3.

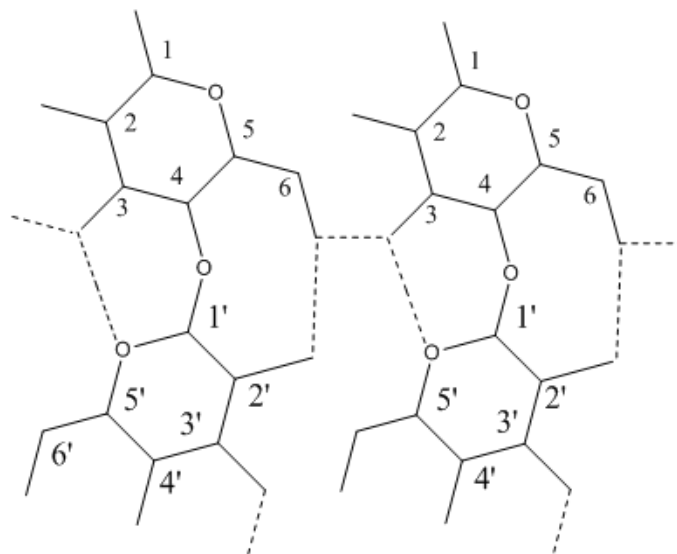


Figure 3. Inter and intra-molecular hydrogen bonds formed in cellulose (adapted from reference¹⁰³)

In the recent years great efforts are made to find rather “green” solubilization process.

2.4.3 Methods of Cellulose Solubilization and Processing

According to the literature, there are different pathways used in the past to achieve the solubilization of cellulose. Using a reaction to functionalize it before dissolving has been the most successful past strategy¹¹¹;

The benefit of further investigation of cellulose dissolution and functionalization for membrane application is explored in this work, as well cellulose application in separation tasks, for which fouling is normally an important. Due to the present of a large number of OH groups, cellulose can be easily further functionalized for specific applications. Figure 4 summarizes different methods leading to cellulose dissolution.

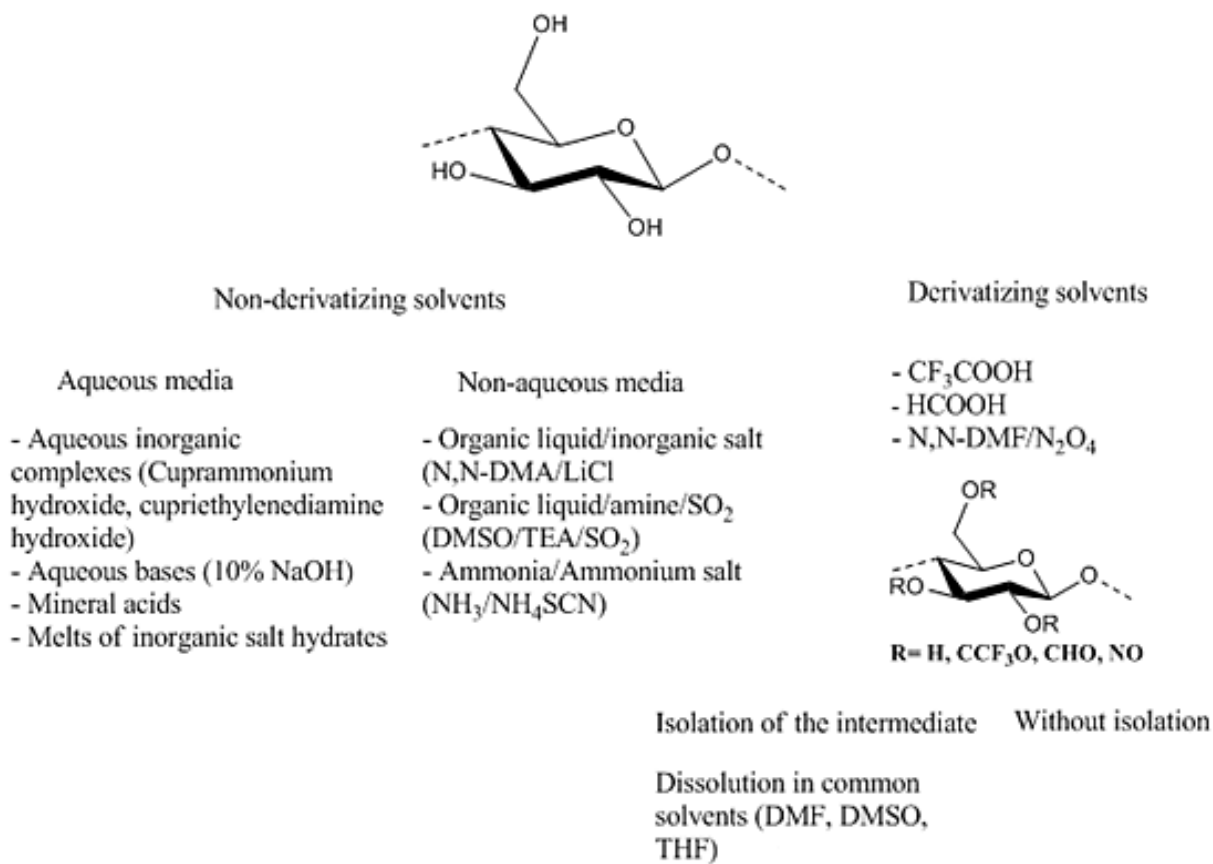


Figure 4. Classification of cellulose solvents suitable as medium for chemical functionalization reactions (adapted from reference¹¹¹)

2.4.3.1 Cellulose Xanthogenate

Cellulose fibers (e. g. viscose and rayon) and films (cellophane) are being produced for more than a century by the viscose technology, which uses a metastable solution of cellulose xanthogenate, with hazardous byproducts like heavy metals, CS₂ and H₂S.¹¹² The harsh process involves mercerization followed by treatment with carbon disulfide and esterification. The xanthogenate was then treated and washed thoroughly with 300 gL⁻¹ ammonium chloride.¹¹³

2.4.3.2 Cuprammonium Process

The other well-known method for production of regenerated cellulose as well as cupro silk and cuprophane is the cuprammonium process also with negative environmental impacts.¹¹⁴ The cuprammonium process involves addition of copper oxide and ammonia in the system.

Rayon has a negative impact on marine life, where researchers have found that rayon contributed with 59.6 % to the total amount of fibers found in the deep ocean and that several types of fish can accidentally consume it.¹¹⁵ The more water repellent the rayon based fibers are, the slower the degradation.

2.4.3.3 Cyclic Amine Oxides

In the 60s cyclic amine oxides have been proposed to dissolve cellulose.¹¹⁶ The cyclic amine oxide can be prepared by reaction between the saturated tertiary amine and hydrogen peroxide in water. N-methylmorpholine-N-oxide can be prepared by reacting N-methylmorpholine with hydrogen peroxide in water to yield generous amount of amine oxide. Advantage of cyclic amine oxide is that, because of its inert nature and neutral pH it is not prone to degradation or further chemical reaction. Amine oxide is also soluble in most common organic solvents e.g. water, methanol, acetonitrile, and dimethyl sulfoxide. Preparation of cellulose compounds, e.g. cellulose esters, requires steps comprising of dissolution, precipitation,

distillation, second precipitation and trituration. Solvents, such as methanol, dimethyl sulfoxide, methyl butyrate and acetone, are used along the process.¹¹⁶

2.4.3.4 N-methylmorpholine-N-oxide

N-methylmorpholine-N-oxide (NMMO) has then been used for production of films and membranes.¹¹⁷ The membrane manufactured with cellulose/NMMO is considered a more environmentally friendly technology.^{6, 118, 119} Although the NMMO is a relatively green solvent and the commercialized production of NMMO-cellulose fibers named Lyocell is a rather simpler technique than others, still the process exhibits some difficulties. Expensive cost, need for recovery of expensive solvent and adjustments of properties of Lyocell fibers are some of the challenges.¹¹²

2.4.3.5 Cellulose in Ionic Liquids

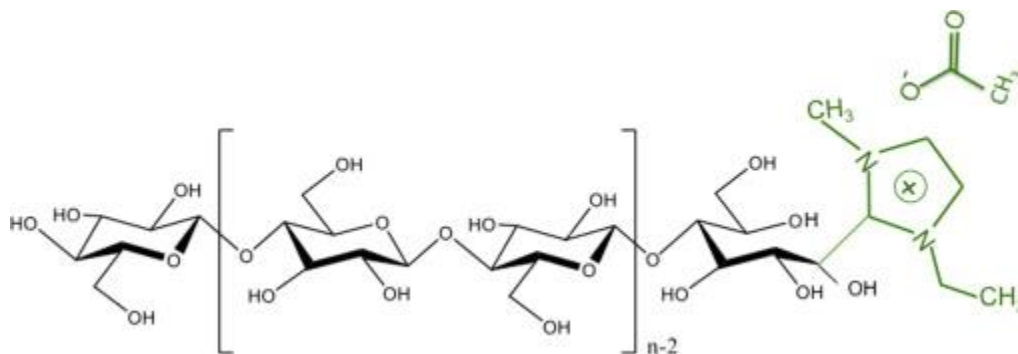
Ionic liquids have a growing interest, being considered as green solvents,¹²⁰ and can dissolve lignocellulosic biomass partially or in total, depending on the subsequent addition of water and solvent. It is important to mention that the production of ionic liquids is still costly. Due to the very low vapor pressure they are expected to bring less health risks to process operators, when compared to volatile solvents, but the toxicity of some ionic liquids in water might be a cause of concern.¹²¹ Therefore for environmental and cost reasons the recovery of ionic liquids is important. Most of

the recovery is done through the evaporation and precipitation processes, but a significant recovery of ionic liquid with a purity of 80%, using nanofiltration has been reported by Abels et al.¹²²

Independent of the level of toxicity, ionic liquids are among the few solvents for cellulose without chemical modification. The dissolution of the cellulosic materials is driven by the anion of the ionic liquid, as reviewed by different groups.^{120, 123-127} Anions such as halides, carboxylates and phosphates have the ability to break the hydrogen bonds within the cellulose structure. We chose 1-ethyl-3-methyl imidazolium acetate [C2mim]OAc (Scheme 1) in this work, which is liquid at room temperature and highly miscible with water¹²⁴; it has high dissolving power even in the presence of up to 10 wt% of water and relatively low viscosity compared to other ionic liquids, and shows no corrosion against stainless steel.¹²⁴ In addition, [C2mim]OAc has low toxicity, melting point lower than -20°C , viscosity 10 mPa s at 80°C and high hydrogen bond acceptor abilities.^{125, 128}

Hydrogen bond acceptor sites in the anion structure and lack of hydrogen bond donors in the ionic liquid cation favor the dissolution of cellulose. The acetate anion in the [C2mim]OAc can form hydrogen bonds with hydroxyl protons of cellulose. Heinze et al.¹²⁷ and Pinkert et al.¹²³ proposed that [C2mim]OAc forms even covalent bond between the glucose unit of cellulose and the imidazolium ring (Scheme 1). This is specific for acetates and not observed for the analog chloride, although it also dissolves cellulose. Even if the covalent in Scheme 1 is formed, the ionic liquid is

expected to be washed out in water, making [C2mim]OAc a good solvent for cellulose coatings.



Scheme 1. Schematic representation of cellulose and 1-ethyl-3-methylimidazolium acetate [C2mim]OAc covalent binding.

Research regarding ionic liquids and cellulose has been mainly towards the fractionation of lignocellulosic biomass, fractionation into mono- and disaccharides as well as the usage of ionic liquids as a pretreatment for the enzymatic hydrolysis. The most exploited usage of ionic liquids in respect to cellulose is as media for homogeneous reactions in order to obtain polysaccharide derivatives from cellulosic materials.¹²⁶

As far as membrane manufacture is concerned a pioneer work has been published by Xing et al.^{129, 130}, based on a cellulose acetate, dissolved in [C2mim]SCN. Li et al.¹¹⁸ reported so far the only work using non-modified cellulose dissolved in ionic liquid for membrane purpose. They used the ionic liquid 1-allyl-3-

methylimidazolium chloride. We explore in this work [C2mim]OAc for the preparation of cellulose membranes by phase inversion.

2.4.4. Cellulose Nanomaterials and Applications

Cellulose nanomaterials, derived from natural sources have numerous applications, from paper and packing industry to automotive and construction, cosmetics, food and very promising biomedical and water treatment industry.¹³¹

In the water treatment and remediation applications, nanotechnology is an emerging technology due to its cost effectiveness and remediation efficiency. Cellulose nanomaterials are vastly used as sorbents for contaminants, mainly heavy metals and as scaffolds for toxic pollutants.

Among various techniques for heavy metal removal, sorption is one of the most efficient with activated carbon as most frequently used sorbent. Cellulose nanomaterials have natural occurrence, they are environmentally friendly and have an immense surface area. For the removal of cationic pollutants such as Pb^{2+} and Ca^{2+} carboxylation of cellulose nanocrystals and cellulose nanofibrils with succinic acid and carboxylate group increases the sorption ability, respectively.^{132, 133} Besides lead and cadmium, carboxylated cellulose nanofibrils sorb 3 to 10 % more Ni^{2+} and Cr^{3+} than unmodified nanofibrils.¹³³ Remediation of radioactive uranyl UO_2^{2+} in water was accomplished by oxidation of wood pulp using the (2,2,6,6-tetramethylpiperidin-1-yl)oxyl (TEMPO)/NaBr/NaClO process followed by

mechanical treatment. The adsorption capability of cellulose nanofibers towards uranyl ion was 167 mg/g, which is two to three times greater than the adsorption of distinctive adsorbents.¹³⁴

Remediation of anionic chromate containing Cr (VI) included succination and amination of cellulose nanocrystals reaching more than 98 % removal.¹³⁵

Hydrophilic nature of cellulose and cellulose nanomaterials prevents its affinity towards hydrophobic compounds e.g. oil. Deposition of TiO₂ onto nanocellulose aerogel via ALD yielded a rather oleophilic surface capable of oil adsorption.¹³⁶ Silanation of cellulose nanofibril aerogel with addition of hydrophobic silane¹³⁷ or freeze-drying of nanofibrillated cellulose in the presence of methyltrimethoxysilane improves oil and organic sorption.¹³⁸

Reinforcement of polymers with nanoparticles is an effective technique in remediation technologies to impart particle aggregation and hence reduce the efficacy. Cellulose nanomaterials prevent the aggregation and promote particle transport. Iron oxide nanoparticles are used in arsenic remediation and aggregation presents one of the drawbacks of system; growth of iron oxide particles onto cellulose nanofibrils, where nanofibrils prevented aggregation, increased the arsenic removal to 36.49 mg/g for As(V).¹³⁹

Polymeric membrane have been reinforced with cellulose nanomaterial due to the increase of membrane tensile strength, hydrophilicity and hence permeability and selectivity, biofouling ability as well as biocompatibility. Ultrafiltration polyethersulfone membrane was reinforced with cellulose nanofibrils yielding a

narrower pore size distribution and permeability enhancement (813.3 L/m² /h) and similar bovine serum albumin (BSA) rejection (92%) compared to pure PES membranes (340 L/m² /h and 94.6%, respectively).¹⁴⁰ Hsiao and Chu et al. (2014) prepared NF membranes via interfacial polymerization and reverse interfacial polymerization on nanofibrous substrate. Sodium chloride rejection was improved from 74% to 91% while permeability of divalent salt solution increased for membranes after modification.¹⁴¹

Bacterial cellulose is produced by bacteria *Gluconacetobacter xylinus* from sugar via uridine diphosphate glucose. Controllable nanostructure via in situ biofabrication opens possibilities for various applications. Due to its natural formation and hence biocompatibility, bacterial cellulose is applicable in biomedical application where this biocompatible material can be used in tissue engineering, scaffold and blood-vessel fabrication as well as nanopaper.¹¹⁰

2.4.5 Cellulose Membranes

One of the first mentioning of cellulose-based membranes for desalination was in the 1950's, when C.E. Reid¹⁴² prepared a cellulose acetate RO membrane that exhibited good separation of salt from water but with rather modest permeability not feasible enough. Although the first nitro cellulose UF membranes were prepared in the early 1900's¹⁴³, but only in the 1960's, after the work of Loeb and Sourirajan¹⁴⁴, asymmetric RO cellulose acetate membranes were prepared with good separation and high permeability. Since then, cellulose acetate (CA) has been

applied in preparation of all filtration processes, from microfiltration (MF) to reverse osmosis (RO). Due to its natural hydrophilicity and low cost, cellulose acetate has been also blended with hydrophobic polymers to yield low fouling composite membrane. To improve the performance of hydrophobic PVDF, Sun et al. (2010)¹⁴⁵ blended CA with PVDF for the preparation of phase inversion membrane in a wet process. Prepared MF membrane showed high flux recovery ratio and low fouling towards BSA protein. Tavakolmoghadam et al. (2014)¹⁴⁶ investigated PVDF/CA blend via phase inversion process induced by immersion precipitation in different concentration ratio and examined their behavior in regard to water permeance and fouling tendency. Membrane blend of 20/80 (CA/PVDF) showed highest water permeability and the lowest total fouling ratio. Mohan et al. (2004)¹⁴⁷ blended CA and PES via precipitation phase inversion technique in different blend compositions. CA/PES blend membranes were tested for pure water permeability, protein rejection (BSA, EA, pepsin, and trypsin) and heavy metal rejection (Cu (II), Ni (II), and Cd (II)) with PEI complexation. Maximum rejection for proteins was observed for BSA (93 %), for heavy metal rejection for Cu (II) (94 %). Compared to unmodified CA membranes, the protein and heavy metal rejection was lower and the permeability was higher. Cellulose based nanomaterials (nanowhiskers, nanocrystals, nanofibers) extracted from natural sources of wood and pulp or produced by bacteria (bacterial cellulose) offer unique network structure and with remarkable mechanical properties e.g. Young modulus of bacterial cellulose reaches more than 15 GPa.¹⁴⁸ UF membrane reinforced with CA nanofibers exhibited ultrahigh permeability of 3450 Lm⁻²h⁻¹ and ferritin rejection of 90.7 %.⁴⁶ Chu and

Hsiao et al. (2014)¹⁴⁹ prepared a composite thin-film nanofibrous UF membrane with cellulose nanofibers. Nanofibers were fabricated from wood pulp using TEMPO (2,2,6,6-Tetramethyl-piperidin-1-yl)oxyl) /NaBr/NaClO system and served as a top barrier layer. Polyacrylonitrile (PAN) electrospun scaffold was the mid-layer and polyethylene terephthalate (PET) functioned as a non-woven substrate. Modified membrane showed permeance five times higher than commercial UF membrane (PAN10) with high rejection ratio (99.9 %) of microsphere latex suspension. Mohammadi et al. (2009)¹⁵⁰ studied the performance and behavior of CA-PEG blends under different conditions and the relation to permeability and selectivity performance. Matsuyama et al. (2011)⁴⁵ prepared three types of hollow fibers from cellulose acetate (CA), cellulose acetate butyrate (CAB), and cellulose acetate propionate (CAP) via the thermally induced phase separation (TIPS) method. The membranes had similar permeability although their hydrophilicities differ, from CA having the highest hydrophilicity and CAP the lowest. CA also showed highest fouling resistance towards BSA and humic acid.

The preparation of multilayer cellulose (non-derivative) has been restricted, mainly because of the lack of suitable solvents.

3. Methodology

In this chapter the methodology used for dissolving the cellulose and preparing membranes is described, as well as their characterization.

3.1 Materials

3.1.1. Cellulose Modification by Silanization and Regeneration

Avicel® PH-101 microcrystalline cellulose ($MW=160,000-560,000 \text{ g mol}^{-1}$) and hexamethyldisilazane (HDMS $\geq 97.0\%$) were purchased from Fluka Analytical, latter produced by Wacker Chemie AG, Burghausen, Germany, both used as received. Hexane (95%, anhydrous) was supplied by Sigma Aldrich®. Hydrochloride acid (HCl, 36.5–38.0%) and sodium chloride (99%) were purchased from Alfa Aesar. Tetrahydrofurane (THF, $\geq 99.5\%$, for synthesis) was purchased from ROTH® and used as received. Poly (ethylene glycol) (PEG) or poly(ethylene oxide) (PEO) of different molecular weights (0.2, 1.5, 3, 6, 10, 35, 100, 300 and 600 kg mol^{-1}) was purchased from Sigma Aldrich®, produced by BASF. The asymmetric porous supports based on polyetherimide (PEI), polyacrylonitrile (PAN), polysulfone (PSU) and polyvinylidene fluoride (PVDF) were prepared at KAUST by phase inversion using continuously operating machine. The polyester wet-laid nonwoven fabric, type 05TH-100 approximately 161 μm thick used for the preparation of

cellulose/ionic liquid membranes was purchased from Hirose Paper, Japan. Milli-Q® water (Millipore) with specific resistivity 18.2 MΩ cm at 26.1 °C was used for membrane preparation and testing.

3.1.2. Cellulose Membranes from Solutions in Ionic liquid

Avicel® PH-101 microcrystalline cellulose (MW=160,000–560,000 g mol⁻¹) and hexamethyldisilazane (≥97.0%) were purchased from Fluka Analytical, latter produced by Wacker Chemie AG, Burghausen, Germany, both used as received. Ionic liquid 1-ethyl-3-methylimidazolium acetate (≥90%) was purchased from Sigma Aldrich®, produced by BASF. Solvents N,N-dimethylformamide (DMF, anhydrous, 99.8%), N,N-dimethylacetamide (DMAc, CHROMASOLV® Plus, for HPLC, ≥99.9%) and 1-methyl-2-pyrrolidinone (NMP, ACS reagent, ≥99.0%) were purchased from Sigma Aldrich® and used as received. Poly (ethylene glycol) (PEG) or poly(ethylene oxide) (PEO) of different molecular weights (0.2, 1.5, 3, 6, 10, 35, 100, 300 and 600 kg mol⁻¹) was purchased from Sigma Aldrich®, produced by BASF. The asymmetric porous supports based on polyetherimide (PEI), polyacrylonitrile (PAN), polysulfone (PSU) and polyvinylidene fluoride (PVDF) were prepared at KAUST by phase inversion using continuously operating machine. The polyester wet-laid nonwoven fabric, type 05TH-100 approximately 161 μm thick used for the preparation of cellulose/ionic liquid membranes was purchased from Hirose Paper, Japan. Milli-Q® water (Millipore) with specific resistivity 18.2 MΩ cm at 26.1 °C was

used for membrane preparation and testing. Sodium chloride (99%) was purchased from Alfa Aesar.

3.1.3. Fouling Evaluation of Cellulose Membranes

Avicel® PH-101 microcrystalline cellulose (MW=160,000–560,000 g mol⁻¹) and hexamethyldisilazane (≥97.0%) were purchased from Fluka Analytical, latter produced by Wacker Chemie AG, Burghausen, Germany, both used as received. Ionic liquid 1-ethyl-3-methylimidazolium acetate (≥90%) was purchased from Sigma Aldrich®, produced by BASF. Bovine serum albumin, lyophilized powder (≥96 %, agarose gel electrophoresis) was purchased from Sigma Aldrich® and used as received. Γ -Globulins from bovine blood (≥99 %, agarose gel electrophoresis, ≤ 4 % NaCl) was purchased from Sigma Aldrich® and used as received. Phosphate Buffered Saline 10X solution was purchased from Fischer Scientific. Suwanee River Humic acid (Suwanee River Humic Acid Standard II (100 mg)) was purchased from International Humic Substances Society.

3.1.4. Oil-Water separation by Cellulose Membrane

Avicel® PH-101 microcrystalline cellulose (MW=160,000–560,000 g mol⁻¹) was purchased from Fluka Analytical, latter produced by Wacker Chemie AG, Burghausen, Germany, used as received. Hydrochloride acid (HCl, 36.5–38.0%) and sodium chloride (99%) were purchased from Alfa Aesar®. Sodium hydroxide

(NaOH, $\geq 99\%$) was purchased from Sigma Aldrich® and used as received. Ionic liquid 1-ethyl-3-methylimidazolium acetate ($\geq 90\%$) was purchased from Sigma Aldrich®, produced by BASF. Milli-Q® water (Millipore) with specific resistivity 18.2 M Ω cm at 26.1°C was used for membrane preparation and testing. The asymmetric porous support based on polysulfone (PSU) was prepared at KAUST by phase inversion using continuously operating machine. The polyester wet-laid nonwoven fabric, type 05TH-100 approximately 161 μm thick used for the preparation of cellulose/ionic liquid membranes was purchased from Hirose Paper. Crude oil was kindly provided from petrochemical company. Surfactants sodium dodecylbenzenesulfonate ($\text{CH}_3(\text{CH}_2)_{11}\text{C}_6\text{H}_4\text{SO}_3\text{Na}$), hexadecyltrimethylammonium bromide ($\text{N}(\text{CH}_3)_3\text{Br}$) and polysorbate 80 (Tween® 80) were purchased from Sigma Aldrich and used as received.

3.2. Membrane Preparation

3.2.1. Cellulose Modification by Silanization and Regeneration

3.2.1.1. Preparation of Trimethylsilyl Cellulose

Cellulose (3 g) was swollen in 150 ml water and 30 ml DMAc, followed by filtration, further dissolution in 300 ml DMAc and heating at 165 °C for 30 min under reflux. After cooling the solution to 100 °C, 15 g of LiCl was added and stirred until complete dissolution. After cooling down to room temperature a clear solution was obtained after stirring for 8 h to 12 h stirring. 45 ml of HDMS was then slowly added

to the solution at 80 °C in 3 h. The hot solution was precipitated in methanol, filtered, thoroughly washed and dried in vacuum oven at 60 °C over night.

3.2.1.2. Preparation of Regenerated Silyl Cellulose

Silylated cellulose was dissolved in THF and used as coating solution. As porous substrate PAN, PSU, PEI or PVDF asymmetric porous membranes, previously manufactured by phase inversion in a continuous machine were used (Figure 8). Polymers were dissolved in following conditions; polyetherimide (Ultem 1000) 17.5 wt%, gamma-butyrolactone 30 wt%, dimethylacetamide 50 wt%; polyacrylonitrile 12 wt%; dimethylformamide 88 wt% and polyethersulfone 18 wt% and dimethylformamide 82 wt% solutions were heated at 60-65°C over night; polysulfone 18 wt% and dimethylformamide 82 wt%; polyvinylidene fluoride (PVDF 900) 10 wt% and N-Methyl-2-pyrrolidone 90 wt% solutions were heated at 80°C over night prior to casting. The non-woven polyester was 100 µm thick and the casting knife was fixed at 100 µm thickness.

They were dip coated with 0.6–1.9 wt% silylated cellulose solutions in THF and dried with briefly hot air. The dried membrane was then immersed in 1 M hydrochloric acid aqueous solution for 15–30 min to regenerate the cellulose. The 1 M hydrochloride acid was prepared from 36.5% to 38.0% hydrochloride acid purchased from Alfa Aesar®.



Figure 5. Flat sheet membrane machine at KAUST

3.2.2. Cellulose Membranes from Solutions in Ionic Liquid

The unmodified cellulose was dissolved in the ionic liquid [C2mim]OAc, at 60 °C during 24 h. The cellulose concentration was 2, 5 and 10 and 14 wt %. The solutions were then cast after cooling down to 23 °C, with the doctor blade adjusted to 150 μm gap, on asymmetric porous supports (PAN, PEI, PSU or PVDF) and polyester nonwoven, respectively, or directly on glass plates. After casting, the membranes were immersed for 2–4 h in deionized water to induce phase separation and dried in air.

3.2.2.1. Preparation of multilayer membranes with polyamide selective layer

Thin film composite membranes with a selective polyamide layer were prepared using interfacial polymerization (IP)¹⁵¹ with m-phenylenediamine and trimesoyl chloride as reactants in aqueous and organic phase, respectively. The polymerization was directly performed on asymmetric porous supports or on cellulose membranes prepared as described in Section 3.2.1.

3.2.3. Fouling Evaluation of Cellulose Membranes

The preparation of cellulose membranes from solutions in ionic liquid is described in Section 3.2.2. Briefly, unmodified cellulose was dissolved in ionic liquid at 60°C constantly stirring for 24 hours. Cellulose concentration was 2 %, 5 % and 10 wt %. Solution was then casted onto polysulfone (PSU) porous support backed up with polyester nonwoven fabric with the casting rod having 150 µm thicknesses. Membranes were immediately immersed in water bath to induce phase inversion for approximately 2-4 hours and air dried.

3.2.4. Oil-Water Separation by Cellulose Membrane

The preparation of cellulose membranes from solutions in ionic liquid is described in Section 3.2.2. Briefly, unmodified cellulose was dissolved in ionic liquid at 60°C constantly stirring for 24 hours. Cellulose concentration was 2 %, 5 % and 10 wt %.

Solution was then casted onto polysulfone (PSU) porous support backed up with polyester nonwoven fabric with the casting rod having 150 μm thicknesses. Membranes were immediately immersed in water bath to induce phase inversion for approximately 2-4 hours and air dried.

3.3. Experimental Methods of Characterization

3.3.1. Chemical Characterization

The functional groups of unmodified cellulose, silylated cellulose and regenerated cellulose as well as a non-modified support were analyzed by attenuated total reflectance mode (ATR) using Fourier Transform Infrared Spectroscopy (FTIR) Perkin Elmer Spectrometer. The number of scans for each sample was 16 with the resolution of 4 cm^{-1} , conducted at room temperature using the ATR unit with a nominal incident angle of 45°. ^1H NMR spectrum was recorded on Bruker Avance III 400 MHz spectrometer using CCl_3D as a solvent.

3.3.2. Morphological Characterization

For the surface and cross-section membrane characterization FEI Nova Nano 630, FEI Magellan, FEI Quanta 200 or 600 field emission scanning electron microscopes (FESEM) were used. To reduce surface charging, the samples were coated with

either iridium or platinum inside K575X or Q150ES (Quorum technologies, UK) sputter coaters.

Cryo SEM experiments were carried out using a PP2000T cryo transfer system (Quorum Technologies, UK) attached to a FEI on Nova Nano 630 SEM with field emission source and through-the-lens detector. To examine the top surface or cross section morphology of membranes, the samples (approximately 2 mm×5 mm) were mounted either flat onto an aluminum stub using aluminum tape or vertically inside slot and secured mechanically between two parallel jaws. The stub was then secured on the cryo specimen holder, rapidly plunged into the liquid nitrogen slush and transferred under vacuum into a PP2000T cryo preparation chamber precooled at $-180\text{ }^{\circ}\text{C}$. To obtain fractured surface of membrane cross section, the sample temperature was raised to $-150\text{ }^{\circ}\text{C}$ and the top part of the vertically mounted membrane was hit with a knife precooled at $-150\text{ }^{\circ}\text{C}$. In order to remove residual ice contamination and further reveal the structure of the surface and the fractured plane, samples were sublimed inside the SEM chamber at $-90\text{ }^{\circ}\text{C}$. To avoid charging problems, samples were transferred back to the preparation chamber and sputter coated with 5 nm thick platinum in an argon atmosphere at $-150\text{ }^{\circ}\text{C}$. The samples were then transferred back to SEM cryo stage, held at $-130\text{ }^{\circ}\text{C}$, and high quality SEM images were captured. In all cases, the imaging was performed using an accelerating voltage of 2–3 kV and working distance of 5 mm.

Atomic Force Microscopy (AFM) image was obtained using a 5500 Scanning Probe Microscope (5500 SPM, Agilent Technologies, USA) in tapping mode. The cantilever

had force constant of 0.5–9.5 N/m (NANOSENSORS), resonance frequency 45 kHz to 115 kHz and was Pt/Ir-coated on tip and detector side.

Transmission Electron Microscopy (TEM) images of cellulose coated membranes and non-modified polysulfone membranes after oil solution filtration were obtained using Spirit Bio Twin (FEI Company) microscope operating at 120 k with camera Eagle 4K (FEI Company) . Membranes were gently rinsed and freeze dried for 24 hours after filtration to preserve the structure. Afterwards they were embedded in an epoxy resin EMBed-812 (EMS) and cured at 60 °C for 24 hours. Ultrathin sections of 120 nm thickness of the embedded membranes were prepared using ultramicrotome (Leica EM UC6) equipped with a diamond knife Ultra 45°(Diatome). The thin slices were placed on a copper grid and imaged in TEM.

3.3.3. Surface Characterization

Surface zeta potential, zeta potential of the solution and particle size was obtained using Malvern Zetasizer Nano ZS that incorporates dynamic light scattering, electrophoresis and static light scattering. The sample of 0.5 mm² was placed on a membrane holder which was inserted in the instrument. Various pH ranging from 3-11 were examined with each measurement taking up to 30 minutes. The pH was adjusted manually each time. Besides the streaming potential of the membranes, zeta potential of the feeds itself was measured with the same instrument.

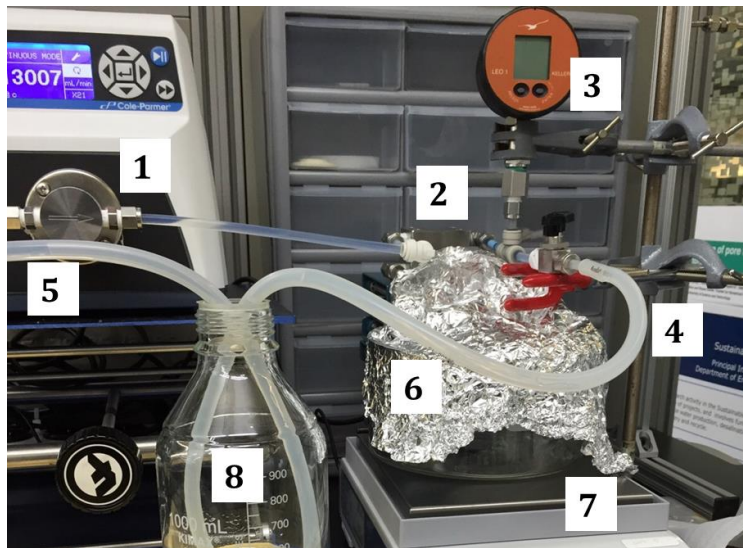
Zeta potential of the aqueous solutions was measured using disposable folded capillary cell to avoid any contamination. Measurement is based on electrophoretic light scattering. The experiment had three runs each repeating 100 times and the average was taken into account. Particle size was measured using disposable 12 mm square polystyrene cuvettes.

3.3.4. Permeance Measurement

Water permeances of non-modified PAN, PEI, PSU asymmetric porous supports and cellulose multilayer membranes were measured using a dead-end set-up at 5 bar, with effective membrane area of 14.6 cm² and using Milli-Q® water as the feed.

Cross flow set up

For humic acid experiment, a cross flow set up was used. The membrane (4.1 cm² area) was placed in a stainless steel cell. A gear pump was used to apply a constant pressure of 3.5 bars unless stated otherwise, controlled with valve. The gear pump suction speed was kept constant at 1300 ml/min. The permeate was collected in a glass beaker placed on a balance, connected to a computer, which continuously collected the data (Figure 6). An ice bath was used to keep the humic acid solution at room temperature if needed (23°C).

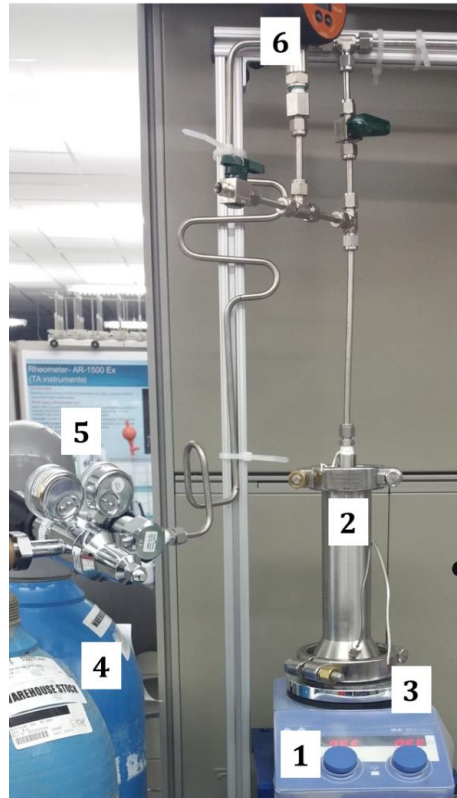
**Legend:**

- 1 - Gear pump**
- 2 - Stainless steel cell**
- 3 - Pressure gauge**
- 4 - Outlet**
- 5 - Inlet**
- 6 - Collection beaker/permeate**
- 7 - Balance**
- 8 - Feed reservoir**

Figure 6. Cross-flow set-up

Dead end set up

For the oil in water separation experiment, a dead end set up was used. Membranes were placed in stainless steel cell and connected with tubing to the nitrogen gas cylinder, while 5 bars pressure was used for all experiments. Permeates were collected in a beaker and analyzed immediately. Continuous stirring was used inside the stainless steel cells with oil in water emulsion (Figure 7).

**Legend:**

- 1 - Magnetic stirrer**
- 2 - Stainless steel dead-end cell**
- 3 - Cell outlet/collection point**
- 4 - Nitrogen gas cylinder**
- 5 - Pressure regulator**
- 6 - Pressure gauge**

Figure 7. Dead-end set-up

3.3.5. Rejection Measurement and Permeate Characterization

To measure the molecular weight cut-off (MWCO) of the membranes, PEG solutions (0.1 wt % single solutions or 0.5 wt % of a mixture of 5 PEG molecular weights) were used as feed in dead-end filtration experiments at 5 bars with an effective membrane area of approximately 14.6 cm². The chosen PEG molecular weights were 200, 1500, 3000, 6000, 10,000, 35,000, 100,000 and 300,000 g mol⁻¹. The solute rejection was calculated from the concentrations of the solute in the feed and permeate, analyzed by GPC.

Gel permeation chromatographs for the determination of molecular weight cut-off (MWCO) were measured using the GPC System-Agilent 1200 Series. The GPC/SEC columns were used together, Agilent PL aquagel OH 60 8 μm and Agilent PL aquagel OH 40 8 μm . Columns were calibrated with polyethylene oxide/glycol EasiVial PEG/PEO (4 ml), the standard for SEC. Three EasiVial PEG/PEO standards for Agilent gel-permeation chromatography cover the molecular range from 106 gmol^{-1} to $1,258,000 \text{ gmol}^{-1}$.

Rejections were calculated by the following equation;

$$R = (1 - C_p/C_f) \times 100 \% \quad (3)$$

where C_p and C_f are final solute concentrations in permeate and feed, respectively.

The MWCO is defined as the smallest molecular weight with 90% rejection.

Salt rejection was measured for selected membranes, with 2000 ppm sodium chloride solution used as feed in a dead-end set-up under pressure of 5 bars with effective membrane area of 14.6 cm^2 . The salt concentration was evaluated by measuring conductivity with WTW ProfiLine Cond 3310 equipment. The feed initial volume was 300 mL; the permeation was conducted for 30 min before collecting samples for conductivity measurement.

3.3.6. Fouling Characterization

3.3.6.1. Extent of Fouling (Humic acid, BSA and γ -globulin)

BSA and γ -globulin were dissolved in phosphate buffered saline (PBS) 10 X solution. Firstly, PBS was prepared in PBS: water ratio (1:10), following preparation of 1 mg/mL BSA solution and 1 mg/mL γ -globulin solution. As prepared solutions were used right away as foulant solutions in a cross flow set up (3.5 bar pressure, 1300 ml/min suction speed) for fouling resistance tests.

Secondly 100 mg/L of humic acid (Suwannee River Humic Acid) was prepared and tested in aforementioned conditions, respectively.

Experiments with humic acid were performed in a cross flow set up described earlier. In short, pure water permeance was measured for 2, 5 and 10 % cell/ionic liquid membranes until steady state was reached. After that, the pure water feed was replaced with humic acid feed and humic and the permeance was measured for several hours . Permeate was collected in a beaker standing on the balance for continuous data collection. Humic acid feed was inside the ice box for controlled temperature experiment. Tubing and cell were cleaned each day to prevent accumulation of humics with removing the membrane and thoroughly cleaning inside the cell.

3.3.7. Oil-Water Separation

3.3.7.1. Extent of Fouling in Experiments with Oil in Water Emulsion and Real Produced Water

Membranes prepared from solutions in ionic liquid were first tested with pure water, followed by oil-in-water emulsion, prepared by mixing water and crude oil; feed, permeate and retentate were collected for further analysis. The cell was filled with 150 ml of oil in water emulsion and 75 ml was collected as permeate. Without taking out the membrane, the cell was rinsed with water, refilled with pure water and the flux was measured again. The flux was measured as functions of time, by weighting the amount of permeate on a balance. To observe any visible adsorption, the membrane was taken out from the cell, rinsed with water.

For each experiment, membranes prepared from 2, 5 and 10 % cell/ionic liquid solutions were used. Testing was performed with three different surfactants and three different pH values ranging from neutral, acid and basic. The oil concentrations used were 200, 500 and 1000 ppm. Surfactants were added in 1:10 ratio in accordance to the oil. Sodium chloride was added in 80 g/L concentration, if not stated differently. The emulsion was mechanically mixed in a laboratory blender for 180 seconds twice.

An experiment was performed also with real produced water received from a petrochemical partner.

A cross-flow experiment was conducted with membranes prepared with 2, 5 and 10 wt % cellulose in ionic liquid now using samples of real produced water as feed. Membranes were placed in a stainless steel cell (4.1 cm² area) and connected with the tubing to the feed and the inlet that was recycled back to the feed. A gear pump was used to apply a constant pressure of 3.5 bars. The gear pump suction speed was kept constant at 1300 ml/min. The permeate was collected in a glass beaker placed on a balance connected to a computer (Figure 8).

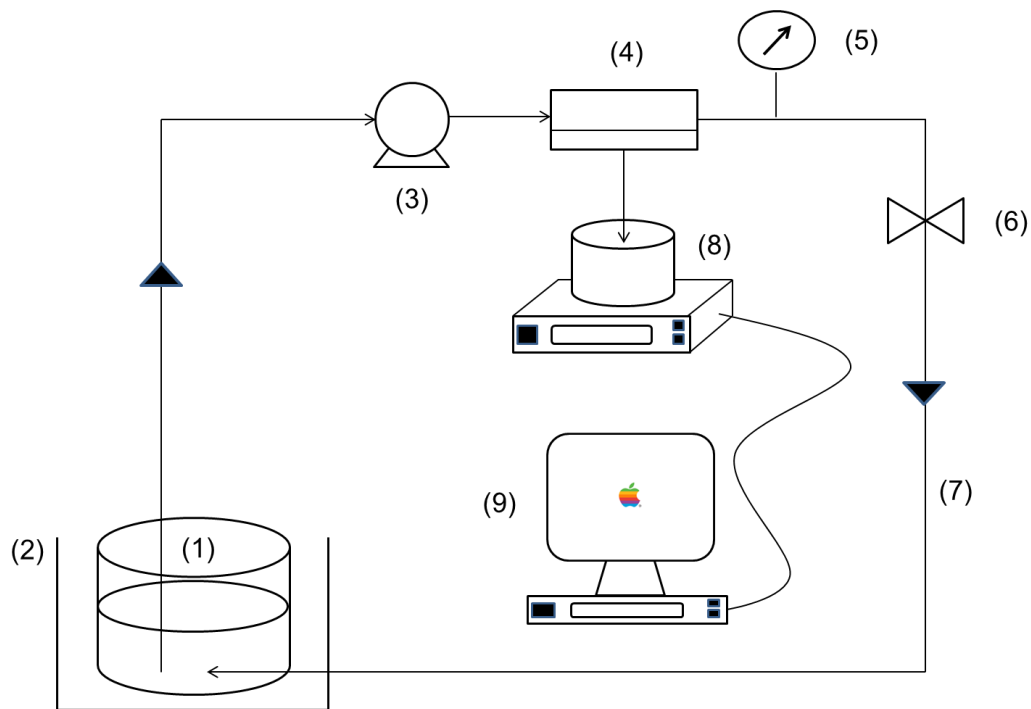


Figure 8. Cross-flow experiment. Legend: (1) Feed tank; (2) Thermostatic bath (if needed); (3) Gear pump; (4) Membrane module; (5) Pressure gauge; (6) Valve; (7) Retentate return; (8) Permeate collection with electronic balance and (9) Computer for data collection.

3.3.7.1.1. Turbidity

Turbidity was measured using a 2100Q HACH portable turbidimeter, which measures turbidity in NTU units of produced water feeds and permeates. The device is compliant with USEPA Method 180.1 design criteria.

3.3.7.1.2. Oil in Water Analysis

To assess the oil-water separation ability of cellulose membranes, oil concentration (ppm) in the feed, permeate and the retentate was evaluated using HD 1000 oil-in-water analyzer.

The HD 1000 analyzer for oil in water measurement has a probe, which gives spectral analysis and laser induced fluorescence in real time measurement to obtain oil concentration in relation to water. When exposed to UV or low blue light, the aromatic hydrocarbons in oil absorb and emit light in different wavelengths which helps to evaluate the amount of oil present in water. Spectroscopy was used to differentiate between several types of oils.

Concentration of oil in the feed and permeate was used to calculate oil rejection using equation (3) mentioned in Chapter 3.3.5.

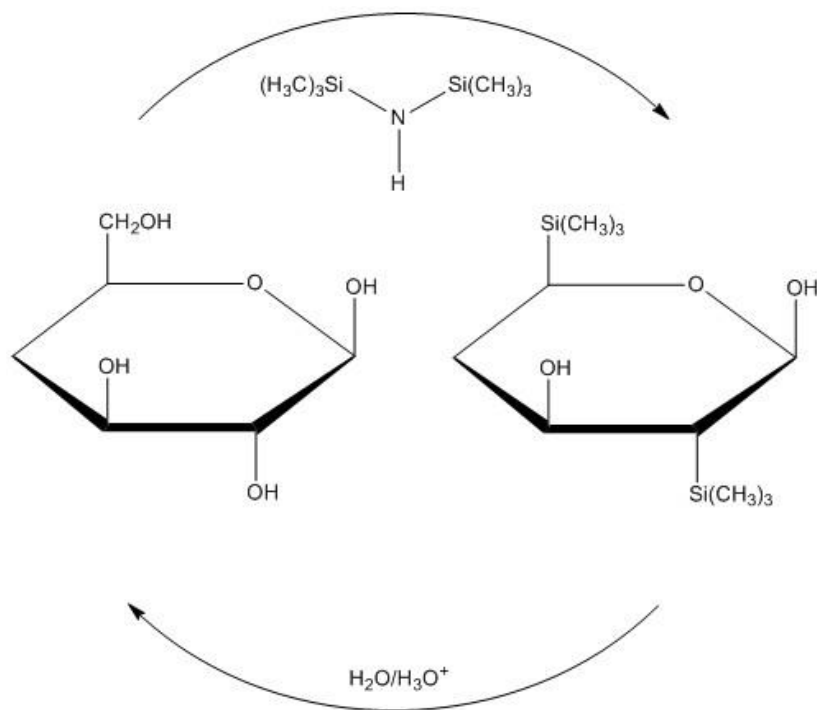
4. Results and Discussion

4.1. Cellulose Modification by Silanization/Regeneration

Cellulose can be hardly dissolved in common solvents due to strong hydrogen bonds and crystallinity. For the manufacture of multilayer membranes, by dip coating, a solvent is needed, which dissolves the coating polymer without damaging the substrate. However the application of cellulose coating for multilayer membranes has been hindered by the lack of solvent for cellulose, which would not damage the morphology of the porous polymeric support. Preliminary results using the silylated cellulose method have been previously mentioned only in a patent of our group.¹⁵² Silylation protects the hydroxyl groups, inhibiting H-bond formation, making the polymer hydrophobic and soluble in apolar solvents. After the coating cellulose can be easily regenerated to its original form by acid hydrolysis.

Multilayer membranes were obtained by dip coating of asymmetric porous polymeric supports based on PSU, PEI, PAN and PVDF. PVDF is the most hydrophobic membrane, followed by PSU, PAN and PEI, respectively. The MWCO in the range of ultrafiltration are usually prepared by phase inversion from solutions in polar solvents like DMAc, DMF or NMP. Deposition of a second polymer layer is an important method for preparing nanofiltration, forward osmosis or gas separation membranes. Cellulose is soluble in DMAc/LiCl, however this would also solubilize or at least damage most of the mentioned polymeric supports. When silylated, cellulose

becomes apolar and soluble in hexane or THF, which do not affect commonly used polymeric supports. After coating, the cellulose can be regenerated to its hydrophilic and less soluble original form by acid treatment (Scheme 2).



Scheme 2. Silylation and regeneration of cellulose

The success of different steps of silylation and regeneration were proven by spectroscopic methods of characterization. Non-modified microcrystalline cellulose and silylated cellulose as well as the cellulose regenerated by acid treatment were characterized by ATR-FTIR. The FTIR spectra in Figure 9 indicates the structural changes of the pristine cellulose into trimethylsilylcellulose due to the etherification with OH groups substituted by O-Si(CH₃)₃ groups. The peaks for the substituted

groups that reflect the valence vibrations in the trimethylsilyl cellulose can be seen at 760 cm^{-1} , 1260 cm^{-1} ($\text{Si}(\text{CH}_3)_3$) and 850 cm^{-1} ($\text{Si}-\text{C}$). The peaks representing the deformation vibrations can be identified at 970 cm^{-1} ($\text{Si}-\text{O}$) and 1470 cm^{-1} (SiCH_3). Characteristic absorption band associated to the OH valence vibration at $\sim 3500\text{ cm}^{-1}$ is much lower in the silylated trimethylsilylcellulose, but some unreacted OH group still remained.

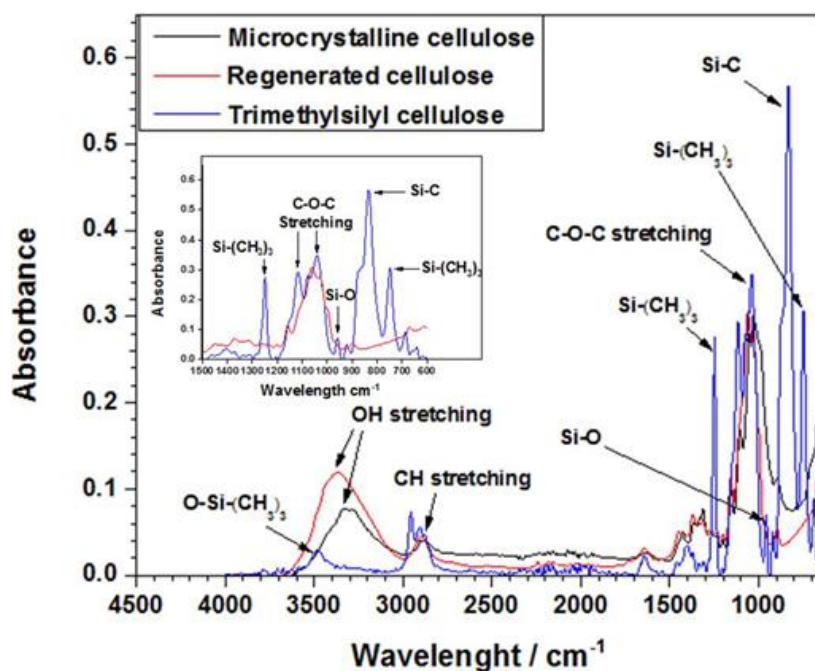


Figure 9. FTIR spectra of non-modified microcrystalline cellulose (black), TMS-cellulose (blue) and regenerated cellulose (red); inset: expanded spectra at low wavelength range.

Regeneration of OH groups after treatment by HCl is proven by the increase of the broad band at 3400 cm^{-1} , which is related to OH stretching vibration. The peak has

The contact angles for non-modified porous supports and those coated by regenerated silyl cellulose are shown in Table 1. For the latter the value is 32.6°, clearly lower than that of unmodified porous supports. However the contact angle is still higher than for coatings obtained by dissolving cellulose in ionic liquid. This could indicate that the cellulose is not completely regenerated, still containing some rest of silyl hydrophobic groups on the surface, which can however not be detected by FTIR.

Table 1. Contact angle of investigated membranes.

Membrane	Contact Angle (°)
PSU	86.0 ± 1.6
PEI	73.0 ± 7.9
PAN	51.2 ± 0.5
1 wt% Cellulose (regenerated)/ PAN	32.6 ± 0.4
1 wt% Cellulose (regenerated)/ PAN/IP	62.7 ± 0.8
2 wt% Cellulose/ [C ₂ mim]OAc/ Nonwoven	26.1 ± 1.8
2 wt% Cellulose/ [C ₂ mim]OAc/ PEI	25.7 ± 0.9
2 wt% Cellulose/ [C ₂ mim]OAc/ PSU	22.0 ± 1.8

The surface morphology indicating order and possible crystallization of the regenerated cellulose layer coating is visible in Figure 11 a. To confirm it, X-ray experiments were conducted. The diffractograms of cellulose before the silylation and after the regeneration are shown in Figure 11 b and c, respectively.

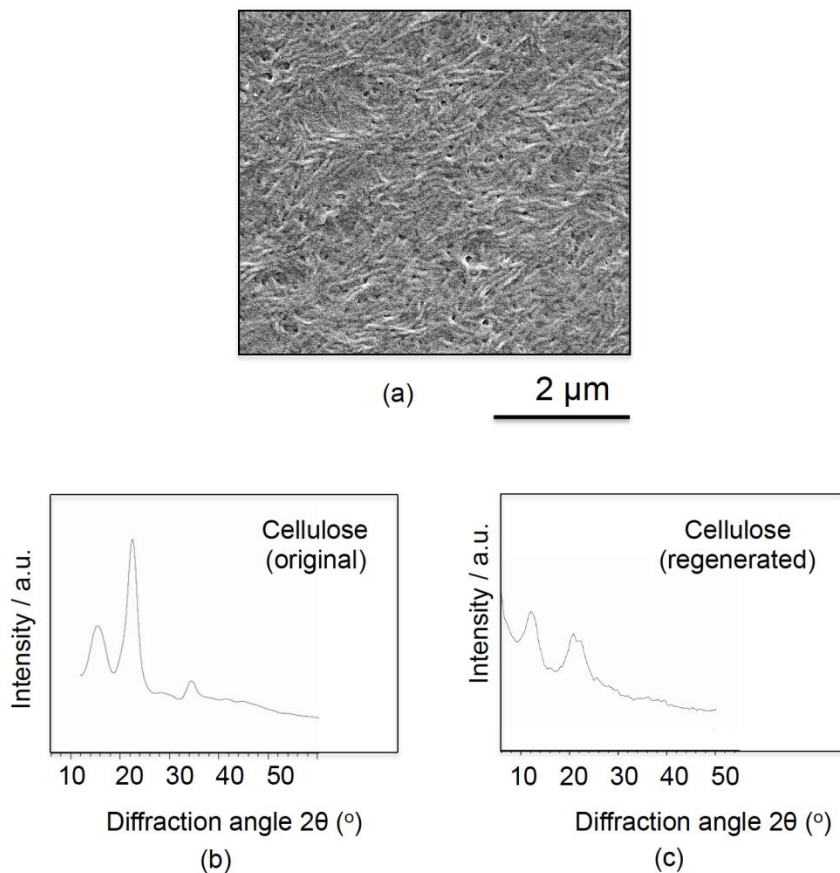


Figure 11. Surface FESEM image and X-ray diffractograms of (a) dry polyacrylonitrile porous membrane coated with 1 wt% silylated cellulose in THF, followed by regeneration with acid treatment; X-Ray diffractograms of (b) unmodified cellulose and (c) regenerated cellulose.

Cellulose can exist in six different cellulose polymorphs, which can be interconverted.¹⁵³ Cellulose I is commonly found in native cellulose. Cellulose III_I or III_{II} can be obtained by treatment of cellulose I or II with liquid ammonia while cellulose IV_I and IV_{II} are observed by heating cellulose III_I or III_{II}, respectively.

Crystallinity was confirmed in all cases. The angles corresponding to the peak maximum in different diffractograms are shown in Table 2. For each case the

probable polymorph was identified, based on previous cellulose characterization reports.¹⁵⁴ The cellulose coating prepared by silylation and treatment with acid is probably polymorph type II, following the same pattern reported before for cellulose regenerated by other procedures.^{116, 124, 154}

Table 2. Cellulose diffractogram and polymorphs.

Material and/or Membrane	2 θ			Cellulose polymorph
	1 st Peak	2 st Peak	3 st Peak	
Non-modified cellulose	14 °	16 °	22 °	I
Regenerated cellulose	12 °	20 °	22 °	II
Cellulose/[C ₂ mim]OAc	12 °	20 °	22 °	II

The performance of regenerated cellulose membranes, prepared from silylated cellulose on PAN asymmetric porous supports, can be seen in Table 3 and Figure 12, including rejection of PEG with different molecular weights and water permeance. The thickness of coating layer was increased with higher cellulose concentration in THF, consequently reduced the water permeability and MWCO, but increased salt and PEG rejection. Higher cellulose concentrations led to thicker coatings of lower water permeances. The lowest MWCO was 5000 gmol⁻¹, reached with 1.6 wt % cellulose in THF, corresponding to a water permeance of 8.1 L m⁻² h⁻¹ bar⁻¹.

Table 3. Performance of membranes prepared from silylated cellulose/THF solution on PAN porous support, followed by regeneration in acid.

Coating solution (wt% Cellulose in THF)	Coating thickness ^a (μm)	Water permeance ($\text{L m}^{-2} \text{h}^{-1} \text{bar}^{-1}$)	MWCO (g mol^{-1})	NaCl Rejection ^b (%)
0	0	102.5	90,000	0
0.6	0.3	28.1 ± 0.6	47,000	1.8
1.0	1.0	16.8 ± 2.7	10,000	2.2
1.6	1.8	8.1 ± 0.3	5,000	3.1
1.9	2.0	5.7 ± 1.4	5,000	9.1

a Estimated from FESEM; b 2000 ppm NaCl as feed solution

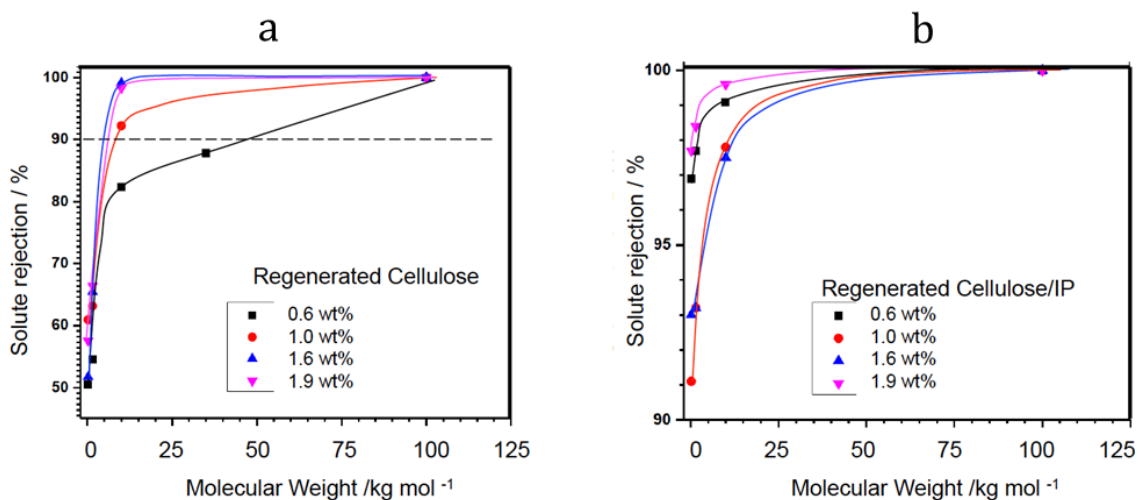


Figure 12. PEG rejections of cellulose membranes prepared by coating with different concentrations of silylated cellulose on PAN porous supports, followed by regeneration with acid solutions: (a) cellulose coating and (b) cellulose coating with polyamide layer.

In part of the membranes, a top polyamide selective layer was formed on the cellulose coating by interfacial polymerization. For comparison, the interfacial polymerization was also performed directly on the porous PAN and PVDF supports without cellulose. The morphology of the polyamide layer directly on the porous

supports is respectively shown in Figure 13 and Figure 14 and on cellulose is shown in Figure 15. A clear difference was observed, depending on the substrate.

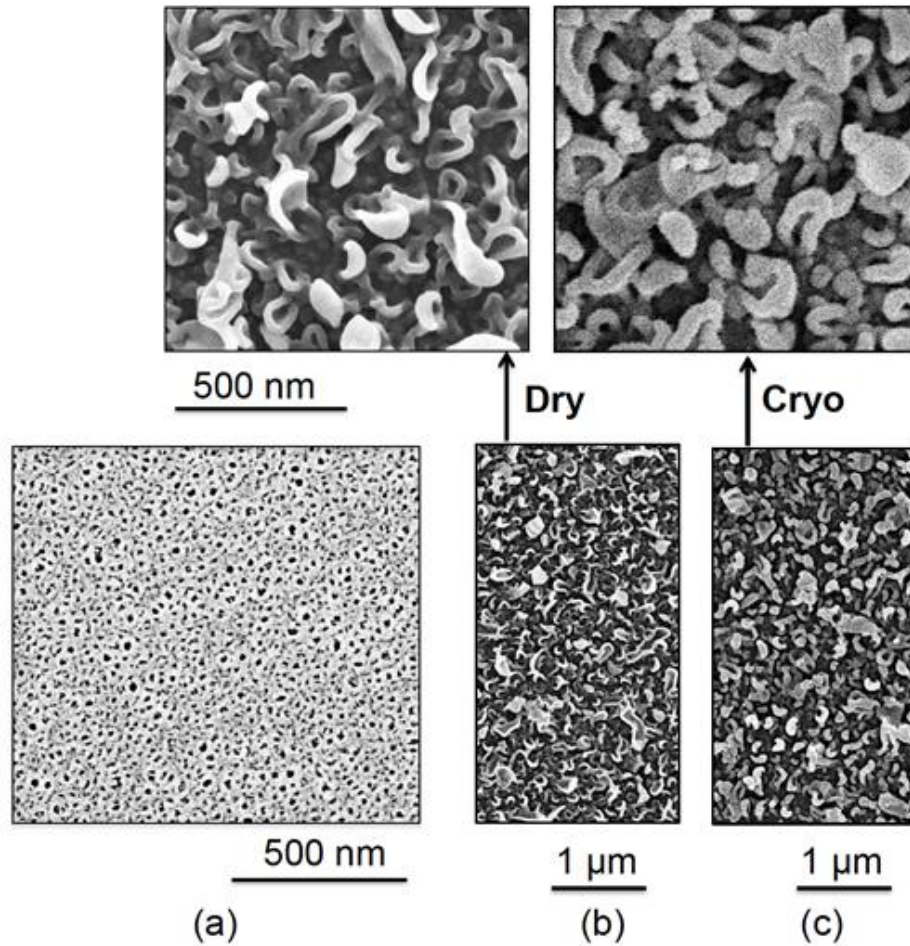


Figure 13. Surface (FESEM image) of a dry (a) PAN porous membranes and (b, c) the same membrane coated with polyamide by interfacial polymerization: (b) dry and (c) cryo images of wet membranes.

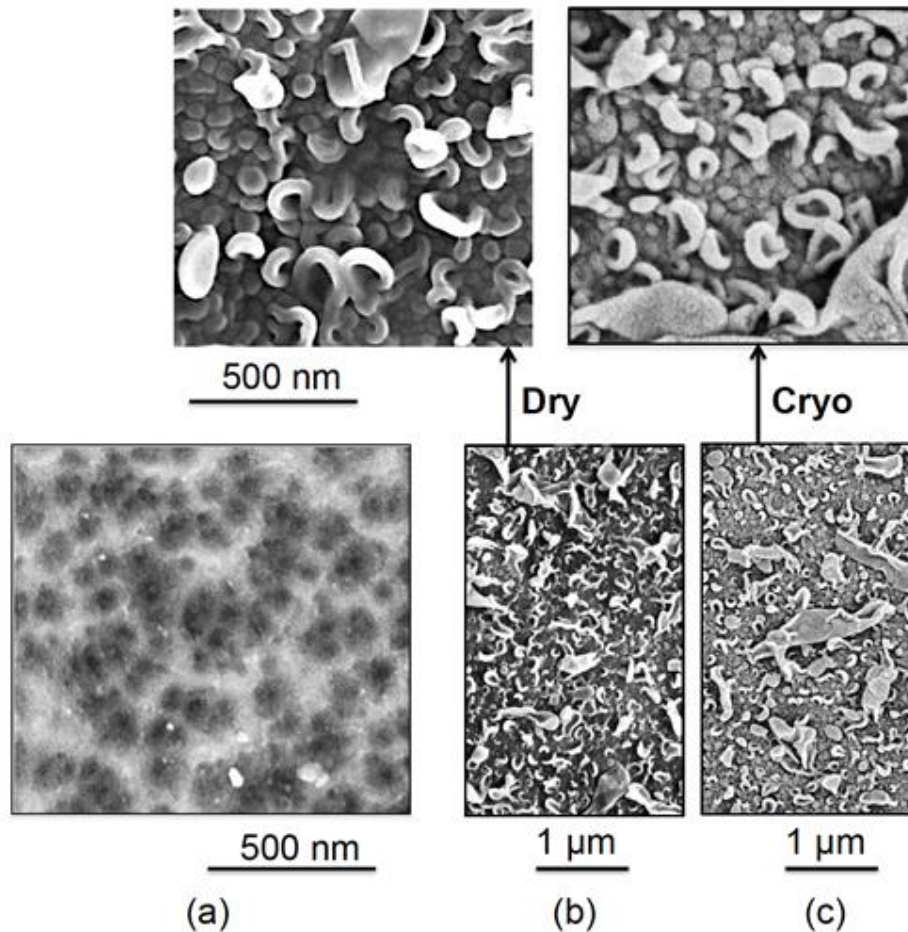


Figure 14. Surface (FESEM image) of (a) PVDF porous membranes and (b, c) the same membrane coated with polyamide by interfacial polymerization: (b) dry and (c) cryo images of wet polyamide/PVDF membrane.

The images in Figure 13 and Figure 14 also reveal the effect of the support on the morphology of the interfacial polymerized layer. PVDF is more hydrophobic and has larger and more scattered pores, while PAN is hydrophilic and has higher density of smaller pores. The polyamide layer is more homogenous with smaller nodules when prepared on PAN. The influence of the porous support on the polyamide layer has been pointed out before by Li et al.¹¹⁸, Ghosh et al.¹⁵⁵ and Pacheco et al.¹⁵⁶ The dense (non-porous) areas of the membranes locally obstruct the growth of the

interfacial polymerized layer, while the contact between organic and aqueous phase is favored through the pores. Yeh et al.¹⁵⁷ explained that large pores during the interfacial polymerization lead to a rapid transport of amine from the aqueous phase, filling the membrane pores, and the organic phase to react with trimesoyl chloride. Convection due to Marangoni effect leads then to turbulent mixture of monomers and formation of larger globules.

Interfacial polymerization was also performed on a membrane coated with cellulose. Well-distributed small pockets were seen in Figure 15 a, b. A significant difference was observed between images obtained for the dry membrane with regular SEM and the wet membrane by cryo microscopy. The wet multilayer membrane has a more swollen polyamide layer (Figure 15 c, d) indicating that water is kept below it. The polyamide thin film layer seems to be less adhered to the substrate in the case of regenerated cellulose support. In addition, the polyamide thin film is smoother than those on PAN and PVDF porous supports (Figure 13, Figure 14 and Figure 15). The reason for the unexpected morphology observed in Figure 15 c can be understood as following. The cellulose layer on the porous support probably absorbs and better holds the amine solution during the interfacial polymerization process. The diffusion of amine from the cellulose layer to the organic phase is gentler, resulting in a smoother polyamide thin film layer. When the interfacial polymerization is conducted on a hydrophobic support with large pores, like the PVDF membranes shown in Figure 14, there is a turbulent amine transport into the organic phase to react with trimesoyl chloride and immediately form a rough polyamide layer. The probable mechanism for the thin polyamide layer

formation on substrates of different porosity is illustrated in Figure 16, based in a model proposed by Li et al.¹⁵⁸ Additionally the swelling of the highly hydrophilic cellulose layer itself with water might also affect the cryo image in Figure 15.¹⁵⁸

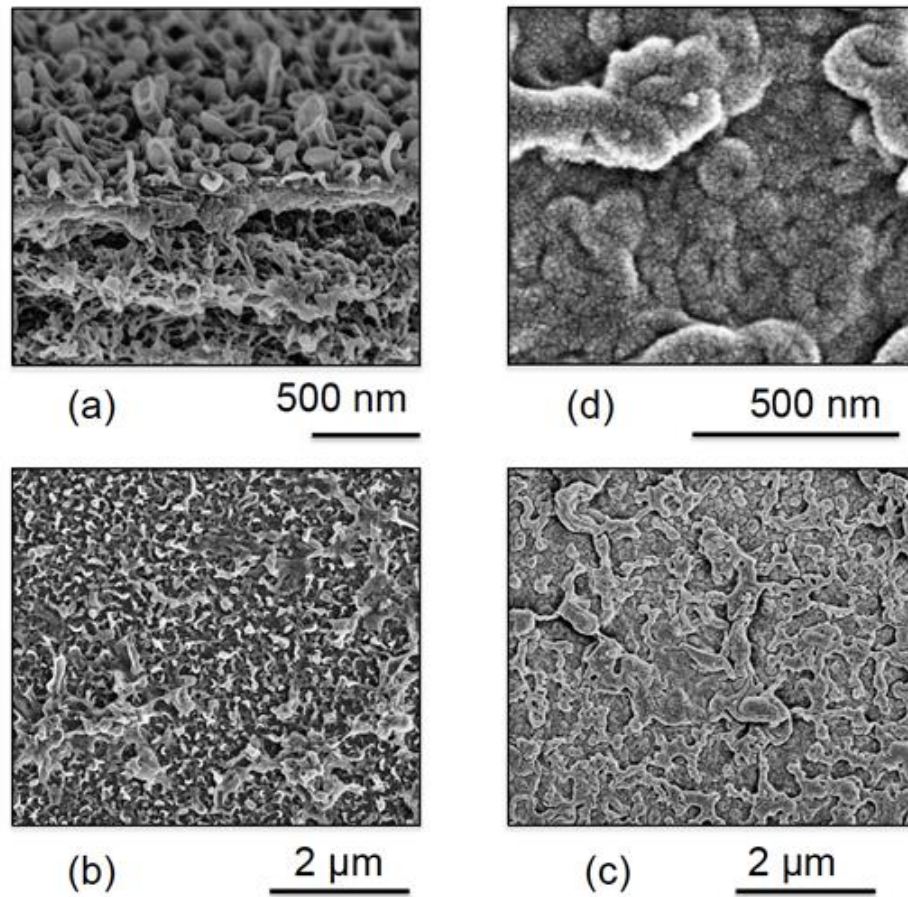


Figure 15. FESEM images of membranes prepared by interfacial polymerization on asymmetric porous polyacrylonitrile supports coated with 1 wt% regenerated cellulose: (a) cross section and (b, c, d) surface images of (a, b) dry and (c, d) cryo wet membranes.

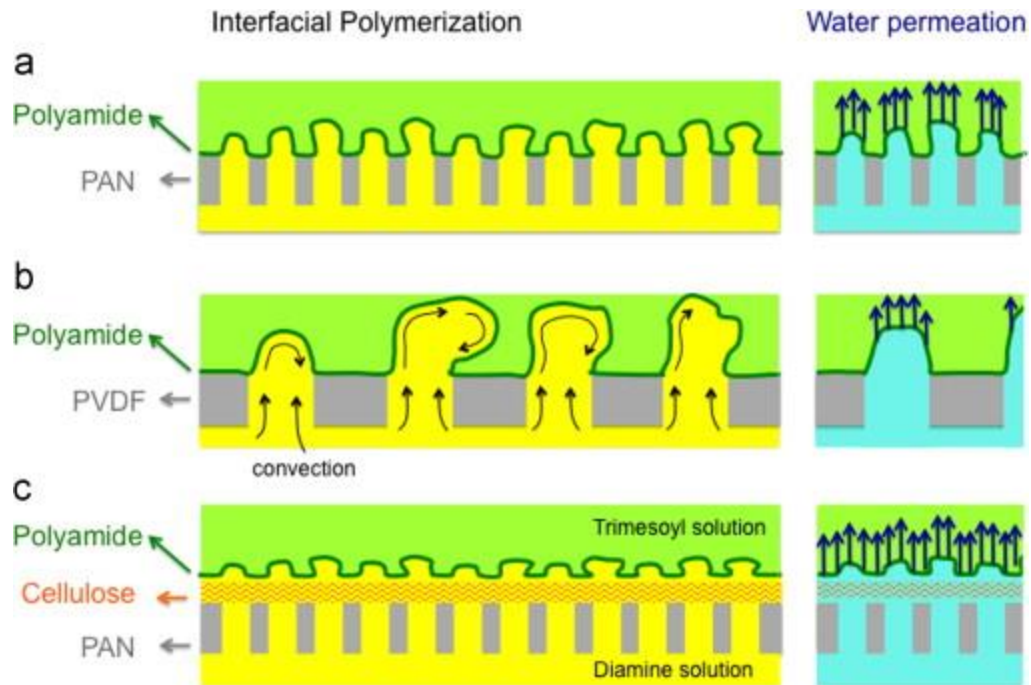


Figure 16. Thin polyamide layer formed by interfacial polymerization on supports of different porosities: (a) PAN, (b) PVDF and (c) cellulose coating on porous PAN. Membrane soaked in diamine aqueous solution (yellow) in contact to trimesoyl chloride organic solution (green). Right: Probable water permeation path. (Adapted from reference¹⁵⁸)

Table 4 summarizes the permeances, MWCO and NaCl rejections of multilayer membranes prepared with cellulose and polyamide. The rejection of PEG molecules with molecular weight of 200 g mol^{-1} was higher than 90% for all membranes. A 5-fold increase of water permeance was observed when introducing a thin cellulose layer, keeping the MWCO below 200 g mol^{-1} , but with much lower salt rejection (only 5.4 %). This kind of membrane could be useful for separation of mixed organic/inorganic waste streams in pharmaceutical, food and agrochemical industries. For instance in biotechnology, reactions or treatments using microorganisms in many cases requires salt removal, since they cannot withstand the osmotic pressure caused by high salt concentration.¹⁵⁹

Table 4. Water permeance of membranes constituted by layers of interfacial polymerized polyamide on regenerated cellulose and on PAN porous support.

Coating solution (wt% Cellulose in THF)	Water permeance (L m ⁻² h ⁻¹ bar ⁻¹)	MWCO (g mol ⁻¹)	NaCl Rejection ^a (%)
0	0.6 ± 0.7	< 200	58 ± 22
0.6	3.2 ± 0.8	< 200	5.4 ± 0.4
1.0	1.7 ± 0.1	< 200	19 ± 1
1.6	1.4 ± 0.2	< 200	36 ± 3
1.9	1.1 ± 0.1	< 200	82 ± 6

A significant improvement of salt rejection was obtained with a thicker cellulose interlayer (coating solution concentration 1.9 wt %). In this case the salt rejection was 41 % higher and at the same time the water permeance was 83 % higher than when the polyamide layer prepared directly on PAN. Also the reproducibility was higher. It is important to note that this comparison was done using the same monomers, same PAN support and under the same preparation conditions. Changing the support, monomers and/or further optimization of the interfacial polymerization preparation conditions might lead to other tuned salt rejection and permeance values.

The reason for the larger permeance with cellulose interlayer might be the following. In the case of polyamide cast directly on porous supports (Figure 13 and Figure 14) probably only the part of the layer forming pockets or globular nodules coming out of the pores will be available for water transport. The areas of

the polyamide layer between the pores are strongly adhered to the PVDF or PAN dense surface and are practically impermeable to water. The hydrophilic cellulose swells with water, which can then freely permeate the whole polyamide layer above it without restrictions (Figure 16, right). The effective total area for water permeation is therefore larger with the cellulose layer.

4.2. Cellulose Membranes from Solutions in Ionic Liquid

The second method chosen for the preparation of cellulose membranes was based on the dissolution of cellulose in ionic liquids and does not require additional solvents other than [C2mim]OAc and water as coagulation bath. For this reason the method can be considered greener than method 1 or any other processes involving cellulose dissolution in aggressive solvents. The cross sections of multilayer cellulose membranes prepared on PSU is shown in Figure 17. Thicknesses of 0.4–5.6 μm were obtained by coating cellulose/[C2mim]OAc solutions with different concentrations on asymmetric porous supports. Thicker cellulose membranes were prepared directly on polyester nonwoven. High magnification of the cellulose coating (Figure 17 c) image shows a regular structuration parallel to the surface. FESEM and AFM images of the coating surface prepared from cellulose/[C2mim]OAc solutions are shown in Figure 18. The surface is slightly different from regenerated silyl cellulose prepared by Method 1. The corresponding X-ray diffractogram is also depicted in Figure 17, confirming the crystallinity of the cellulose coating. Peaks appear in the same scattering angles, indicating that the same form of cellulose, i.e.

cellulose polymorph II predominates in both regenerated celluloses from the silylation process and the dissolution in ionic liquid. Amorphous cellulose has a broad peak with a maximum around 20–22°. ¹⁶⁰ There is an overlap of the broad amorphous peak and the sharper one for the crystalline form II in this region at 20°. Similar is observed for the regenerated cellulose obtained by silylation and acid treatment. However, the peak for the regenerated silyl cellulose at 20° is broader than for that obtained for coatings from dissolved cellulose in ionic liquid, indicating lower crystallinity, smaller crystallites and/or non-uniformity within the crystallites. Cellulose crystallites are normally small (<5 nm), the exact determination of the crystal lattice by X-ray diffractogram is not always possible and the degree of crystallinity might have a large variation for the same sample. ^{161, 162}

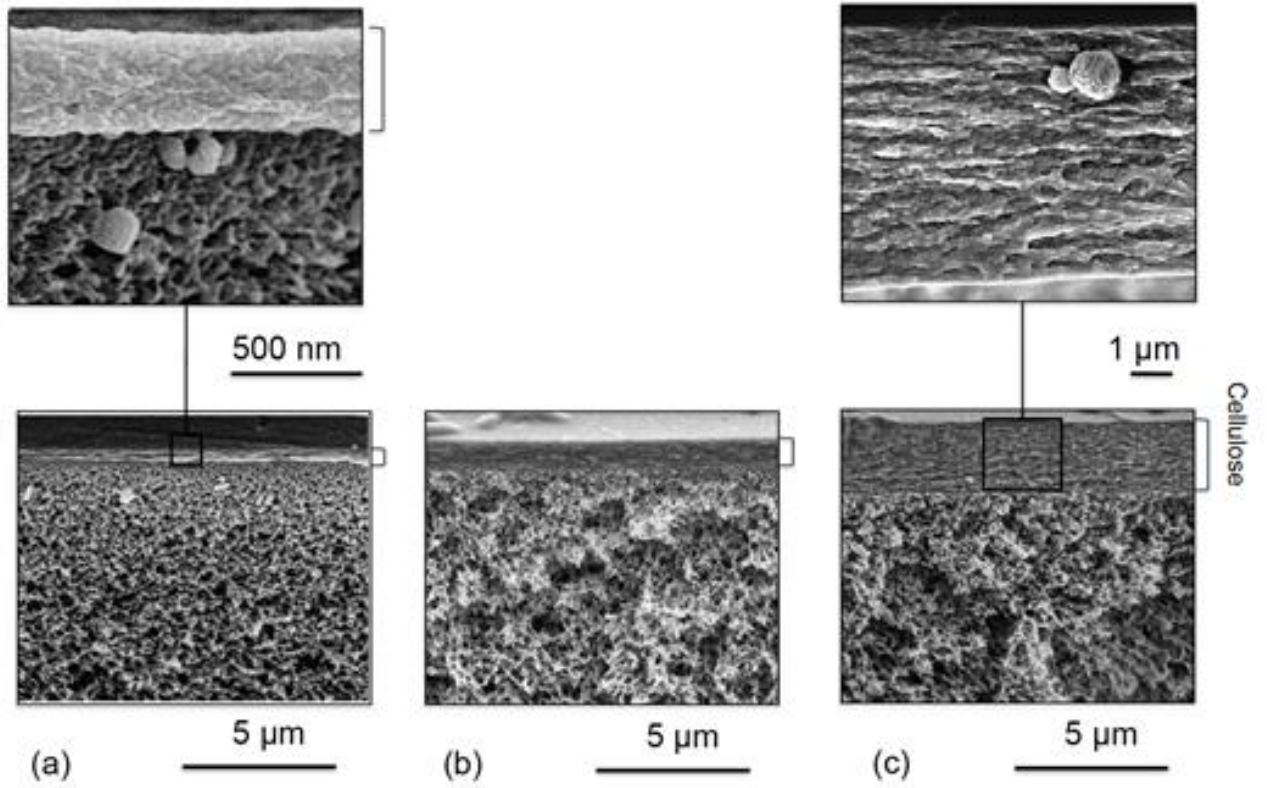


Figure 17. Cross section (FESEM) images of membranes prepared from (a) 2, (b) 5 and (c) 10 wt % cellulose solutions in [C2mim]OAc by casting on polysulfone asymmetric porous supports and immersion in water.

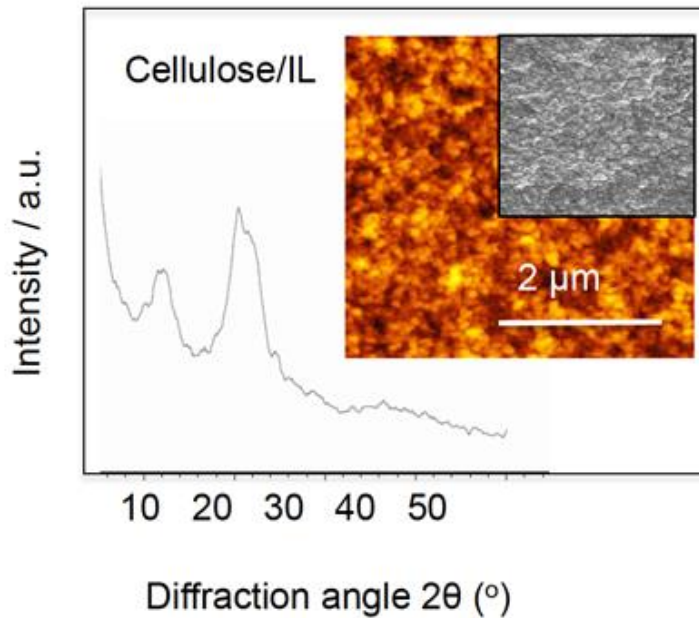


Figure 18. X-Ray diffractogram of cellulose after dissolution in [C2mim]OAc and immersion in water; inset: AFM and FESEM images of coating surfaces prepared with 5 wt % cellulose/[C2mim]OAc solution.

The contact angles of coatings obtained from cellulose/[C2mim]OAc solutions were 22.0–26.1°, lower than for regenerated silyl cellulose (5), confirming the total availability of OH groups for interaction with water.

The performance of membranes prepared from cellulose/[C2mim]OAc solutions is summarized in Table 5 and Figure 19. The increase of cellulose concentration resulted in lower MWCO with simultaneous reduction of the water permeance and increase of coating thickness. PSU as a porous support led to the highest water permeance and lowest MWCO.

Table 5. Water permeance and solute rejection for multilayer membranes prepared from Cellulose/[C₂mim]OAc.

Coating solution (%) Cellulose in / [C ₂ mim]OAc)	Support	Thickness of cellulose layer (μm) ^a	Water permeance (L m ⁻² h ⁻¹ bar ⁻¹)	Rejection of PEO 100 Kg mol ⁻¹ (%)	MWCO (g mol ⁻¹) ^b
0	PSU	0	(1.1 ± 0.2) x 10 ³	100	92,000
2	PSU	0.4	262.9 ± 3.9	95	81,000
5	PSU	0.9	25.6 ± 0.3	95	60,000
10	PSU	2.3	13.8 ± 1.0	100	3,000
0	PEI	0	(1.3 ± 0.2) x 10 ³	48	275,000
5	PEI	0.7	9.9 ± 0.1	100	67,000
10	PEI	3.9	1.75 ± 0.05	100	7,000
5	Polyester no-woven	3.5	11.4 ± 0.9	97	46,000
10	Polyester no-woven	6.8	1.2 ± 0.05	100	5,000

^aEstimated by FESEM (Figure 12). ^bPEO with MW 100 kg mol⁻¹. ^cEstimated by GPC data from Figure

18.

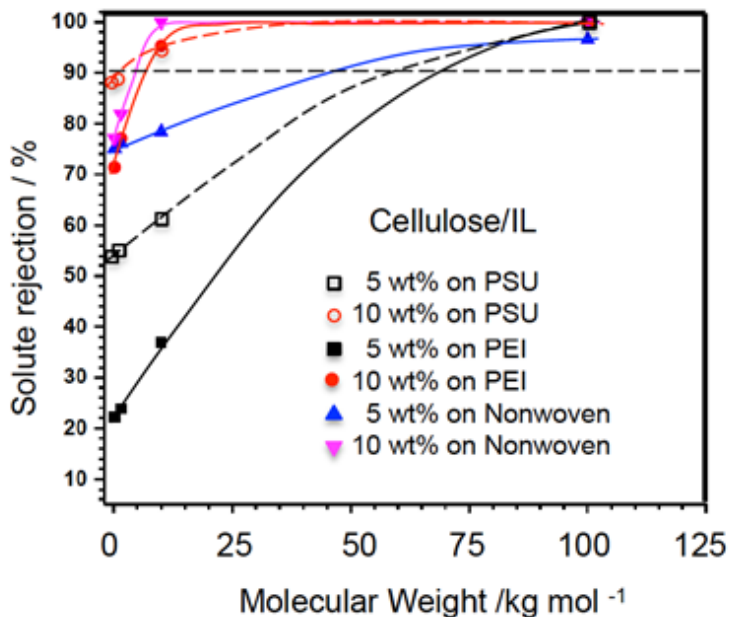


Figure 19. PEG rejections of cellulose membranes prepared from solution in [C2mim]OAc coated on PSU and PEI porous supports or directly on polyester nonwoven.

4.2.1. Stability of Cellulose/Ionic Liquid Membranes in Organic Solvents

One of the advantages of cellulose is the lack of solubility in water and most of the organic solvents. To investigate the solvent resistivity of cellulose membranes prepared with ionic liquid via phase inversion, we immersed regenerated cellulose coatings obtained from 5 wt % and 10 wt % solutions in [C2mim]OAc without any support in THF, hexane, DMF, NMP and DMAc for 1 h, 12 h, 24 h and for one week and the weight loss was measured by measuring the weight before and after the experiment. The membranes showed no visible change and no weight loss, indicating that the cellulosic membranes are resistant in these solvents.

These membranes have potential use in solvent filtration and separation. The challenge would be to use the support that will not be dissolved in harsh organic

solvents. In that case membranes would be prepared on non-woven polyester support or self-standing without any support which in that case, would require less robust cell to measure the separation efficiency or usage of mechanical support during the filtration.

Based on these findings, pristine cellulose membranes could be a potentially valuable in the field of solvent filtration.

4.3. Fouling Evaluation of Cellulose Membranes

In this chapter we report the results of testing membranes with model foulants. Since cellulose membranes have a large number of OH and smooth surface and predominantly negative charge in wide range of pH, the expectation is that the resistance to fouling would be high.

Membranes were tested with Suwanee River Humic Acid (SRHA), as a main foulant model, together with commonly used proteins bovine serum albumin (BSA) and gamma globulin to investigate resistivity. After cross flow experiment with humic acid, no obvious permeance decline was noticed, as compared to commercial membranes, which after had a severe decline (Figure 22, 23, 24).

Most common used and explored foulants in the literature are bovine serum albumin, gamma globulin, polysaccharides and humic or fulvic acids¹⁶³. Humic acid is found in wastewater, sea water, fresh water and brackish water is in very low concentration $0.1 \text{ mgL}^{-1} - 20 \text{ mgL}^{-1}$, but it presents 50-80 % of the dissolved natural

organic matter in the aquatic systems. We chose Suwanee River Humic acid as a foulant model, commonly used in the literature for this purpose, due to its purity (no fulvic acid or ashes). The fouling tendency of the humics is due to their ability to bind divalent salts, e.g. calcium that forms a bridge between the membrane and humic. Nyström et al. (1996)¹⁶⁴ showed that humics were most harmful in membranes that were positively charged and containing alumina or silica.

Schäfer et al. (2000)¹⁶⁵ studied the effect of solution chemistry and concentration polarization on the morphology of the humic acid fouling layer on MF membranes. They reported irreversible fouling on all the membranes, when high calcium concentration was present in the feed. They showed that the hydrophobic part of the humic acid was deposited favorably on the membrane surface. They also demonstrated that calcium-humate complexes caused the highest flux decline due to the compactable floc-like structures. Zydney et al. (1999)¹⁶⁶ pointed out the importance of humic agglomerates on the fouling.

Kabsch-Korbutowicz et al. (1999)¹⁶⁷ demonstrated that the most hydrophilic membrane tested, regenerated cellulose, prepared in a different way than in this work, had the least proneness to fouling by humic acid and that the presence of mineral salts e.g. calcium intensifies the rate of fouling.

Tu et al. (2001)¹⁶⁸ showed that more negatively charged, hydrophilic membrane are less prone to fouling due to the fewer interaction between the functional groups of the organics and the polar groups on the membrane surface.

Fouling by humic acid has been reported to be greatly promoted by low pH, high ionic strength, high calcium concentration and high foulant concentration.¹⁶⁹⁻¹⁷¹

4.3.1. Fouling Evaluation with Bovine Serum Albumin, Gamma Globulin and Humic Acid

The membranes were first tested with 0.01 % BSA (1 gL^{-1}) and γ -Globulin (1 gL^{-1}), dissolved in PBS buffer and used fresh for each test (3.5 bar pressure, 1300 ml/min suction speed). Secondly in a separate experiment the membranes were tested with 100 mg/L of aqueous humic, (Suwannee River Humic Acid) at pH 8.

The membranes showed stable BSA permeance and high rejection (Figure 20, A Table 6). Thin cellulose coating showed higher flux recovery when compared to control polysulfone membrane (Figure 20 B). This indicates that the membrane would need only hydraulic backwash for cleaning.

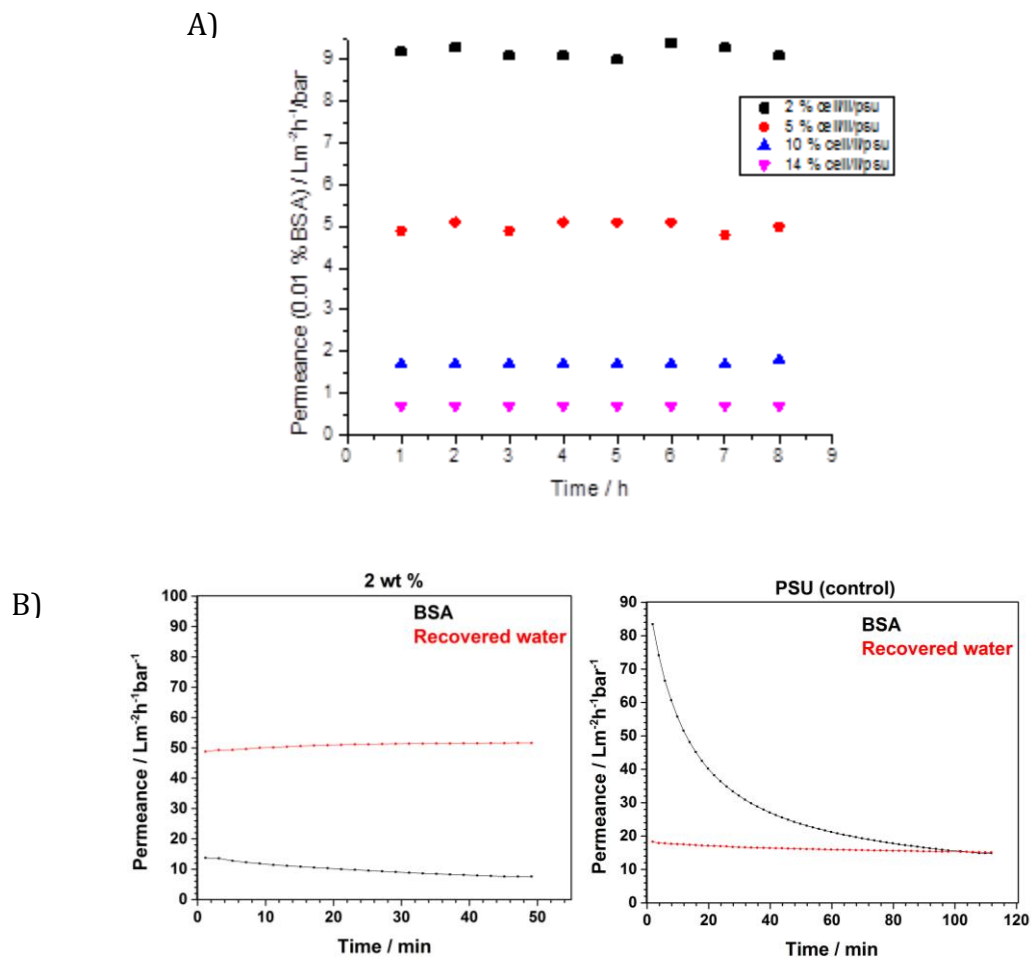


Figure 20. A) BSA solution permeance (1 gL^{-1}) for membranes prepared from 2 %, 5 %, 10 % and 14 % cellulose/ionic liquid solutions. B) Flux recovery and BSA permeance for 2 wt % and control PSU membrane

Table 6. Pure water permeance and rejection for BSA and gamma globulin for 2 %, 5 %, 10 % and 14 % cellulose/ionic liquid membranes

Cellulose coating	Pure water permeance $\text{Lm}^{-2}\text{h}^{-1}\text{bar}^{-1}$	BSA (1 mg/mL) rejection	γ -Globulin (1 mg/mL) rejection
2 wt %	70	72 %	100 %
5 wt %	22	100 %	100 %
10 wt %	5	100 %	100 %
14 wt %	2	100 %	100 %

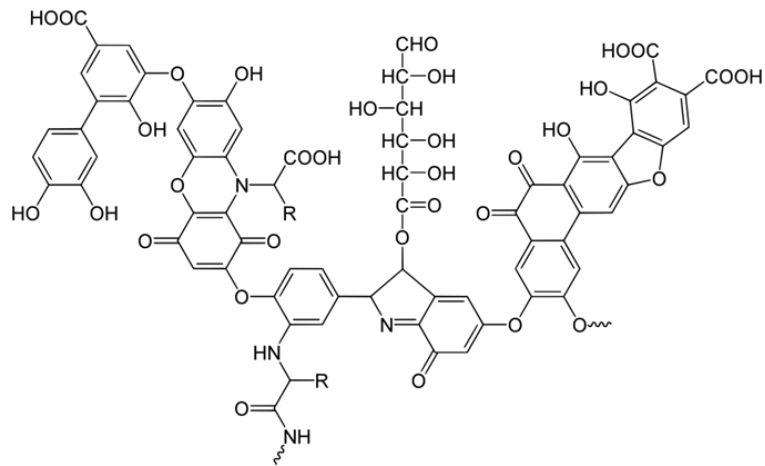


Figure 21. Humic acid structure (adapted from¹⁷²)

Humic acid (Figure 21), main component of humic substances, is a complex mixture of many acids and its main functional groups are phenolic and carboxylic. It is a naturally oxidized molecule and this makes it mainly negatively charged. To investigate the membrane resistivity towards humic acid, cellulose membranes have been filtered with humic acid solution for several hours and compared to commercial PVDF and PSU as well as control PSU membrane.

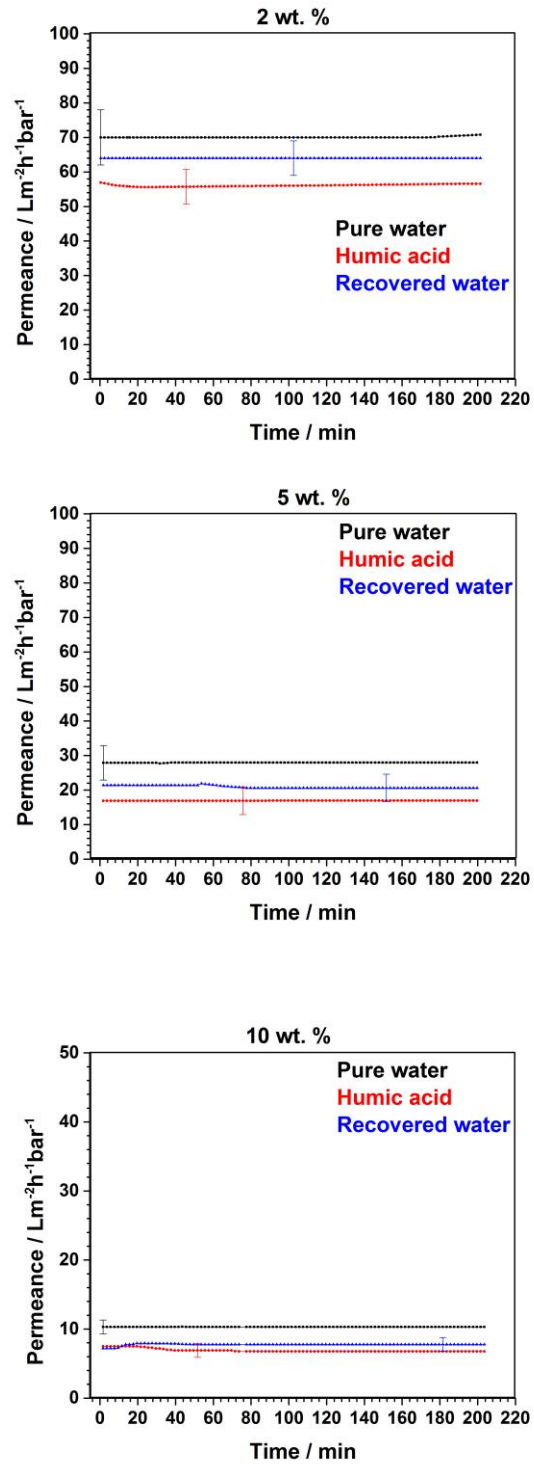


Figure 22. Pure water permeance and water permeance in the presence of humic acid for membranes prepared from 2, 5 and 10 wt. % cellulose solutions

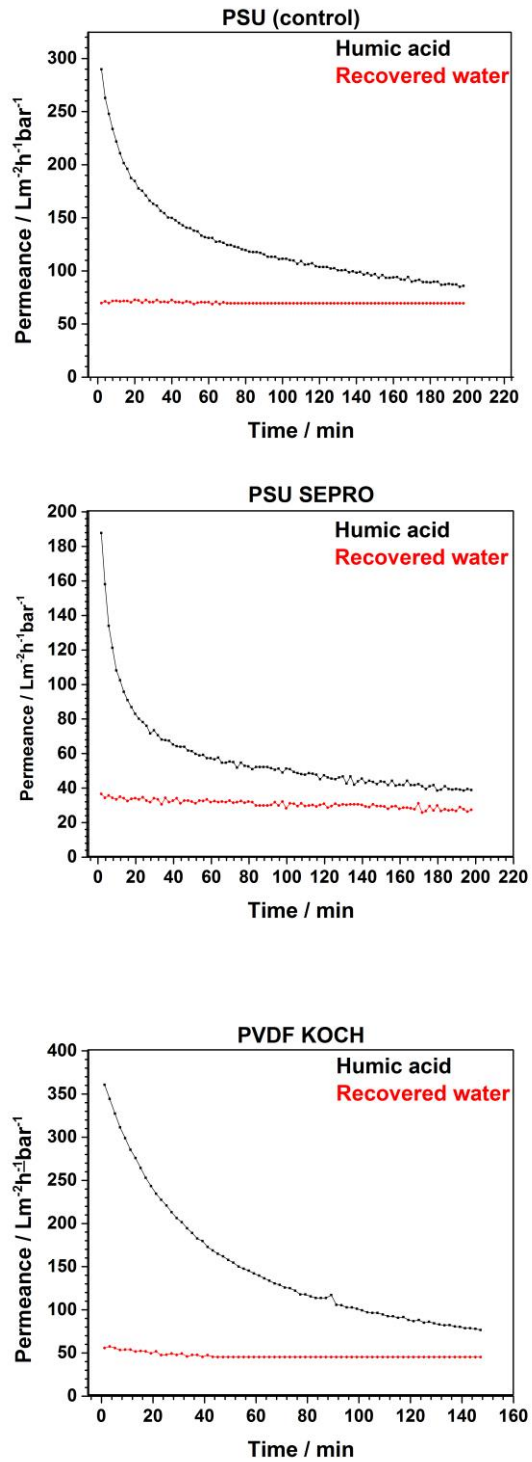


Figure 23. Water permeance in the presence of humic acids for commercial PVDF and PSU membranes as well as PSU membranes prepared in our lab (control).

In Figure 22 the pure water permeance, water permeance with humic acid and recovered water permeance is presented for 2, 5 and 10 wt % cellulose membranes under the same condition for several hours.

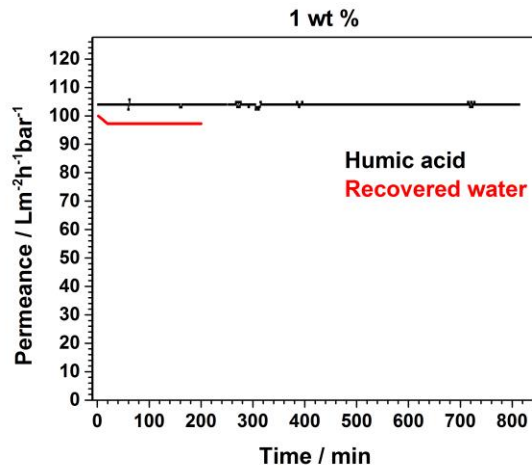


Figure 24. Pure water permeance and water permeance with humic acid for a membrane prepared from a 1 wt % cellulose solution

Commercial membranes with similar MWCO, such as polyvinylidene fluoride (PVDF) and polysulfone (PSU) were used as comparison or control throughout the experiments (Figure 23). These membranes showed severe flux decline and much lower recovery than that of 2 wt % (similar MWCO as PVDF) cellulose membranes. Cellulose membranes manifested no permeance reduction in the presence of humic acid when compared to the control membranes. Even thinner cellulose layer obtained with 1 wt % polymer coating showed no severe flux decline, when the humic acid was introduced in the water used as feed (Figure 24).

At pH 8 humic acid has zeta potential of -26.3 ± 0.3 and cellulose membrane is negatively charged. Thus electrostatic repulsion will cause less severe humic

adsorption. PVDF is negatively charged membrane (KOCH) with large pore size (120 kDa MWCO) and initial permeance of approximately $400 \text{ Lm}^{-2}\text{h}^{-1}\text{bar}^{-1}$, PSU from SEPRO has 20 kDa MWCO and initial permeance around $200 \text{ Lm}^{-2}\text{h}^{-1}\text{bar}^{-1}$ and PSU produced in our lab had MWCO of 90 kDa and initial permeance around $300 \text{ Lm}^{-2}\text{h}^{-1}\text{bar}^{-1}$. Higher initial flux will cause higher permeation drag force thus faster adsorption and internal pore blockage.

4.4. Oil-Water Separation by Cellulose Membranes

For the purpose of extracting crude oil from oil reservoir water is injected into the well in order to increase the reservoir pressure and drive the crude oil up to the surface where it can be pumped. This usually occurs in secondary and tertiary recovery. The method where water is used to pump out the oil is often referred to as the water flooding.

Water injection provides additional pressure in the reservoir stimulating oil production and it pushes it towards the well. The water used for flooding is commonly reused as "produced water". Since it is not sufficient, other sources of so called "make-up" water are used, which can be seawater, aquifer water and river water.

Produced water is frequently contaminated with various hydrocarbons, metals and salts, depending on their origin. Water injected in the well is most likely quite salty, giving that seawater is the most abundant choice especially for offshore refineries.

Salt concentration in produced water can be from several ppm to 300,000 ppm.^{67, 173, 174} Salt exacerbates scaling and corrosion, causing problems in process equipment and piping. Presence of salt is practically inevitable in oil and gas industry. Sodium chloride was added in our tests with a concentration of 80 g/L to mimic real produced water conditions and to prepare solution that should promote more severe fouling to evaluate the performance of cellulose layer.

Introduction of salt decreases the critical micelle concentration and also the partitioning of the surfactant between the two phases (oil/water). Salt can compress the electric double layer around particles or oil droplets in emulsions or on membrane surfaces.

Fouling can be classified as reversible and irreversible, backwashable and non-backwashable. Reversible fouling is due to partial pore blockage and cake filtration, whilst irreversible fouling is due to the internal pore blockage and adsorption of foulants onto the membrane surface.⁶² Non-backwashable fouling cannot be removed with hydraulic backwash but it can be removed by chemical cleaning. On the other hand, irreversible fouling cannot be removed with chemical cleaning or any other method (backwash, flushing, wiping) and membrane will not recover its original permeability.⁵⁹

To assess the extent of fouling of cellulose membranes towards oil in water emulsions, the flux recovery ratio and the total flux loss or flux decay were calculated from equations (1) and (2) mentioned in Chapter 2.2.

The flux recovery ratio represents the amount of pure water permeance that can be recovered after testing the membrane with oil in water emulsion. The flux decay ratio is the ratio between the pure water permeance and that of the emulsion, tested with the same membrane.

Several factors affect the extent of fouling. Charge characteristic is an important one. Foulant-foulant and membrane-foulant electrostatic and hydrophobic interactions are the main reason for adsorption or lack of that. Besides fouling, concentration polarization can be a reason for the flux decline.

Oil-water separation was carried out under constant pressure of 5 bars, investigating the effect of concentration, pH and surfactants on the oil removal when compared to the control polysulfone membranes. In Figure 25 a schematic illustration of the experiments is presented. Membranes were placed in stainless steel cell connected to the nitrogen gas cylinder under constant stirring. Firstly, pure water permeation was measured, followed by oil in water emulsion permeation. Finally pure water permeation was measured again. Between the measurements, the membranes were not removed; they were simply rinsed with water.

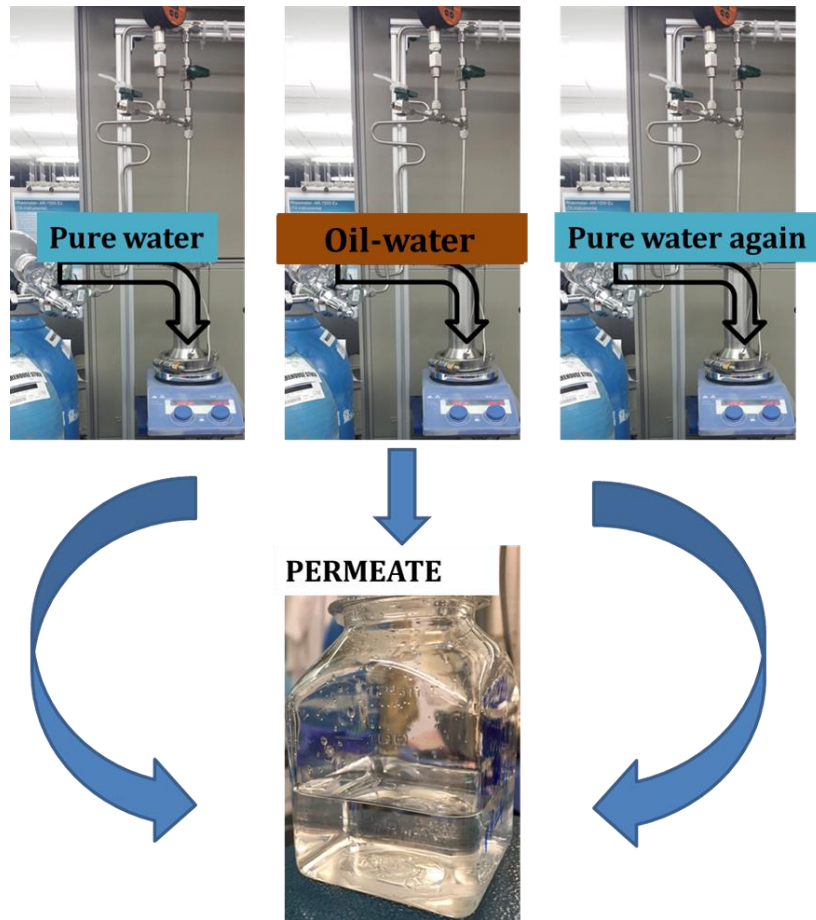


Figure 25. Oil-water filtration experiment

Surfactants are widely used in the petroleum industry due to their ability to decrease the interfacial tension between water and oil, stabilizing emulsions and facilitating water intrusion in rock capillary pores. In order to prepare an emulsion where the size of oil droplets is less than $10\ \mu\text{m}$, the addition of surfactant is crucial. Surfactants are amphiphilic compounds constituted by a hydrophilic (water soluble) head and a hydrophobic (oil soluble) tail.

Three different surfactants were used, anionic sodium dodecylbenzylsulfonate (SDBS), cationic hexadecyltrimethylammonium bromide (CTAB) and neutral Polysorbate® 80 (Tween® 80) (Figure 26).

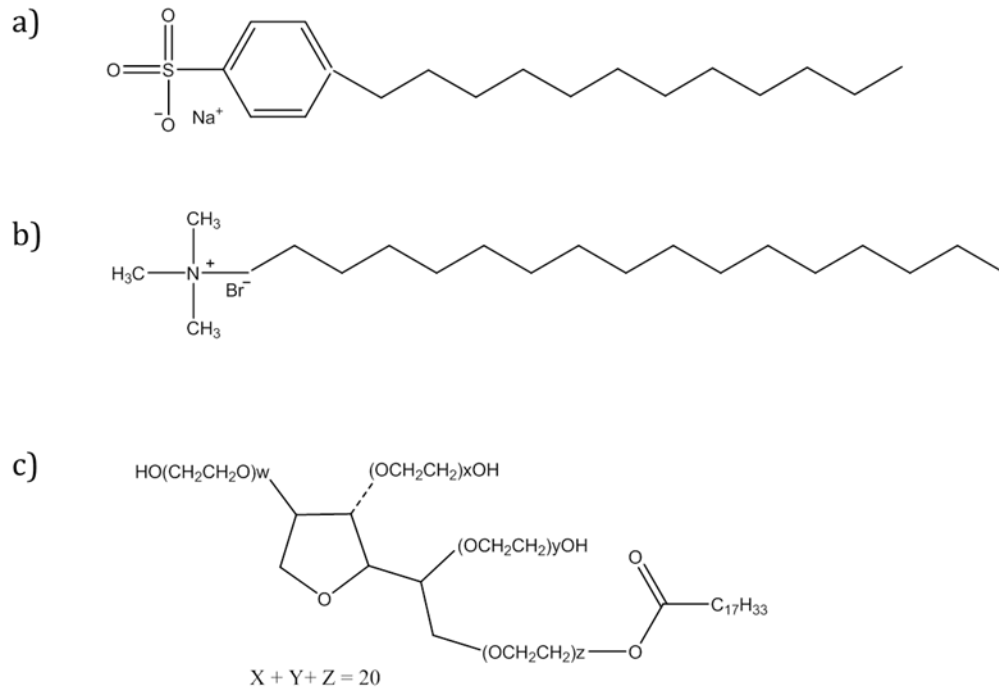


Figure 26. Three surfactants used in the experiment: (a) sodium dodecylbenzenesulfonate (SDBS); (b) hexadecyltrimethylammonium bromide (CTAB) and (c) Polysorbate 80 (Tween 80)¹⁷⁵

The anionic surfactant contained an anionic benzenesulfonate group as head. The cationic one contained quaternary ammonium and the neutral surfactant does not have a charged group.

Particle size analysis revealed that the oil in water emulsion stabilized by the anionic surfactant has droplets with size in a range of 1-2 μm , while those stabilized by cationic and non-ionic surfactants have droplets with size in range of 200-300 nm and 200 nm, respectively.

Droplet sizes and the average zeta potential of 200 ppm oil in water emulsions containing different surfactants at pH 4, 8 and 11 are shown in Table 7-9.

Table 7. Droplet size and zeta potential of 200 ppm oil in water emulsion with SDBS at pH 4, 8 and 11.

	200 SDBS pH 4	200 SDBS pH 8	200 SDBS pH 11
Droplet size / nm	2425 \pm 759.0	1619 \pm 76	759 \pm 136
Zeta potential / mV	-34 \pm 9	-36 \pm 4	-62 \pm 2

Table 8. Droplet size and zeta potential of 200 ppm oil in water emulsion with CTAB at pH 4, 8 and 11.

	200 CTAB pH 4	200 CTAB pH 8	200 CTAB pH 11
Droplet size / nm	218 \pm 6	315 \pm 72	231 \pm 12
Zeta potential / mV	12.1 \pm 0.3	-2 \pm 1	-12 \pm 4

Table 9. Droplet size and zeta potential of 200 ppm oil in water emulsion with Tween 80 at pH 4, 8 and 11.

	200 TWEEN pH 4	200 TWEEN pH 8	200 TWEEN pH 11
Droplet size / nm	210 \pm 3	227 \pm 11	214 \pm 5
Zeta potential / mV	-4.3 \pm 0.2	-4.7 \pm 0.6	-2 \pm 1

The larger droplet sizes detected with anionic surfactant reflect higher interface tension and a less stable emulsion, when compared to the other two surfactants. Oil-in-water emulsions containing anionic surfactant were the least stable ones, having oil visually separated from water within 3 days of preparation. Emulsions containing cationic surfactant were stable for 7 days, while emulsions containing non-ionic surfactant were stable for several weeks.

To investigate the stability of cellulose membrane in a broad range of pH, the prepared oil-in-water emulsions were characterized in at pH 4, 8 and 11.

The change of pH might affect the membrane and the emulsion itself. Membrane functional groups might protonate and deprotonate over wide pH range, and so will the surfactant molecules in the emulsion, leading to different charge density values. Charge of the membrane and charge of the ions in the solution will cause either electrostatic repulsion or attraction, which will directly affect the performance of the membrane.

The zeta potential of a membrane prepared from a 2 wt % cellulose solution and the zeta potential of surfactant-oil droplets in an emulsion containing 200 ppm crude oil and three surfactants are shown in Figure 27a and 27b.

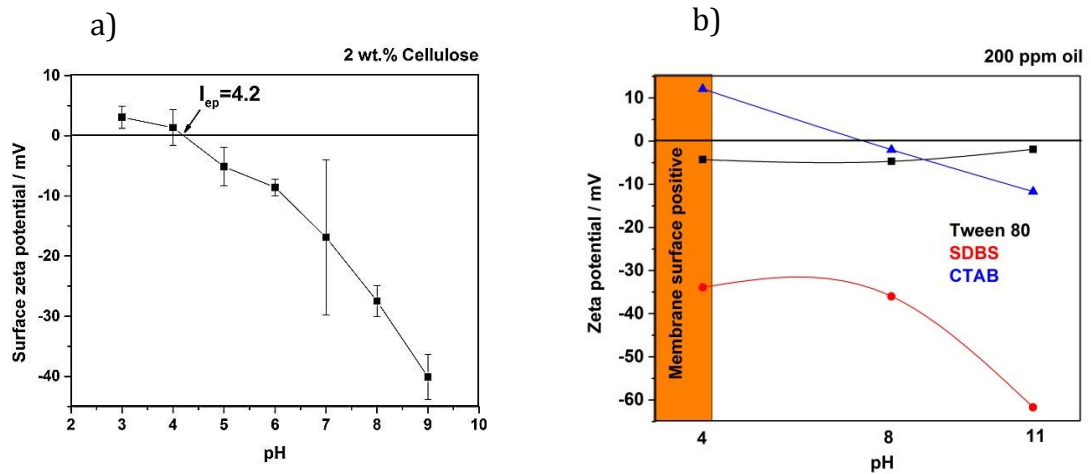


Figure 27.(a) Zeta potential of a membrane prepared from 2 wt % cellulose solution, measured with water at different pH values and (b) Zeta potential of surfactant-oil droplets in water for an emulsion containing 200 ppm crude oil and 20 ppm SDBS, CTAB and Tween.

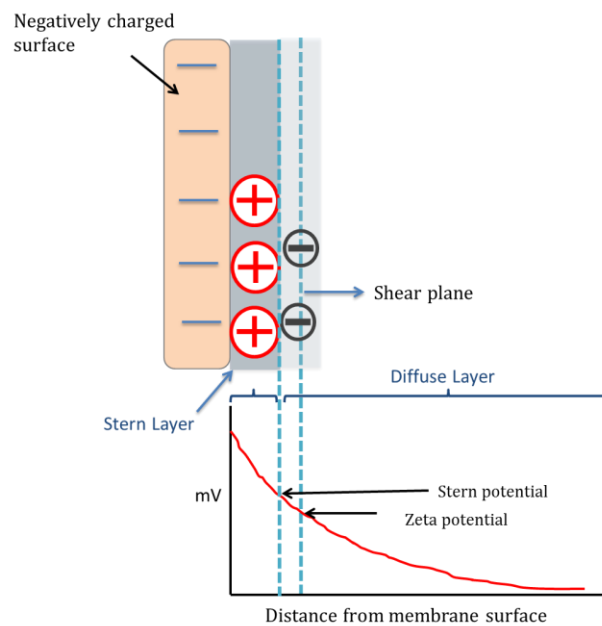


Figure 28. Zeta potential

When a charged particle or droplet is suspended in liquid, ions of opposite charge will be attracted to its surface. Cellulose membrane, having negative charge at high

pH will attract positive ions to bind to its surface. The first layer of ions close to the surface of the membrane will be strongly bound (Stern layer) to it and ions that are further away will be more loosely bounded, forming what is called a diffuse layer.¹⁷⁶

The layer of counter-ions next to the Stern layer is still relatively strongly bounded to the surface constituting the outer Helmholtz layer. If the surface is moved, this ion layer would move with it and in a practical measurement, the zeta potential corresponds to the potential at this layer (Figure 28). Changes in pH will change how strongly the ions and counter ions will be bounded to the surface, affecting the zeta potential.

Similarly, the zeta potential of the surfactant-oil droplets depends on pH too. Low pH, favor a positive (or less negative) zeta potential; high pH favors a more negative zeta potential (Figure 27).

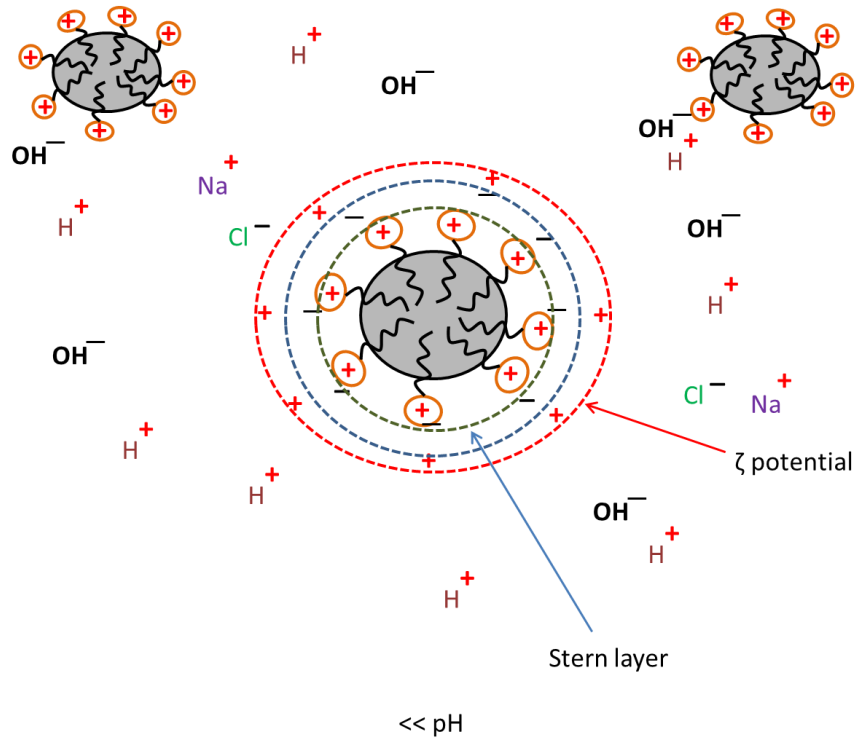


Figure 29. CTAB-oil droplet at low pH

The surfactant molecules place themselves in the interface between the oil droplets and the water, with the hydrophobic tail penetrating the oil phase while the water soluble head remains in the contact with the water phase. A positively charged head attracts negative counter ions from the water phase, which then attract positive ions, determining the zeta potential (Figure 29). Similarly, negatively charged water soluble head of anionic surfactant will attract positive counter-ions from the aqueous phase, which then attract negative counter-ions, leading to a negative zeta potential, as depicted for SDBS-oil droplets in Figure 30.

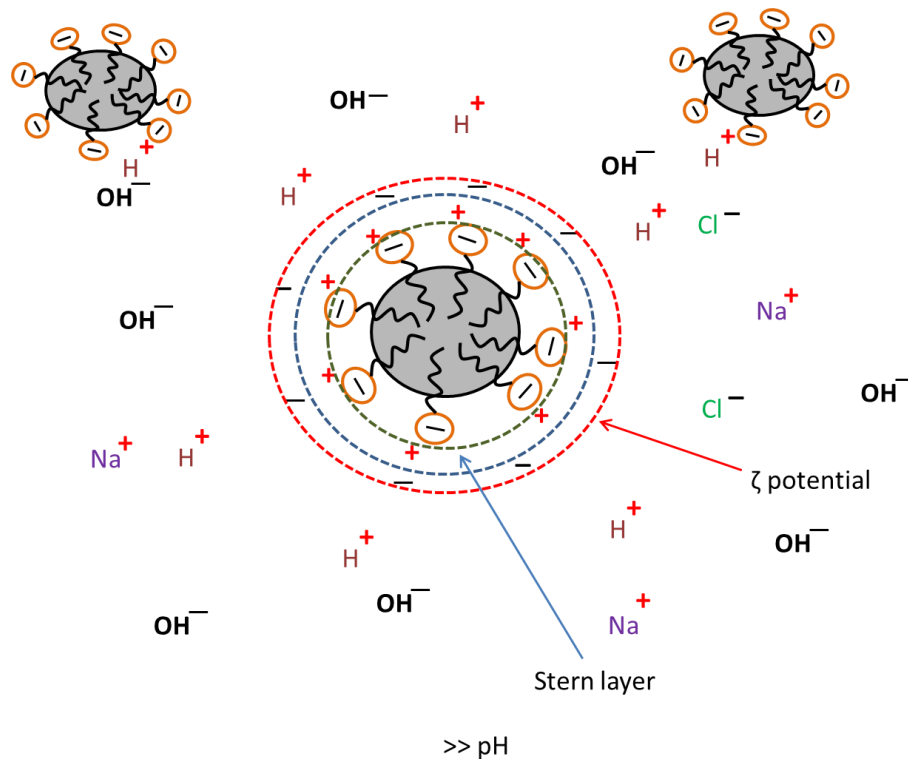


Figure 30. SDBS-oil droplet at high pH

At low pH, positively charged CTAB-oil droplets would be repelled by the positively charged membrane. The membrane becomes negative above pH 4.2. SDBS-oil droplets are negative in the whole investigated pH range and should be more effectively repelled as the pH is increased above 4.2. Droplets in emulsions containing non-ionic surfactants have zeta potential not far from zero (slightly negative) in the whole pH range.

Membranes prepared from 2, 5 and 10 wt % cellulose solutions were investigated using oil in water emulsions with 200, 500 and 1000 ppm oil at pH values 4, 8 and 11. Representative results are chosen here. The performance of 5 wt % cellulose membrane is shown in terms of flux recovery in Figure 31. Low flux recovery

indicates higher adsorption onto the membrane surface and therefore more irreversible fouling. Filtration of emulsions containing anionic surfactant had the highest flux recovery, similar to those with non-ionic surfactant, whilst emulsions containing cationic surfactant had the least flux recovery.

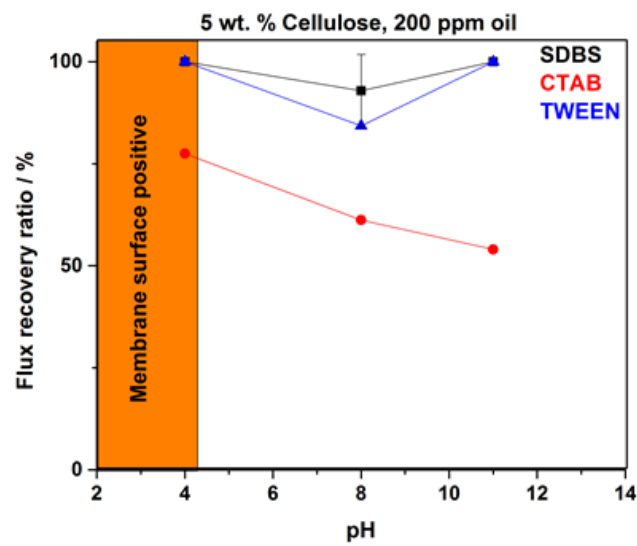


Figure 31. Flux recovery ratio for filtration of emulsions with SDBS, CTAB and Tween through 5 wt % cellulose membrane.

The effect of different surfactant and oil concentration on permeance is shown in Figure 31 and Figure 32.

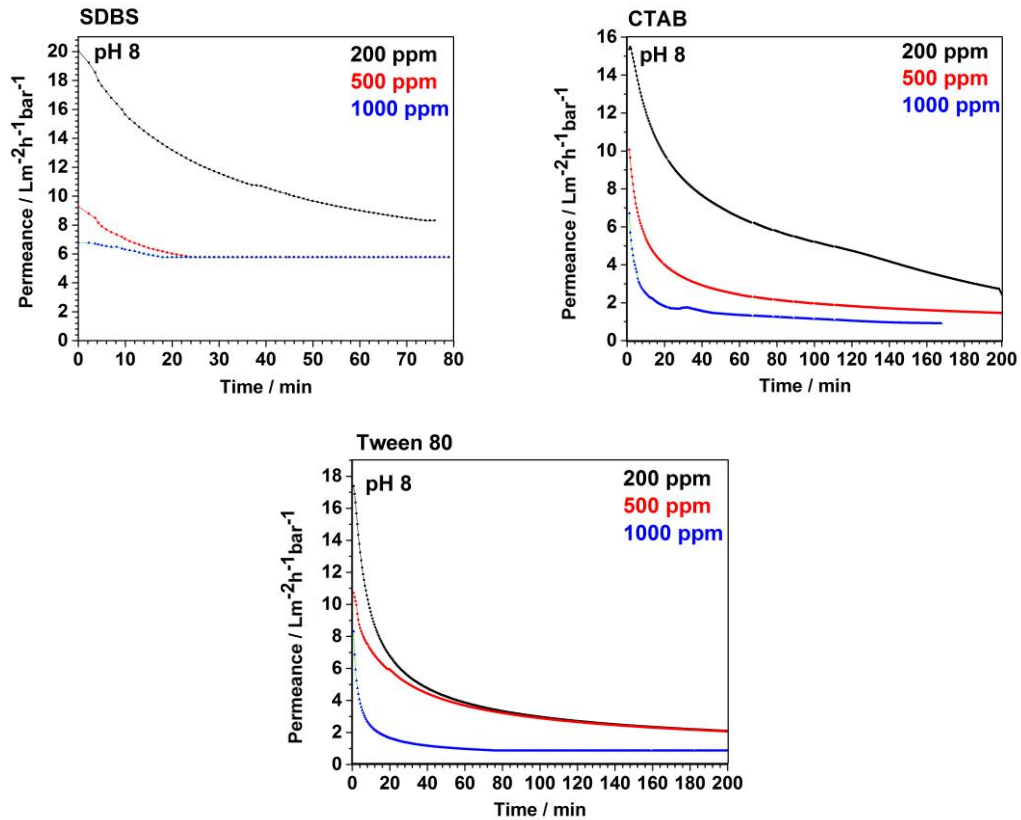


Figure 32. Emulsion permeance through 5 wt % cellulose membranes containing SDBS, CTAB and Tween and 200, 500 and 1000 ppm of crude oil at pH 8.

Filtration at pH 4 and pH 11 showed similar trend. Filtration with SDBS had the least flux decline even at higher oil concentrations (Figure 32). This is consistent with the fact that the membrane has a negative zeta potential in the whole pH range above 4.2.

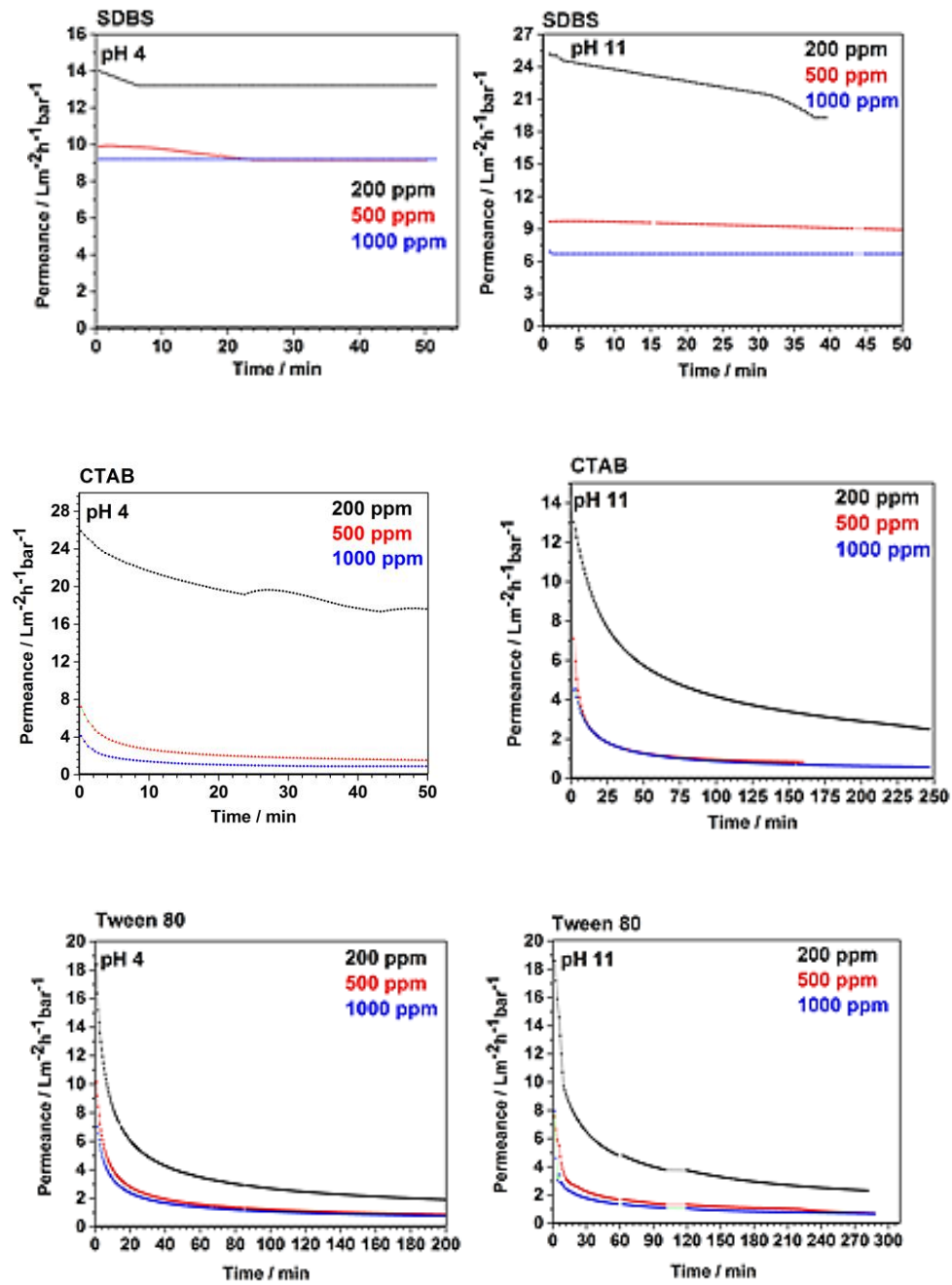
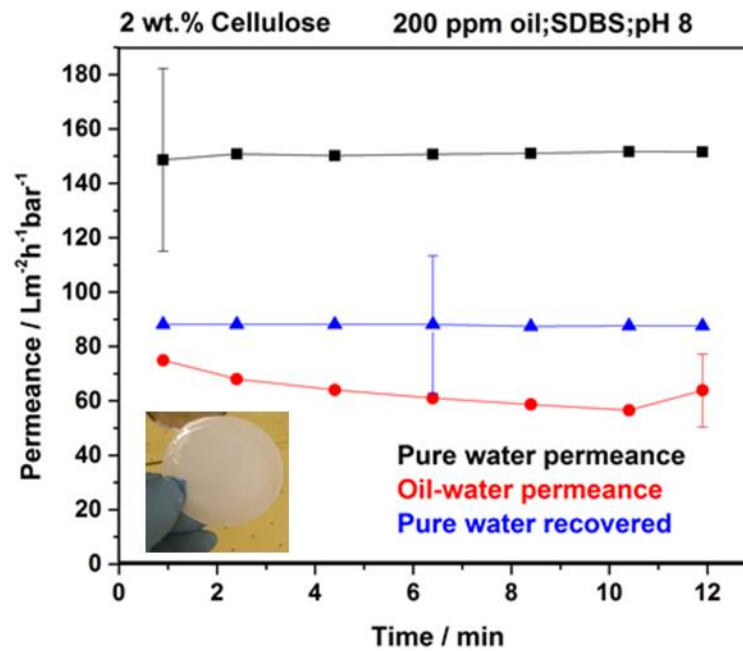
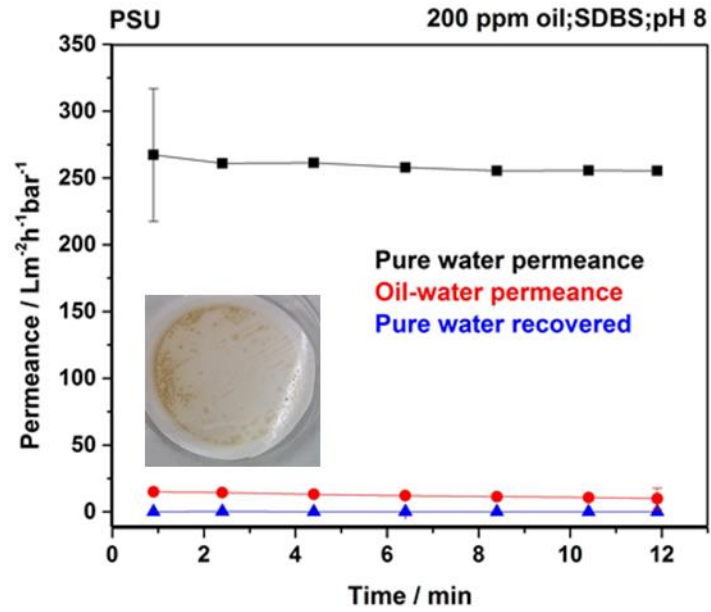


Figure 33. Emulsion permeance through 5 wt % cellulose membrane, containing SDBS, CTAB and Tween and 200, 500 and 1000 ppm of crude oil at pH 4 and pH 11.

At higher oil concentration the surface coverage with emulsified oil is faster leading to faster flux stabilization. Apart from fouling flux decline can be caused by concentration polarization, as well as membrane being mechanically compressed under pressure in a dead-end set up. A complete flux recovery eliminates a possible contribution of mechanical compression.



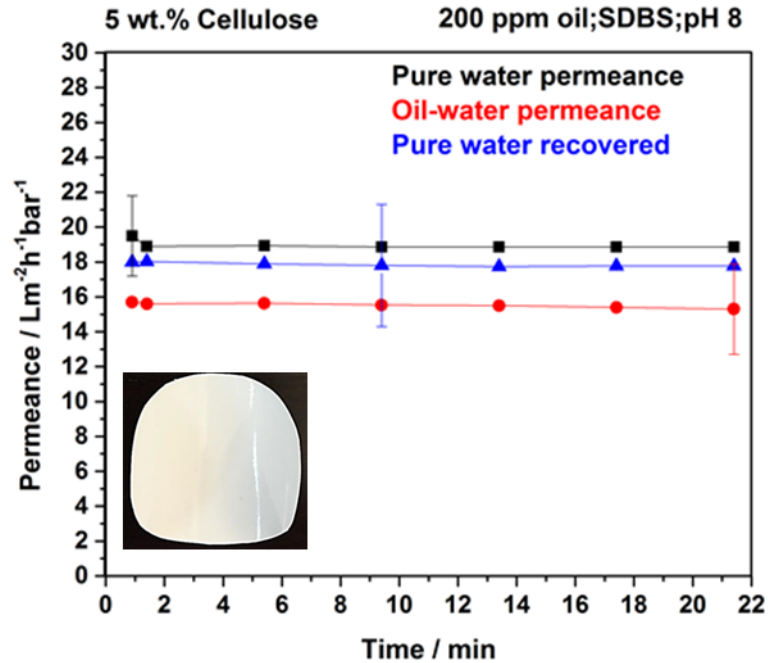


Figure 34. Pure water permeance, emulsion permeance and recovered water permeance for PSU and membranes prepared from 2 wt %, 5 wt % solutions with 200 ppm crude oil and 20 ppm SDBS at pH 8. Inset: rinsed membranes after filtration.

To confirm that emulsified oil didn't adsorb to great extent onto the thin cellulose layer, transmission electron microscopy (TEM) was used (Figure 35). Compared to polysulfone, which showed a prominent layer on top of the membrane surface, the cellulose-coated membrane had practically no foulant on the surface. The cross sections of unmodified polysulfone membranes and cellulose-coated membranes after filtering oil-water emulsion, containing SDBS and 200 ppm of crude oil at pH 8 are imaged in Figure 34.

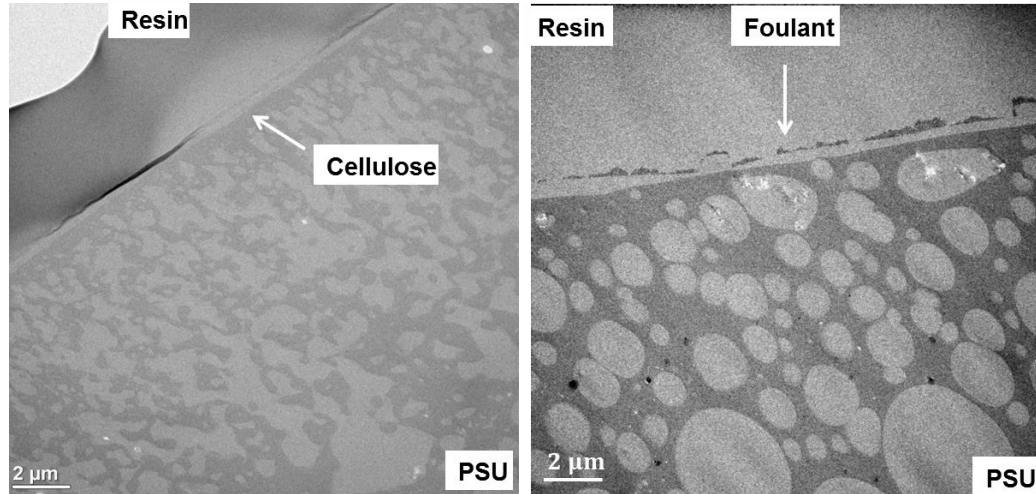


Figure 35. TEM images of membrane cross sections after filtration of oil-water emulsions containing 200 ppm of crude oil and SDBS at pH 8. A 2 wt % cellulose membrane is shown on the left side and polysulfone is shown on the right.

Although PSU had higher initial water permeance and reasonable emulsion permeance, the water permeance recovery was almost zero. This leads to the conclusion that the PSU surface was irreversibly fouled by adsorption and internal pore blockage, which was also visible on the membrane even after rinsing. The membrane with the thinnest cellulose coating ($0.4 \mu\text{m}$), obtained with 2 wt % cellulose solution, had a water permeance of $150 \text{ Lm}^{-2}\text{h}^{-1}\text{bar}^{-1}$, which is about 60% of the value for the uncoated PSU membrane. The emulsion permeance was much higher than for the uncoated PSU and the recovered flux was around $90 \text{ Lm}^{-2}\text{h}^{-1}\text{bar}^{-1}$. The recovered water permeance for uncoated PSU was close to zero. The membrane coated with 5 wt % cellulose (layer thickness around $0.9 \mu\text{m}$) had a reduced initial water permeance, when compared to PSU and the membrane coated with 2 wt % cellulose solution, but its emulsion permeance was similar to PSU and the water flux recovery was more than 90 %. The thickness of the cellulose layer

affects the permeance. Membranes prepared from 2 wt % and 5 wt % solutions didn't show visual changes after filtration. The polysulfone membrane used for filtration of emulsions containing SDBS had zero flux recovery (Figure 27, 28 and 29).

Cellulose membrane from three different coating solution concentrations, 2, 5, and 10 wt %, lead to complete oil removal in all conditions i.e. with cationic, anionic and non-ionic surfactant as well as at pH 4, 8 and 11. The images of 200 ppm, 500 ppm and 1000 ppm feed with SDBS and corresponding permeates, using a 2 wt % cellulose membrane, are shown in Figure 36 and Table 10.

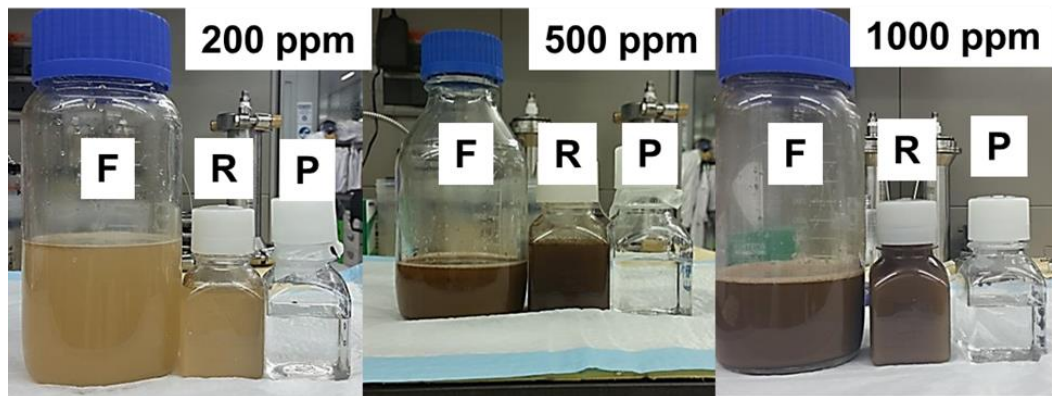


Figure 36. Feed (a), retentate (b) and permeate (c) for emulsions with 200 ppm, 500 ppm and 1000 ppm oil with SDBS at pH 8 filtered through 2 wt % cellulose membranes.

Table 10. Feed, retentate and permeate concentrations for emulsions with 200, 500 and 1000 ppm oil with SDBS at pH 8 for 2 wt % cellulose membrane.

Feed oil concentration / ppm	Retentate oil concentration / ppm	Permeate oil concentration / ppm	Permeate Turbidity NTU
204 ± 6	216 ± 5	0	0.3±0.1
412 ± 104	397 ± 12	0	0.1±0.0
953±113	917±97	0	0.1±0.0

The least flux decline and highest permeance were measured with emulsions with SDBS. As mentioned above SDBS is an anionic surfactant and the membrane is negatively charged in practically all investigated pH range. Electrostatic repulsion leads to no significant adsorption onto the membrane surface. The emulsions with SDBS have bigger droplet size than with other surfactants, indicating lower stability. Fluctuations in the feed and retentate values could be due to the least stabilized SDBS-oil droplets while measuring rather larger volume of different sizes with a fluorescence probe. Emulsion containing 200 ppm of oil, stabilized with SDBS was tested with oil extraction method using tetrachloroethylene as extraction solvent. Feed had approximately 200 ppm of oil, retentate 150 ppm of oil and permeate 3 ppm of oil.

Unmodified ultrafiltration polysulfone membranes exhibited completely irreversible fouling, showing no flux recovery. The membranes were blocked immediately after the start of the emulsion filtration and pure water permeance measured afterwards was significantly less than the initial permeance.

Experiments with 5 and 10 wt % cellulose membranes and emulsion with CTAB and Tween confirmed a complete oil removal with turbidity below 1 NTU for 96 % of the permeates and under 5 NTU for 4 % of the permeates, which is within the obligatory laws and restrictions issues of WHO, European standards and USEPA. The reason for fluctuations in oil concentration is due to the losses during emulsion preparation and mixing in the laboratory blender.

Cellulose membranes were finally investigated for the filtration of real produced water (Figure 37). During 4 hour long filtration experiment, the permeance of three different cellulose membranes was practically constant. The turbidity was reduced from 629 ± 3 NTU in the feed to the 6.3 ± 0.1 NTU in the permeate.

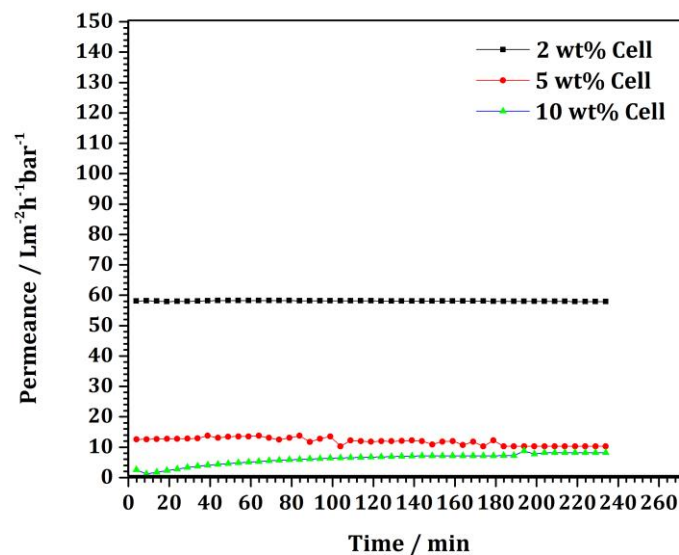


Figure 37. Real produced water permeance with time using membranes prepared from 2, 5 and 10 wt % cellulose solutions in ionic liquid.

From this experiment we can conclude that cellulose membranes of various thin film thicknesses can be of potential use in downstream application for real produced water produced in the last stages of filtration where the oil concentration is low.

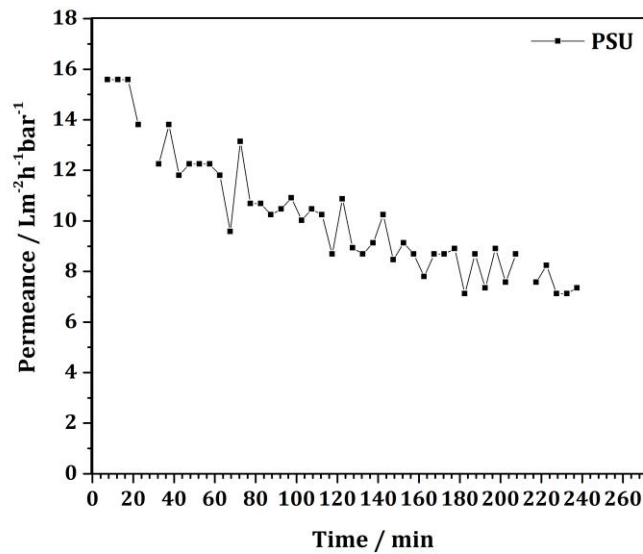


Figure 38. Real produced water permeance with time for unmodified PSU membrane.

The same filtration was conducted on unmodified PSU membranes under the same conditions (Figure 38). The produced water flux declined significantly, when compared to pure water permeance, indicating that adsorption and internal pore blockage occurred.

5. Conclusion

In this Chapter we provide the main research conclusions as well recommendations for future research.

5.1. Summary of Research Conclusions

5.1.1. Cellulose Membrane Prepared via Silanization and Regeneration

Membranes prepared via silanization exhibited a thin cellulose layer with high hydrophilicity with molecular weight cut-off within the UF membrane range.

The prepared membranes were further modified by promoting interfacial polymerization on top of the thin-cellulose composite membrane. In this case, the cellulose layer served as an intermediate layer leading to faster water transport through polyamide layer and extending the application to nanofiltration range with MWCO of 200 Da and highest sodium chloride retention of 82 %. The surface of polyamide layer was smoothened by presence of cellulose, promoting faster transport and additional layer tightened the membrane.

5.1.2. Cellulose Membrane Prepared with Ionic Liquid

Imidazolium based ionic liquid with acetate anion ([C2mim]OAc) is capable of breaking the hydrogen bonds due to the hydrogen acceptor sites in the anion

structure and lack of hydrogen bond donors in the ionic liquid cation. Membranes prepared from ionic liquid with contact angle of 22° exhibited MWCO as low as 3 kDa and water permeance as high as $13.8 \text{ Lm}^{-2}\text{h}^{-1}\text{bar}^{-1}$. Cellulose membrane prepared without support are resistant to common organic solvents and can withstand wide range of pH from 3-11.

5.1.3. Low Fouling Tendency of Cellulose/Ionic Liquid Membranes Towards Humic and Non-Humic Foulants

Cellulose membranes prepared with ionic liquid showed resistivity to humic acid fouling, where membranes have been in contact with humic acid for several hours, without permeance decline. Compared to commercial membranes, for the cellulose membranes the flux decline was very small; e.g. 20 % flux decline for 2 wt % cellulose membrane and 75 % for control polysulfone membrane.

Cellulose/ionic liquid membranes were not susceptible to non-humic fouling, as well as to BSA and gamma globulin proteins, having practically constant permeance and rejection of 100 %.

5.1.4. Complete Removal of Crude Oil with Cellulose/Ionic Liquid Membranes

Cellulose/Ionic liquid membranes showed excellent performance in complete removal of crude oil from oil-in-water emulsions. Membranes were subjected to several filtration tests investigating the influences of crude oil concentration, pH

range and different surfactants. By varying pH of the solution and charge of the emulsion droplets and the membrane charge and the fouling is affected. Emulsions with SDBS had the least flux decline and highest permeance.

The thinnest cellulose coating (2 wt % cellulose) provided high permeance and much higher flux recovery than the control PSU membrane. Unmodified ultrafiltration polysulfone membranes exhibited complete irreversible fouling, with tremendously reduced emulsion permeance.

This finding indicated that the cellulose coated layer was very effective for oil-water complete separation and flux recovery.

5.2. Recommendations for Future Research

5.2.1. Scale-up Potential, Environmental Impact and Recovery of Ionic Liquid

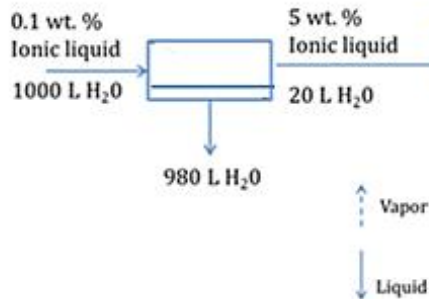
In this Chapter we present solely the estimated cost for production of 1 m² of cellulose/ionic liquid membranes and two potential processes for recovery of ionic liquid, hybrid RO-distillation and distillation alone process calculating only the energy required without considering e.g. pressure exchanger or booster pump in RO process or energy required for cooling the water in distillation process etc.

One of the main challenges in membrane technology, besides fouling, is the ability to scale up the process and to reduce consumption of toxic solvents thus having less harsh environmental impact.

Cellulose membranes have the advantage of being comprised of a natural abundant material, available in a variety of forms, including the natural one, wood pulp. Usage of green solvent such as ionic liquid is less harmful for the environment compared to the common organic solvents.

The economic efficiency of shifting from lab scale to pilot scale membrane fabrication should be evaluated. We discuss here a preliminary evaluation. Using water soluble ionic liquid with no vapor pressure gives the possibility of waste reduction as ionic liquid can be regenerated. Regeneration of ionic liquid by implementing membrane technology and column distillation can recover 90 % of ionic liquid thus minimizing the waste (Figure 39).

1. Membrane process



2. Distillation process

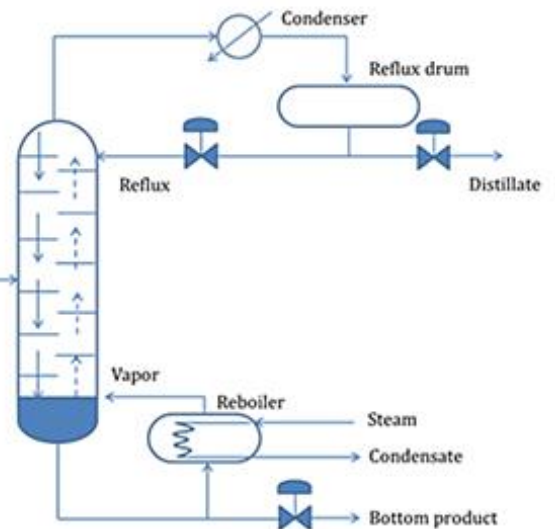


Figure 39. Recovery of ionic liquid by (a) membrane process and (b) distillation process.

The operational route starts with membrane manufacturing where the goal product is cellulose membrane manufactured with ionic liquid.

1. Hybrid process (membrane filtration and distillation)

Membrane process (Figure 39 a))

To prepare 15 m x 0.3 m (4.5 m²) of cellulose membrane in a continuous machine 500 ml volume solution containing 5 wt % cellulose and 95 wt % ionic liquid are required, leading to 0.1 wt % ionic liquid in the water bath having volume of 1000 L. For effective distillation the feed entering the column should have 5 wt % ionic liquid. From the mass balance if the feed has 0.1 wt % ionic liquid in 1000 L, and to get a retentate with 5 wt % and 20 L of water, 980L of water have to be removed (permeate) (equation shown in Appendix A1). The osmotic pressure of the retentate is approximately 14 bars calculated from Van't Hoff equation (Appendix A2). The proposed membrane could be a RO one (OSMO HR(PA)) from GE.¹⁷⁷ The energy consumption for the aforementioned membrane process would be approximately 3 kWh/m³ if we assume that the energy consumption for RO desalination is between 2.5 and 4 kWh/m³.¹⁷⁸ (Appendix A3)

Distillation process (Figure 39 b))

A feed containing 5 wt % of ionic liquid and 20 L of water would go into the distillation column. It has been reported that the distillation of [C2mim]OAc can produce 90 % yield.¹⁷⁹ The energy required to heat 20 L of solution (assume 20° C) to boiling point would be 6.7 MJ (1.8 kWh).¹⁸⁰ The energy required to evaporate 20 L of water to steam at atmospheric pressure would be 45.2 MJ (12.5 kWh). The total

energy required to distillate 20 L of solution containing 5 wt % ionic liquid with 90 % yield is 51.9 MJ (14.4 kWh) (Appendix A4a and A5a). The total energy consumption of a hybrid RO-distillation system is 17.4 kWh.

2. Distillation process (only)

Recovery of ionic liquid could be possible with only distillation. Energy requirement will increase because the feed would have 1000 L of water with 0.1 wt % of ionic liquid. The energy required to heat 1000 L of solution (assume 20°C) to the boiling point would be 336.0 MJ (93.3 kWh). The energy required to evaporate 1000 L of water to steam at atmospheric pressure would be 2260 MJ (627.7 kWh) (Appendix A4b and A5b). The total energy consumption of a distillation system is 721 kWh. The energy consumption tariff for Saudi Arabia for industrial facilities is fixed at 5 US \$ cents/kWh.¹⁸¹

Although a hybrid RO-distillation process would be more cost effective still distillation alone in Saudi Arabia is not as expensive as it would be in USA (9.43 US \$ cents/kWh) or Germany (15.22 US \$ cents/kWh).¹⁸²

The advantage of using hybrid system would be less energy consumption, thus decreased gas emission. The disadvantage is the usage of two systems with a more complicated operation, increase in operation and maintenance cost.

The advantage of using distillation as a sole process is simplicity, being a rapid method but rather energy consuming. Equations are shown in Appendix A.

In summary, cellulose membrane manufacture from ionic liquid are susceptible for scale up with estimated cost of 10 \$/m². Using cellulose doesn't cause considerable depletion of natural resources due to, firstly, its abundance; secondly, cellulose can be from wood, pulp or cotton, which is a residue from e.g. wood industry or textile industry. Ionic liquid is a non-volatile and environmentally benign solvent therefore its usage reduced the negative environmental impact.

Another advantage of ionic liquid is the possibility of recovery, which minimizes the waste. Hybrid RO-distillation system consumes less energy than distillation alone although distillation is a simpler method.

Usage of ionic liquid reduces the release of toxic chemical in the environment based on the fact that ionic liquid is not toxic chemical and that [C2mim]OAc is the least toxic among ionic liquids.

By recovering ionic liquid we reduced the waste, minimize negative environmental impact and have more cost efficient process.

5.2.2. Cellulose Membranes in Biomedical Application

The application of cellulose in membrane technology and beyond is numerous. Aforementioned characteristics as well as countless derivatives such as nanocrystals and bacterial cellulose extend the application from membranes to every day personal products, automotive and medicinal.

Cellulose and cellulose derivatives are already used in biomedical application due to their biocompatibility and biodegradability. They are used as hemodialysis membranes for artificial kidneys, membranes in plasmapheresis and as drug delivery precursors.

Electrospun cellulose fibers from ionic liquids call for further research for biomedical application taking the advantage of cellulose dissolution in ionic liquid and reduced toxicity with modification of the electrospinning instrumentation and procedure.¹⁸³

REFERENCES

1. Coping with Water Scarcity: Challenge of the Twenty-first Century, Report from the UN-Water, FAO, 2007, Human Development Report, UNDP, 2006.
2. Report Assesses Market for Membrane-based Equipment for Water Treatment, Membrane Technology 2010, 2010, 6.
3. Zheng, C.; Liu, J., China's "Love Canal" Moment? *Science* 2013, 340, (6134), 810-810.
4. Zhou, Y.; Khu, S.-T.; Xi, B.; Su, J.; Hao, F.; Wu, J.; Huo, S., Status and challenges of water pollution problems in China: learning from the European experience. *Environmental earth sciences* 2014, 72, (4), 1243-1254.
5. Figoli, A.; Marino, T.; Simone, S.; Di Nicolo, E.; Li, X.-M.; He, T.; Tornaghi, S.; Drioli, E., Towards non-toxic solvents for membrane preparation: a review. *Green Chemistry* 2014, 16, (9), 4034-4059.
6. Szekely, G.; Jimenez-Solomon, M. F.; Marchetti, P.; Kim, J. F.; Livingston, A. G., Sustainability assessment of organic solvent nanofiltration: from fabrication to application. *Green Chemistry* 2014, 16, (10), 4440-4473.
7. Zhang, H.; Zhao, H.; Liu, P.; Zhang, S.; Li, G., Direct growth of hierarchically structured titanate nanotube filtration membrane for removal of waterborne pathogens. *Journal of Membrane Science* 2009, 343, (1), 212-218.
8. Zhang, X.; Zhang, T.; Ng, J.; Sun, D. D., High-Performance Multifunctional TiO₂ Nanowire Ultrafiltration Membrane with a Hierarchical Layer Structure for Water Treatment. *Advanced Functional Materials* 2009, 19, (23), 3731-3736.
9. Liu, L.; Liu, Z.; Bai, H.; Sun, D. D., Concurrent filtration and solar photocatalytic disinfection/degradation using high-performance Ag/TiO₂ nanofiber membrane. *Water research* 2012, 46, (4), 1101-1112.
10. Zhang, X.; Du, A. J.; Lee, P.; Sun, D. D.; Leckie, J. O., Grafted multifunctional titanium dioxide nanotube membrane: separation and photodegradation of aquatic pollutant. *Applied Catalysis B: Environmental* 2008, 84, (1), 262-267.
11. Karabelas, A.; Plakas, K.; Sarasidis, V.; Patsios, S., The effect of humic acids on the removal of atrazine from water in a continuous photocatalytic membrane reactor. *Global NEST Journal* 2014, 16, (3), 516-524.
12. Ma, N.; Zhang, Y.; Quan, X.; Fan, X.; Zhao, H., Performing a microfiltration integrated with photocatalysis using an Ag-TiO₂/HAP/Al₂O₃ composite membrane for water treatment: Evaluating effectiveness for humic acid removal and anti-fouling properties. *Water research* 2010, 44, (20), 6104-6114.
13. Lazar, M. A.; Varghese, S.; Nair, S. S., Photocatalytic water treatment by titanium dioxide: recent updates. *Catalysts* 2012, 2, (4), 572-601.
14. Romão, J.; Barata, D.; Habibovic, P.; Mul, G.; Baltrusaitis, J., High throughput analysis of photocatalytic water purification. *Analytical chemistry* 2014, 86, (15), 7612-7617.
15. Athanasekou, C.; Romanos, G.; Katsaros, F.; Kordatos, K.; Likodimos, V.; Falaras, P., Very efficient composite titania membranes in hybrid ultrafiltration/photocatalysis water treatment processes. *Journal of Membrane Science* 2012, 392, 192-203.

16. König, K.; Boffa, V.; Buchbjerg, B.; Farsi, A.; Christensen, M. L.; Magnacca, G.; Yue, Y., One-step deposition of ultrafiltration SiC membranes on macroporous SiC supports. *Journal of Membrane Science* 2014, *472*, 232-240.
17. Pendergast, M. M.; Hoek, E. M., A review of water treatment membrane nanotechnologies. *Energy & Environmental Science* 2011, *4*, (6), 1946-1971.
18. Pradeep, T., Noble metal nanoparticles for water purification: a critical review. *Thin solid films* 2009, *517*, (24), 6441-6478.
19. Li, J.; Zhao, T.; Chen, T.; Liu, Y.; Ong, C. N.; Xie, J., Engineering noble metal nanomaterials for environmental applications. *Nanoscale* 2015, *7*, (17), 7502-7519.
20. Thatai, S.; Khurana, P.; Boken, J.; Prasad, S.; Kumar, D., Nanoparticles and core-shell nanocomposite based new generation water remediation materials and analytical techniques: A review. *Microchemical Journal* 2014, *116*, 62-76.
21. Alazba, A. A.; Amin, M. T., A review of nanomaterials based membranes for removal of contaminants from polluted waters. *Membrane Water Treatment* 2014, *5*, (2), 123.
22. Stoimenov, P. K.; Klinger, R. L.; Marchin, G. L.; Klabunde, K. J., Metal oxide nanoparticles as bactericidal agents. *Langmuir* 2002, *18*, (17), 6679-6686.
23. Ghasemzadeh, G.; Momenpour, M.; Omid, F.; Hosseini, M. R.; Ahani, M.; Barzegari, A., Applications of nanomaterials in water treatment and environmental remediation. *Frontiers of Environmental Science & Engineering* 2014, *8*, (4), 471-482.
24. Sharma, Y.; Srivastava, V.; Upadhyay, S.; Weng, C., Alumina nanoparticles for the removal of Ni (II) from aqueous solutions. *Industrial & Engineering Chemistry Research* 2008, *47*, (21), 8095-8100.
25. Ponder, S. M.; Darab, J. G.; Mallouk, T. E., Remediation of Cr (VI) and Pb (II) aqueous solutions using supported, nanoscale zero-valent iron. *Environmental Science & Technology* 2000, *34*, (12), 2564-2569.
26. Allred, B. J.; Tost, B. C., Laboratory comparison of four iron-based filter materials for water treatment of trace element contaminants. *Water Environment Research* 2014, *86*, (11), 2221-2232.
27. Kawada, S.; Saeki, D.; Matsuyama, H., Development of ultrafiltration membrane by stacking of silver nanoparticles stabilized with oppositely charged polyelectrolytes. *Colloids and Surfaces A: Physicochemical and Engineering Aspects* 2014, *451*, 33-37.
28. Hu, M.; Mi, B., Enabling graphene oxide nanosheets as water separation membranes. *Environmental science & technology* 2013, *47*, (8), 3715-3723.
29. Han, Y.; Xu, Z.; Gao, C., Ultrathin graphene nanofiltration membrane for water purification. *Advanced Functional Materials* 2013, *23*, (29), 3693-3700.
30. Liu, H.; Wang, H.; Zhang, X., Facile fabrication of freestanding ultrathin reduced graphene oxide membranes for water purification. *Advanced materials* 2015, *27*, (2), 249-254.
31. Srivastava, A.; Srivastava, O.; Talapatra, S.; Vajtai, R.; Ajayan, P., Carbon nanotube filters. *Nature materials* 2004, *3*, (9), 610-614.
32. Cohen-Tanugi, D.; Grossman, J. C., Water desalination across nanoporous graphene. *Nano letters* 2012, *12*, (7), 3602-3608.
33. Rahaman, M. S.; Vecitis, C. D.; Elimelech, M., Electrochemical carbon-nanotube filter performance toward virus removal and inactivation in the presence

- of natural organic matter. *Environmental science & technology* 2012, 46, (3), 1556-1564.
34. Baek, Y.; Kim, C.; Seo, D. K.; Kim, T.; Lee, J. S.; Kim, Y. H.; Ahn, K. H.; Bae, S. S.; Lee, S. C.; Lim, J., High performance and antifouling vertically aligned carbon nanotube membrane for water purification. *Journal of Membrane Science* 2014, 460, 171-177.
35. Das, R.; Ali, M. E.; Hamid, S. B. A.; Ramakrishna, S.; Chowdhury, Z. Z., Carbon nanotube membranes for water purification: a bright future in water desalination. *Desalination* 2014, 336, 97-109.
36. Brady-Estévez, A. S.; Schnoor, M. H.; Kang, S.; Elimelech, M., SWNT- MWNT hybrid filter attains high viral removal and bacterial inactivation. *Langmuir* 2010, 26, (24), 19153-19158.
37. Huang, H.; Ying, Y.; Peng, X., Graphene oxide nanosheet: an emerging star material for novel separation membranes. *Journal of Materials Chemistry A* 2014, 2, (34), 13772-13782.
38. Saljoughi, E.; Mousavi, S. M., Preparation and characterization of novel polysulfone nanofiltration membranes for removal of cadmium from contaminated water. *Separation and purification technology* 2012, 90, 22-30.
39. Ahmad, A.; Abdulkarim, A.; Ooi, B.; Ismail, S., Recent development in additives modifications of polyethersulfone membrane for flux enhancement. *Chemical engineering journal* 2013, 223, 246-267.
40. Yuliwati, E.; Ismail, A. F., Effect of additives concentration on the surface properties and performance of PVDF ultrafiltration membranes for refinery produced wastewater treatment. *Desalination* 2011, 273, (1), 226-234.
41. Liu, F.; Hashim, N. A.; Liu, Y.; Abed, M. M.; Li, K., Progress in the production and modification of PVDF membranes. *Journal of Membrane Science* 2011, 375, (1), 1-27.
42. Lohokare, H.; Muthu, M.; Agarwal, G.; Kharul, U., Effective arsenic removal using polyacrylonitrile-based ultrafiltration (UF) membrane. *Journal of Membrane Science* 2008, 320, (1), 159-166.
43. Kim, I.-C.; Yun, H.-G.; Lee, K.-H., Preparation of asymmetric polyacrylonitrile membrane with small pore size by phase inversion and post-treatment process. *Journal of Membrane Science* 2002, 199, (1), 75-84.
44. Qin, J.-J.; Li, Y.; Lee, L.-S.; Lee, H., Cellulose acetate hollow fiber ultrafiltration membranes made from CA/PVP 360 K/NMP/water. *Journal of membrane science* 2003, 218, (1), 173-183.
45. Shibusaki, T.; Kitaura, T.; Ohmukai, Y.; Maruyama, T.; Nakatsuka, S.; Watabe, T.; Matsuyama, H., Membrane fouling properties of hollow fiber membranes prepared from cellulose acetate derivatives. *Journal of Membrane Science* 2011, 376, (1), 102-109.
46. Soyekwo, F.; Zhang, Q. G.; Deng, C.; Gong, Y.; Zhu, A. M.; Liu, Q. L., Highly permeable cellulose acetate nanofibrous composite membranes by freeze-extraction. *Journal of Membrane Science* 2014, 454, 339-345.
47. Eren, E.; Sarihan, A.; Eren, B.; Gumus, H.; Kocak, F. O., Preparation, characterization and performance enhancement of polysulfone ultrafiltration

- membrane using PBI as hydrophilic modifier. *Journal of Membrane Science* 2015, 475, 1-8.
48. Xie, Y.; Tayouo, R.; Nunes, S. P., Low fouling polysulfone ultrafiltration membrane via click chemistry. *Journal of Applied Polymer Science* 2015, 132, (21).
49. Sinha, M.; Purkait, M., Increase in hydrophilicity of polysulfone membrane using polyethylene glycol methyl ether. *Journal of Membrane Science* 2013, 437, 7-16.
50. Derlon, N.; Mimoso, J.; Klein, T.; Koetzsch, S.; Morgenroth, E., Presence of biofilms on ultrafiltration membrane surfaces increases the quality of permeate produced during ultra-low pressure gravity-driven membrane filtration. *Water research* 2014, 60, 164-173.
51. Sheng, T.; Chen, H.; Xiong, S.; Chen, X.; Wang, Y., Atomic layer deposition of polyimide on microporous polyethersulfone membranes for enhanced and tunable performances. *AIChE Journal* 2014, 60, (10), 3614-3622.
52. Pezeshk, N.; Rana, D.; Narbaitz, R.; Matsuura, T., Novel modified PVDF ultrafiltration flat-sheet membranes. *Journal of Membrane Science* 2012, 389, 280-286.
53. Qin, A.; Li, X.; Zhao, X.; Liu, D.; He, C., Preparation and characterization of nano-chitin whisker reinforced PVDF membrane with excellent antifouling property. *Journal of Membrane Science* 2015, 480, 1-10.
54. Pan, K.; Ren, R.; Liang, B.; Li, L.; Li, H.; Cao, B., Synthesis of pH-responsive polyethylene terephthalate track-etched membranes by grafting hydroxyethyl-methacrylate using atom-transfer radical polymerization method. *Journal of Applied Polymer Science* 2014, 131, (20).
55. Van Wagner, E. M.; Sagle, A. C.; Sharma, M. M.; La, Y.-H.; Freeman, B. D., Surface modification of commercial polyamide desalination membranes using poly (ethylene glycol) diglycidyl ether to enhance membrane fouling resistance. *Journal of Membrane Science* 2011, 367, (1), 273-287.
56. Nunes, S. P.; Car, A., From charge-mosaic to micelle self-assembly: block copolymer membranes in the last 40 years. *Industrial & Engineering Chemistry Research* 2012, 52, (3), 993-1003.
57. Marques, D. S.; Vainio, U.; Chaparro, N. M.; Calo, V. M.; Bezahd, A. R.; Pitera, J. W.; Peinemann, K.-V.; Nunes, S. P., Self-assembly in casting solutions of block copolymer membranes. *Soft Matter* 2013, 9, (23), 5557-5564.
58. Madhavan, P.; Peinemann, K.-V.; Nunes, S. P., Complexation-tailored morphology of asymmetric block copolymer membranes. *ACS applied materials & interfaces* 2013, 5, (15), 7152-7159.
59. Abdelrasoul, A.; Doan, H.; Lohi, A., Fouling in membrane filtration and remediation methods. *Mass Transfer-Advances in Sustainable Energy and Environment Oriented Numerical Modeling* 2013, 195-218.
60. Tang, C. Y.; Chong, T.; Fane, A. G., Colloidal interactions and fouling of NF and RO membranes: a review. *Advances in colloid and interface science* 2011, 164, (1), 126-143.
61. Dramas, L.; Croué, J.-P., Ceramic membrane as a pretreatment for reverse osmosis: interaction between marine organic matter and metal oxides. *Desalination and Water Treatment* 2013, 51, (7-9), 1781-1789.

62. Field, R., *Fundamentals of fouling*. Wiley-VCH: 2010; Vol. 4, p 1-23.
63. Madaeni, S.; Gheshlaghi, A.; Rekabdar, F., Membrane treatment of oily wastewater from refinery processes. *Asia-Pacific Journal of Chemical Engineering* 2013, 8, (1), 45-53.
64. Elimelech, M.; Chen, W. H.; Waypa, J. J., Measuring the zeta (electrokinetic) potential of reverse osmosis membranes by a streaming potential analyzer. *Desalination* 1994, 95, (3), 269-286.
65. Childress, A. E.; Elimelech, M., Effect of solution chemistry on the surface charge of polymeric reverse osmosis and nanofiltration membranes. *Journal of Membrane Science* 1996, 119, (2), 253-268.
66. Amy E. Childress, M. E., Relating Nanofiltration Membrane Performance to Membrane Charge (Electrokinetic) *Environmental Science and technology* 2000, 34, 3710-3716.
67. Neff, J. M., *Bioaccumulation in marine organisms: effect of contaminants from oil well produced water*. Elsevier: 2002.
68. Tellez, G. T.; Nirmalakhandan, N.; Gardea-Torresdey, J. L., Performance evaluation of an activated sludge system for removing petroleum hydrocarbons from oilfield produced water. *Advances in Environmental Research* 2002, 6, (4), 455-470.
69. Commission, O., OSPAR report on discharges, spills and emissions from offshore oil and gas installations in 2012. In 2014.
70. US Environment Protection Agency. <http://www.3epa.org/> (April 2016),
71. World Health Organization: WHO. <http://www.who.int/> (April 2016),
72. European Commission. <http://ec.europa.eu/> (April 2016),
73. International Energy Agency. <http://www.iea.org/> (April 2016),
74. Lu, D.; Zhang, T.; Ma, J., Ceramic membrane fouling during ultrafiltration of oil/water emulsions: Roles played by stabilization surfactants of oil droplets. *Environmental science & technology* 2015, 49, (7), 4235-4244.
75. Fakhru'l-Razi, A.; Pendashteh, A.; Abdullah, L. C.; Biak, D. R. A.; Madaeni, S. S.; Abidin, Z. Z., Review of technologies for oil and gas produced water treatment. *Journal of Hazardous Materials* 2009, 170, (2), 530-551.
76. Hong, A.; Fane, A.; Burford, R., Factors affecting membrane coalescence of stable oil-in-water emulsions. *Journal of membrane science* 2003, 222, (1), 19-39.
77. El-Kayar, A.; Hussein, M.; Zatout, A.; Hosny, A.; Amer, A., Removal of oil from stable oil-water emulsion by induced air flotation technique. *Separations Technology* 1993, 3, (1), 25-31.
78. Chakrabarty, B.; Ghoshal, A.; Purkait, M., Ultrafiltration of stable oil-in-water emulsion by polysulfone membrane. *Journal of Membrane Science* 2008, 325, (1), 427-437.
79. Chu, L. Y.; Wang, S.; Chen, W. M., Surface Modification of Ceramic-Supported Polyethersulfone Membranes by Interfacial Polymerization for Reduced Membrane Fouling. *Macromolecular Chemistry and Physics* 2005, 206, (19), 1934-1940.
80. Plebon, M.; Saad, M.; Fraser, S. In *Further advances in produced water de-oiling utilizing a technology that removes and recovers dispersed oil in produced water 2 microns and larger*, 12th international petroleum environmental conference, Houston, TX, Nov, 2005; Citeseer: 2005; pp 8-11.

81. Knudsen, B.; Hjelsvold, M.; Frost, T.; Svarstad, M.; Grini, P.; Willumsen, C.; Torvik, H. In *Meeting the zero discharge challenge for produced water*, SPE International Conference on Health, Safety, and Environment in Oil and Gas Exploration and Production, 2004; Society of Petroleum Engineers: 2004.
82. Seureau, J.; Aurelle, Y.; Hoyack, M. In *A three-phase separator for the removal of oil and solids from produced water*, SPE Annual Technical Conference and Exhibition, 1994; Society of Petroleum Engineers: 1994.
83. Chen, W.; Su, Y.; Zheng, L.; Wang, L.; Jiang, Z., The improved oil/water separation performance of cellulose acetate-graft-polyacrylonitrile membranes. *Journal of Membrane Science* 2009, 337, (1), 98-105.
84. Križan Milić, J.; Murić, A.; Petrinić, I.; Simonić, M., Recent developments in membrane treatment of spent cutting-oils: A review. *Industrial & Engineering Chemistry Research* 2013, 52, (23), 7603-7616.
85. Zhao, C.; Xue, J.; Ran, F.; Sun, S., Modification of polyethersulfone membranes—A review of methods. *Progress in Materials Science* 2013, 58, (1), 76-150.
86. Ulbricht, M.; Belfort, G., Surface modification of ultrafiltration membranes by low temperature plasma II. Graft polymerization onto polyacrylonitrile and polysulfone. *Journal of Membrane Science* 1996, 111, (2), 193-215.
87. Chen, H.; Belfort, G., Surface modification of poly (ether sulfone) ultrafiltration membranes by low-temperature plasma-induced graft polymerization. *Journal of Applied Polymer Science* 1999, 72, (13), 1699-1711.
88. Pieracci, J.; Crivello, J. V.; Belfort, G., UV-assisted graft polymerization of N-vinyl-2-pyrrolidinone onto poly (ether sulfone) ultrafiltration membranes using selective UV wavelengths. *Chemistry of materials* 2002, 14, (1), 256-265.
89. Reddy, A.; Mohan, D. J.; Bhattacharya, A.; Shah, V.; Ghosh, P., Surface modification of ultrafiltration membranes by preadsorption of a negatively charged polymer: I. Permeation of water soluble polymers and inorganic salt solutions and fouling resistance properties. *Journal of Membrane Science* 2003, 214, (2), 211-221.
90. Nunes, S. P.; Sforça, M. L.; Peinemann, K.-V., Dense hydrophilic composite membranes for ultrafiltration. *Journal of Membrane Science* 1995, 106, (1), 49-56.
91. Hester, J.; Banerjee, P.; Mayes, A., Preparation of protein-resistant surfaces on poly (vinylidene fluoride) membranes via surface segregation. *Macromolecules* 1999, 32, (5), 1643-1650.
92. Wang, Y.-q.; Wang, T.; Su, Y.-l.; Peng, F.-b.; Wu, H.; Jiang, Z.-y., Remarkable reduction of irreversible fouling and improvement of the permeation properties of poly (ether sulfone) ultrafiltration membranes by blending with pluronic F127. *Langmuir* 2005, 21, (25), 11856-11862.
93. Su, Y.; Li, C.; Zhao, W.; Shi, Q.; Wang, H.; Jiang, Z.; Zhu, S., Modification of polyethersulfone ultrafiltration membranes with phosphorylcholine copolymer can remarkably improve the antifouling and permeation properties. *Journal of Membrane Science* 2008, 322, (1), 171-177.
94. Shi, Q.; Su, Y.; Zhao, W.; Li, C.; Hu, Y.; Jiang, Z.; Zhu, S., Zwitterionic polyethersulfone ultrafiltration membrane with superior antifouling property. *Journal of Membrane Science* 2008, 319, (1), 271-278.

95. Li, Y. S.; Yan, L.; Xiang, C. B.; Hong, L. J., Treatment of oily wastewater by organic-inorganic composite tubular ultrafiltration (UF) membranes. *Desalination* 2006, 196, (1), 76-83.
96. Bilstad, T.; Espedal, E., Membrane separation of produced water. *Water Science and Technology* 1996, 34, (9), 239-246.
97. Lee, J. M.; Frankiewicz, T. C. In *Treatment of produced water with an ultrafiltration (UF) membrane-a field trial*, SPE Annual Technical Conference and Exhibition, 2005; Society of Petroleum Engineers: 2005.
98. Li, H.-J.; Cao, Y.-M.; Qin, J.-J.; Jie, X.-M.; Wang, T.-H.; Liu, J.-H.; Yuan, Q., Development and characterization of anti-fouling cellulose hollow fiber UF membranes for oil-water separation. *Journal of Membrane science* 2006, 279, (1), 328-335.
99. Shams Ashaghi, K.; Ebrahimi, M.; Czermak, P., Ceramic ultra-and nanofiltration membranes for oilfield produced water treatment: a mini review. *Open Environmental Sciences* 2007, 1, (1).
100. Bader, M., Seawater versus produced water in oil-fields water injection operations. *Desalination* 2007, 208, (1), 159-168.
101. Melin, T.; Rautenbach, R., *Membranverfahren*. Springer Berlin Heidelberg: 2007.
102. Chen, A.; Flynn, J.; Cook, R.; Casaday, A., Removal of oil, grease, and suspended solids from produced water with ceramic crossflow microfiltration. *SPE production engineering* 1991, 6, (02), 131-136.
103. Klemm, D.; Schmauder, H. P.; Heinze, T., Cellulose. *Biopolymers online* 2005.
104. Krässig, H. A.; Krässig, H. A.; Krässig, H. A., *Cellulose: structure, accessibility and reactivity*. Gordon and Breach Science Publishers: 1993.
105. Klemm, D.; Philipp, B.; Heinze, T.; Heinze, U.; Wagenknecht, W., Endpapers. *Comprehensive Cellulose Chemistry: Functionalization of Cellulose, Volume 2* 1998.
106. Payen, A., Mémoire sur la composition du tissu propre des plantes et du ligneux. *Comptes rendus* 1838, 7, 1052-1056.
107. Schweizer, E., Das Kupferoxyd-Ammoniak, ein Auflösungsmittel für die Pflanzenfaser. *Journal für praktische Chemie* 1857, 72, (1), 109-111.
108. Schützenberger, P., Action de l'acide acétique anhydre sur la cellulose, l'amidon, les sucres, la mannite et ses congénères, les glucosides et certaines matières colorantes végétales. *Compt. Rend. Hebd. Séances Acad. Sci* 1865, 61, 484-487.
109. Staudinger, H.; Daumiller, G., Über hochpolymere Verbindungen. 154. Mitteilung. Untersuchungen an Celluloseacetaten und Cellulosen. *Justus Liebigs Annalen der Chemie* 1937, 529, (1), 219-265.
110. Klemm, D.; Kramer, F.; Moritz, S.; Lindström, T.; Ankerfors, M.; Gray, D.; Dorris, A., Nanocelluloses: A New Family of Nature-Based Materials. *Angewandte Chemie International Edition* 2011, 50, (24), 5438-5466.
111. Heinze, T.; Liebert, T., Unconventional methods in cellulose functionalization. *Progress in polymer science* 2001, 26, (9), 1689-1762.
112. Fink, H.-P.; Weigel, P.; Purz, H.; Ganster, J., Structure formation of regenerated cellulose materials from NMMO-solutions. *Progress in Polymer Science* 2001, 26, (9), 1473-1524.

113. Hebeish, A.; Guthrie, J., *The chemistry and technology of cellulosic copolymers*. Springer Science & Business Media: 2012; Vol. 4.
114. Hoelkeskamp, F., Process for production of cuprammonium cellulose articles. In Google Patents: 1963.
115. Plymouth, U. o., Abundance of microplastics in the world's deep seas *Science Daily*.
116. Johnson, D. L., Compounds dissolved in cyclic amine oxides. In Google Patents: 1969.
117. Zhang, Y.; Shao, H.; Wu, C.; Hu, X., Formation and Characterization of Cellulose Membranes from N-Methylmorpholine-N-oxide Solution. *Macromolecular Bioscience* 2001, 1, (4), 141-148.
118. Li, X.-L.; Zhu, L.-P.; Zhu, B.-K.; Xu, Y.-Y., High-flux and anti-fouling cellulose nanofiltration membranes prepared via phase inversion with ionic liquid as solvent. *Separation and purification technology* 2011, 83, 66-73.
119. Wilkes, J. S., A short history of ionic liquids—from molten salts to neoteric solvents. *Green Chemistry* 2002, 4, (2), 73-80.
120. Swatloski, R. P.; Spear, S. K.; Holbrey, J. D.; Rogers, R. D., Dissolution of cellulose with ionic liquids. *Journal of the American Chemical Society* 2002, 124, (18), 4974-4975.
121. Pham, T. P. T.; Cho, C.-W.; Yun, Y.-S., Environmental fate and toxicity of ionic liquids: a review. *Water research* 2010, 44, (2), 352-372.
122. Abels, C.; Redepenning, C.; Moll, A.; Melin, T.; Wessling, M., Simple purification of ionic liquid solvents by nanofiltration in biorefining of lignocellulosic substrates. *Journal of Membrane Science* 2012, 405, 1-10.
123. Pinkert, A.; Marsh, K. N.; Pang, S.; Staiger, M. P., Ionic liquids and their interaction with cellulose. *Chemical Reviews* 2009, 109, (12), 6712-6728.
124. Sun, N.; Rahman, M.; Qin, Y.; Maxim, M. L.; Rodríguez, H.; Rogers, R. D., Complete dissolution and partial delignification of wood in the ionic liquid 1-ethyl-3-methylimidazolium acetate. *Green Chemistry* 2009, 11, (5), 646-655.
125. Remsing, R. C.; Swatloski, R. P.; Rogers, R. D.; Moyna, G., Mechanism of cellulose dissolution in the ionic liquid 1-n-butyl-3-methylimidazolium chloride: a ¹³C and ^{35/37}Cl NMR relaxation study on model systems. *Chemical Communications* 2006, (12), 1271-1273.
126. Gericke, M.; Fardim, P.; Heinze, T., Ionic liquids—promising but challenging solvents for homogeneous derivatization of cellulose. *Molecules* 2012, 17, (6), 7458-7502.
127. Heinze, T.; Dorn, S.; Schöbitz, M.; Liebert, T.; Köhler, S.; Meister, F. In *Interactions of ionic liquids with polysaccharides-2: Cellulose*, Macromolecular Symposia, 2008; Wiley Online Library: 2008; pp 8-22.
128. Youngs, T.; Hardacre, C.; Holbrey, J., Glucose solvation by the ionic liquid 1, 3-dimethylimidazolium chloride: A simulation study. *The Journal of Physical Chemistry B* 2007, 111, (49), 13765-13774.
129. Xing, D. Y.; Peng, N.; Chung, T.-S., Investigation of unique interactions between cellulose acetate and ionic liquid [EMIM] SCN, and their influences on hollow fiber ultrafiltration membranes. *Journal of Membrane Science* 2011, 380, (1), 87-97.

130. Xing, D. Y.; Peng, N.; Chung, T.-S., Formation of cellulose acetate membranes via phase inversion using ionic liquid, [BMIM] SCN, as the solvent. *Industrial & Engineering Chemistry Research* 2010, 49, (18), 8761-8769.
131. Carpenter, A. W.; de Lannoy, C.-F.; Wiesner, M. R., Cellulose nanomaterials in water treatment technologies. *Environmental science & technology* 2015, 49, (9), 5277-5287.
132. Yu, X.; Tong, S.; Ge, M.; Wu, L.; Zuo, J.; Cao, C.; Song, W., Adsorption of heavy metal ions from aqueous solution by carboxylated cellulose nanocrystals. *Journal of Environmental Sciences* 2013, 25, (5), 933-943.
133. Srivastava, S.; Kardam, A.; Raj, K. R., Nanotech reinforcement onto cellulosic fibers: green remediation of toxic metals. *International Journal of Green Nanotechnology* 2012, 4, (1), 46-53.
134. Ma, H.; Hsiao, B. S.; Chu, B., Ultrafine cellulose nanofibers as efficient adsorbents for removal of UO₂²⁺ in water. *ACS Macro Letters* 2011, 1, (1), 213-216.
135. Singh, K.; Arora, J. K.; Sinha, T. J. M.; Srivastava, S., Functionalization of nanocrystalline cellulose for decontamination of Cr (III) and Cr (VI) from aqueous system: computational modeling approach. *Clean Technologies and Environmental Policy* 2014, 16, (6), 1179-1191.
136. Korhonen, J. T.; Kettunen, M.; Ras, R. H.; Ikkala, O., Hydrophobic nanocellulose aerogels as floating, sustainable, reusable, and recyclable oil absorbents. *ACS applied materials & interfaces* 2011, 3, (6), 1813-1816.
137. Jiang, F.; Hsieh, Y.-L., Amphiphilic superabsorbent cellulose nanofibril aerogels. *Journal of Materials Chemistry A* 2014, 2, (18), 6337-6342.
138. Zhang, Z.; Sèbe, G.; Rentsch, D.; Zimmermann, T.; Tingaut, P., Ultralightweight and flexible silylated nanocellulose sponges for the selective removal of oil from water. *Chemistry of Materials* 2014, 26, (8), 2659-2668.
139. Nata, I. F.; Sureshkumar, M.; Lee, C.-K., One-pot preparation of amine-rich magnetite/bacterial cellulose nanocomposite and its application for arsenate removal. *RSC Advances* 2011, 1, (4), 625-631.
140. Qu, P.; Tang, H.; Gao, Y.; Zhang, L.; Wang, S., Polyethersulfone composite membrane blended with cellulose fibrils. *BioResources* 2010, 5, (4), 2323-2336.
141. Wang, X.; Yeh, T.-M.; Wang, Z.; Yang, R.; Wang, R.; Ma, H.; Hsiao, B. S.; Chu, B., Nanofiltration membranes prepared by interfacial polymerization on thin-film nanofibrous composite scaffold. *Polymer* 2014, 55, (6), 1358-1366.
142. Reid, C.; Breton, E., Water and ion flow across cellulosic membranes. *Journal of Applied Polymer Science* 1959, 1, (2), 133-143.
143. Bechhold, H., Kolloidstudien mit der Filtrationsmethode. *Zeitschrift für Elektrochemie und angewandte physikalische Chemie* 1907, 13, (32), 527-533.
144. Loeb, S.; Sourirajan, S., High-flow semipermeable membranes for separation of water from saline solutions. *Adv Chem Ser* 1962, 38, (1), 117-132.
145. Mu, C.; Su, Y.; Sun, M.; Chen, W.; Jiang, Z., Remarkable improvement of the performance of poly (vinylidene fluoride) microfiltration membranes by the additive of cellulose acetate. *Journal of Membrane Science* 2010, 350, (1), 293-300.
146. Razzaghi, M. H.; Safekordi, A.; Tavakolmoghadam, M.; Rekadardar, F.; Hemmati, M., Morphological and separation performance study of PVDF/CA blend membranes. *Journal of Membrane Science* 2014, 470, 547-557.

147. Mahendran, R.; Malaisamy, R.; Arthanareeswaran, G.; Mohan, D., Cellulose acetate-poly (ether sulfone) blend ultrafiltration membranes. II. Application studies. *Journal of applied polymer science* 2004, 92, (6), 3659-3665.
148. Eichhorn, S. J.; Dufresne, A.; Aranguren, M.; Marcovich, N.; Capadona, J.; Rowan, S.; Weder, C.; Thielemans, W.; Roman, M.; Renneckar, S., Review: current international research into cellulose nanofibres and nanocomposites. *Journal of Materials Science* 2010, 45, (1), 1-33.
149. Ma, H.; Burger, C.; Hsiao, B. S.; Chu, B., Fabrication and characterization of cellulose nanofiber based thin-film nanofibrous composite membranes. *Journal of Membrane Science* 2014, 454, 272-282.
150. Mohammadi, T.; Saljoughi, E., Effect of production conditions on morphology and permeability of asymmetric cellulose acetate membranes. *Desalination* 2009, 243, (1), 1-7.
151. Petersen, R. J., Composite reverse osmosis and nanofiltration membranes. *Journal of membrane science* 1993, 83, (1), 81-150.
152. K.V. Peinemann, S.P. Nunes, J. Timmermann, Composite Membrane Made of a Microporous Support Membrane and Interlayer Made of Regenerated Cellulose and Method for the Production of Same, Patent Application no. 1083981, 2005.
153. O'SULLIVAN, A. C., Cellulose: the structure slowly unravels. *Cellulose* 1997, 4, (3), 173-207.
154. Isogai, A., Allomorphs of cellulose and other polysaccharides. *Cellulosic polymers. Hanser, Munich* 1994, 1-24.
155. Ghosh, A. K.; Jeong, B.-H.; Huang, X.; Hoek, E. M., Impacts of reaction and curing conditions on polyamide composite reverse osmosis membrane properties. *Journal of Membrane Science* 2008, 311, (1), 34-45.
156. Pacheco, F. A.; Pinnau, I.; Reinhard, M.; Leckie, J. O., Characterization of isolated polyamide thin films of RO and NF membranes using novel TEM techniques. *Journal of Membrane Science* 2010, 358, (1), 51-59.
157. Ferlita, R. R.; Phipps, D.; Safarik, J.; Yeh, D. H., Cryo-snap: A simple modified freeze-fracture method for SEM imaging of membrane cross-sections. *Environmental Progress* 2008, 27, (2), 204-209.
158. Li, X.; Wang, K. Y.; Helmer, B.; Chung, T.-S., Thin-film composite membranes and formation mechanism of thin-film layers on hydrophilic cellulose acetate propionate substrates for forward osmosis processes. *Industrial & Engineering Chemistry Research* 2012, 51, (30), 10039-10050.
159. Freger, V.; Arnot, T.; Howell, J., Separation of concentrated organic/inorganic salt mixtures by nanofiltration. *Journal of Membrane Science* 2000, 178, (1), 185-193.
160. Hayashi, J.; Sufoka, A.; Ohkita, J.; Watanabe, S., The confirmation of existences of cellulose III, IIII, IVI, and IVII by the X-ray method. *Journal of Polymer Science: Polymer Letters Edition* 1975, 13, (1), 23-27.
161. Park, S.; Baker, J. O.; Himmel, M. E.; Parilla, P. A.; Johnson, D. K., Cellulose crystallinity index: measurement techniques and their impact on interpreting cellulase performance. *Biotechnology for biofuels* 2010, 3, (1), 1.
162. Thygesen, A.; Oddershede, J.; Lilholt, H.; Thomsen, A. B.; Ståhl, K., On the determination of crystallinity and cellulose content in plant fibres. *Cellulose* 2005, 12, (6), 563-576.

163. Burgess, R. R.; Deutscher, M. P., *Guide to protein purification*. Academic Press: 2009; Vol. 463.
164. Nyström, M.; Ruohomäki, K.; Kaipia, L., Humic acid as a fouling agent in filtration. *Desalination* 1996, *106*, (1), 79-87.
165. Schäfer, A.; Schwicker, U.; Fischer, M.; Fane, A. G.; Waite, T., Microfiltration of colloids and natural organic matter. *Journal of Membrane Science* 2000, *171*, (2), 151-172.
166. Yuan, W.; Zydney, A. L., Humic acid fouling during microfiltration. *Journal of Membrane Science* 1999, *157*, (1), 1-12.
167. Kabsch-Korbutowicz, M.; Majewska-Nowak, K.; Winnicki, T., Analysis of membrane fouling in the treatment of water solutions containing humic acids and mineral salts. *Desalination* 1999, *126*, (1), 179-185.
168. Tu, S. C.; Ravindran, V.; Den, W.; Pirbazari, M., Predictive membrane transport model for nanofiltration processes in water treatment. *AIChE Journal* 2001, *47*, (6), 1346-1362.
169. Hong, S.; Elimelech, M., Chemical and physical aspects of natural organic matter (NOM) fouling of nanofiltration membranes. *Journal of membrane science* 1997, *132*, (2), 159-181.
170. Tang, C. Y.; She, Q.; Lay, W. C.; Wang, R.; Fane, A. G., Coupled effects of internal concentration polarization and fouling on flux behavior of forward osmosis membranes during humic acid filtration. *Journal of Membrane Science* 2010, *354*, (1), 123-133.
171. Tang, C. Y.; Kwon, Y.-N.; Leckie, J. O., Characterization of humic acid fouled reverse osmosis and nanofiltration membranes by transmission electron microscopy and streaming potential measurements. *Environmental science & technology* 2007, *41*, (3), 942-949.
172. Stevenson, F. J., *Humus chemistry: genesis, composition, reactions*. John Wiley & Sons: 1994.
173. Pitre, R. In *Produced water discharges into marine ecosystems*, Offshore Technology Conference, 1984; Offshore Technology Conference: 1984.
174. Jacobs, R.; Grant, R.; Kwant, J.; Marquenie, J.; Mentzer, E., The composition of produced water from Shell operated oil and gas production in the North Sea. In *Produced Water*, Springer: 1992; pp 13-21.
175. Sigma-Aldrich Co. <http://www.sigmaaldrich.com/> (April 2016),
176. Malvern Instruments Ltd. <http://www.malvern.com/en/products/product-range/zetasizer-range/zetasizer-nano-range/zetasizer-nano-zs/> (April 2016),
177. GE Power Water and Process Technologies. <https://www.gewater.com> (April 2016),
178. Linares, R. V.; Li, Z.; Yangali-Quintanilla, V.; Ghaffour, N.; Amy, G.; Leiknes, T.; Vrouwenvelder, J., Life cycle cost of a hybrid forward osmosis–low pressure reverse osmosis system for seawater desalination and wastewater recovery. *Water research* 2016, *88*, 225-234.
179. Massonne, K.; Siemer, M.; Mormann, W.; Leng, W., Distillation of ionic liquids. In Google Patents: 2013.
180. Perry, J. H., *Chemical engineers' handbook*. 1950; Vol. 27, p 533.

181. SaudiElectricityCompany.<https://www.se.com.sa/en-us/Customers/Pages/TariffRates.aspx> (May 2016),
182. TheStatistical Portal. <http://www.statista.com/statistics/263492/electricity-prices-in-selected-countries/> (May 2015),
183. Mecerreyes, D., *Applications of Ionic Liquids in Polymer Science and Technology*. Springer: 2015.

APPENDICES

Appendix A

1. Amount of water to be removed.

$$C_1V_1 = C_2V_2$$

$$C_1=0.1 \text{ wt \%}$$

$$V_1=1000 \text{ L}$$

$$C_2=5 \text{ wt \%}$$

Then $V_2=20 \text{ L}$, and water to be removed is 980 L .

2. Osmotic pressure

$$\Pi = iMRT$$

$$i \text{ (1-ethyl-3-methylimidazolium acetate)}=2$$

$$\text{MW (1-ethyl-3-methylimidazolium acetate)} = 170.21 \text{ gmol}^{-1}$$

$$R= 0.082 \text{ L atm}^{-1} \text{ K}^{-1}\text{mol}^{-1}$$

$$T= 293.15 \text{ K}$$

$$M= 0.294 \text{ molL}^{-1}$$

Then $\Pi=14.13 \text{ bars}$

3. RO energy consumption

Assuming energy consumption of RO system is 2.5-4 kWh/m³

For 1000 L of water in the feed, energy consumption will be approximately 3 kWh/m³.

4. Heating the water (assuming from 20° C) to boiling point of 100° C

$$Q = mc_p \Delta T$$

$$C_p (\text{water}) = 4.2 \text{ J}/(\text{g} \cdot ^\circ\text{C})$$

$$\Delta T (\text{water}) = 100 - 20$$

m – mass of water:

a) distillation in hybrid process; m = 20 kg

b) distillation alone; m = 1000 kg

5. Evaporating water to steam

$$Q = m h_v$$

$$h_v (\text{water}) = 2260 \text{ J}/\text{g}$$

m-mass of water:

a) distillation in hybrid process; m = 20 kg

b) distillation alone; m = 1000 kg

LIST OF PUBLICATIONS AND CONFERENCES

1) Part of the chapter regarding preparation and characterization of cellulose membranes via silylation and ionic liquid as well as interfacial polymerization has been published in Journal of Membrane Science. Title and authors are: Cellulose Multilayer Membranes Manufacture with Ionic Liquid prepared by S. Livazovic, Z. Li, A.R. Behzad, K.-V. Peinemann and S.P. Nunes.

Part of the chapters regarding fouling with humic acid and oil in water separation are in the process of being submitted:

2) The work on fouling with Suwanee River Humic Acid (SRHA) and other organics such as bovine serum albumin (BSA) and gamma globulin (γ - globulin) is intended for publication with the following title and authors: Fouling Resistance of Cellulose Multilayer Membranes evaluated with Humic (SRHA) and Non-Humic (BSA, γ -Globulin), S. Livazovic and S.P. Nunes.

3) The work on oil in water separation is intended for publication with the following title and authors: Effect of pH, Surfactants and Concentration on Complete Removal of Crude Oil from Synthetic Produced Water using Cellulose/Ionic Liquid Membranes, by S. Livazovic and S.P. Nunes.

List of conferences:

1. 25th Annual meeting North American Membrane Society (NAMS), Boston, MA, May 30 - June 3, 2015

Poster presentation: "Cellulose composite membranes with ionic liquid as a green solvent"

2. Functional Nanomaterials: Design, Synthesis, and Applications, KAUST, KSA, March 15 – 17, 2015 - Attendee

3. Advanced Membranes and Porous Materials Center / KAUST Research Conference, KAUST, KSA, February 23 – 25, 2015 - Attendee

4. Membrane Science and Technology for Water, KAUST, KSA, November 17 -18, 2014

Poster presentation: "Cellulose nanofiltration membranes"

5. KAUST Polymer Conference: From Synthesis to Properties to Applications, KAUST, KSA, November 9 – 13, 2013 - Attendee

6. European Membrane School (EMS) Middle East, April 29 – May 2, 2012 - Attendee

Intended for abstract submission:

- 9th IMSTEC (The Membrane Society of Australasia), Adelaide, Australia, December 5-8 2016.